AD_____

Award Number: W81XWH-04-1-0456

TITLE: Manipulation of Nf-KappaB Activity In The Macrophage Lineage As A Novel Therapeutic Approach

PRINCIPAL INVESTIGATOR: Fiona Yull, Ph.D.

CONTRACTING ORGANIZATION: Vanderbilt University Medical Center
Nashville, TN 37232

REPORT DATE: May 2008

TYPE OF REPORT: Final

PREPARED FOR: U.S. Army Medical Research and Materiel Command
Fort Detrick, Maryland 21702-5012

REPORT DOCUMENTATION PAGE

Form Approved
OMB No. 0704-0188

1. REPORT DATE	2. REPORT TYPE	3. DATES COVERED
18-05-2008	Final	19 APR 2004 - 18 APR 2008

4. TITLE AND SUBTITLE

Manipulation of Nf-KappaB Activity In The Macrophage Lineage As A Novel Therapeutic Approach

5a. CONTRACT NUMBER

5b. GRANT NUMBER
W81XWH-04-1-0456

5c. PROGRAM ELEMENT NUMBER

6. AUTHOR(S)
Fiona Yull, Ph.D.

Email: fiona.yull@mcmail.vanderbilt.edu

5d. PROJECT NUMBER

5e. TASK NUMBER

5f. WORK UNIT NUMBER

7. PERFORMING ORGANIZATION NAME(S) AND ADDRESS(ES)

Vanderbilt University Medical Center
Nashville, TN 37232

8. PERFORMING ORGANIZATION REPORT NUMBER

9. SPONSORING / MONITORING AGENCY NAME(S) AND ADDRESS(ES)
U.S. Army Medical Research and Materiel Command
Fort Detrick, Maryland 21702-5012

10. SPONSOR/MONITOR'S ACRONYM(S)

11. SPONSOR/MONITOR'S REPORT NUMBER(S)

12. DISTRIBUTION / AVAILABILITY STATEMENT
Approved for Public Release; Distribution Unlimited

13. SUPPLEMENTARY NOTES

14. ABSTRACT

Morphogenesis of the mammary gland when misregulated can result in tumorigenesis. It involves interactions of multiple cell types in a highly regulated manner with complex signal transduction pathways coordinating the physiological processes. Interactions between epithelial and mesenchymal cells are known to be important. Studies have highlighted the importance of macrophages. The nuclear factorkappa B (NF-kB) family of transcription factors appears to be critical in regulating the dynamic changes during normal and neoplastic development. This goal of this proposal was to investigate the contribution of NF-kB signaling within macrophages in normal and neoplastic mammary development. Our data provides insights into the importance of NF-kB signaling in macrophages for mammary and tumor development and progression and suggests the potential for manipulation of NF-kB in macrophages as a novel therapeutic approach. In the course of this study we have used our previously generated IkBa knockout model and more importantly have generated a new set of inducible transgenics that enable us to manipulate NF-kB in macrophages. Our data suggest that altered NF-kappaB activity within macrophages has significant effects on mammary ductal development and impacts at least the metastatic stage of breast tumor progression.

15. SUBJECT TERMS
NF-kappaB, macrophages, mammary ductal development, doxycycline inducible transgenics

16. SECURITY CLASSIFICATION OF:			17. LIMITATION OF ABSTRACT	18. NUMBER OF PAGES	19a. NAME OF RESPONSIBLE PERSON
a. REPORT	b. ABSTRACT	c. THIS PAGE			USAMRMC
U	U	U	UU	47	19b. TELEPHONE NUMBER *(include area code)*

Table of Contents

INTRODUCTION

Morphogenesis of the mammary gland is a highly complex process which when misregulated can result in tumorigenesis. It involves the interactions of multiple cell types in a highly regulated manner with complex signal transduction pathways coordinating the physiological processes. Interactions between epithelial and mesenchymal cells are known to be important. However, as we started this research studies were beginning to highlight the importance of other cell types, such as macrophages. One of the signaling molecules that appears to be critical in regulating the dynamic changes during normal and neoplastic development is the nuclear factor-kappa B (NF-□) family of transcription factors. NF-□B can regulate many genes that are expressed by macrophages that are important for proliferation and apoptosis of cells, as well as remodeling and angiogenesis. We have investigated the contribution of NF-□B signaling within macrophages to normal and neoplastic mammary development. We have developed and characterized several new transgenics and created a model system that enables modulation of NF-□B signaling within macrophages. We have begun to obtain insights into the importance of NF-□B signaling in macrophages for tumor development and progression and our data suggests that modulation of NF-□B within macrophages may represent a novel therapeutic approach.

BODY

Task 1. To investigate the effects of constitutive NF-□B activity within macrophages on mammary development (Months 1-24):

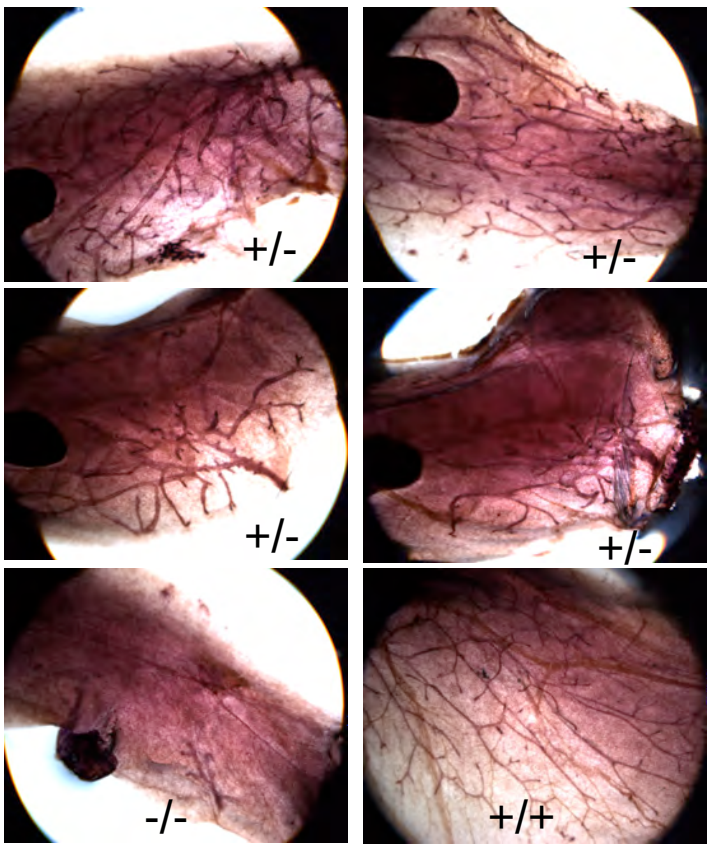

Figure 1 – Wholemount staining of virgin mammary glands after I□B-□ +/-, -/- and +/+ fetal liver transplantation.

a. Perform fetal liver cell transplantation using I□B-□ null and control donors at postnatal day 19 to determine effects on virgin postnatal mammary development of constitutive NF-□B activity in reconstituted hematopoietic cells (Months 1-24). [100 mice]

b. Perform fetal liver cell transplantation using I□B-□ null and control donors into recipients at 6 weeks. Allow hematopoetic cell reconstitution for a further 6 weeks. Mate recipient mice and investigate effects on development during pregnancy of constitutive NF-□B activity in hematopoietic cells (Months 1-24). [100 mice]

Our lab and others generated I□B□ deficient mice (Chen et al., 2000; Chen et al., 2000b; Beg et al., 1995; Klement et al., 1996). In these animals the major inhibitor of NF-□B is absent resulting in constitutive activity. Neonatal lethality precludes the study of adult mammary gland morphogenesis in these animals. However, fetal liver transplantation and reconstitution of hematopoetic cell lineages enables the effects of constitutive NF-□B activation within these lineages to be investigated in an adult animal (Chen et al., 2000; Everhart et al., 2005). Our original hypothesis suggested that constitutive NF-□B activity in mice reconstituted with I□B□ deficient hematopoetic cells would result in increased postnatal ductal proliferation. We were

therefore surprised when our program of fetal liver transplantations suggested that constitutive NF-κB in IκBα -/- reconstituted virgin animals resulted in decreased ductal proliferation with heterozygote knockout animals displaying an intermediate phenotype. Intriguingly, our most recent data (see Aim 3) is in agreement with this effect. Mice reconstituted with heterozygote knockout cells display an interesting phenotype in which the extent to which the ductal tree is able to grow into the recipient fad pad appears to be reduced but the ducts themselves appear thicker, representative examples are shown in **Figure 1**. However, having performed a relatively large number of reconstitution experiments, we became concerned about some of the technical aspects of this approach. Fetal livers are harvested from 14.5dpc embryos resulting from matings between heterozygous knockout animals. The harvested cells are reintroduced into irradiated recipients on the same day. This effectively means that the reconstitutions are performed "blind" because the genotyping of the embryos occurs after the reconstitutions have been completed. This results in a large number of heterozygote reconstitutions and relatively few homozygous or wildtype reconstitutions. We also had several experiments in which when the mammary tissue was finally harvested we discovered that none of the transplantations had reconstituted and suspected that this was due to technical issues with the irradiator. Another issue with the reconstitution strategy is that the resulting chimeras have reconstituted populations of multiple cell types of the hematopoetic lineage. In other words, we were not able to specifically assign phenotypic changes to an effect of changed signaling within macrophages as opposed to within B or T cells or a combinatorial effect. Given these considerations, all of which would be addressed by the inducible model proposed as aim 2, we decided to focus our efforts on the inducible model system (see task 2).

Our attempts to obtain pregnant reconstituted animals proved unsuccessful. We were unable to decrease the dosage of radiation sufficiently to find the balance between a practical level of reconstitution while retaining the fertility of the reconstituted animal. As an alternative approach, we investigated mammary development during pregnancy in wildtype (+/+) versus heterozygote (+/-) IκBα knockout animals. On examination of H&E stained 16.5dpc sections, we were intrigued to observe increased ductal development in heterozygote animals relative to controls. We had previously believed there to be no significant phenotype in heterozygote knockout animals but decided to look more closely at the heterozygotes during pregnancy relative to control wildtype animals. As the involvement of macrophages in both normal development and tumorigenesis was a major focus of this grant, we were curious to determine whether constitutive NF-κB activation in the whole animals without transplantation had an effect on tissue macrophages. In order to investigate the presence of macrophages we used an F4/80 antibody to stain tissue sections (**Figure 2**). The results suggested that increased numbers of macrophages are found in tissue with constitutive NF-κB activity.

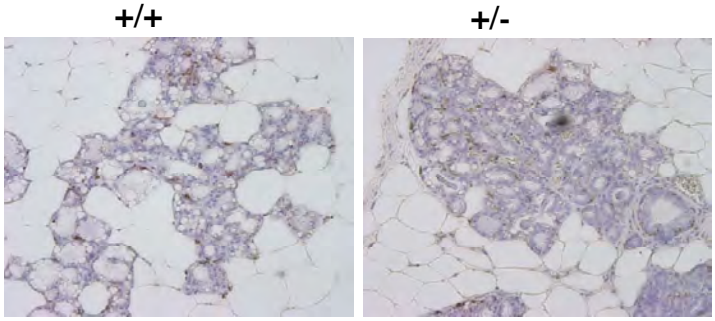

Figure 2 – F4/80 staining of IκBα +/- and +/+ tissue at 16.5dpc shows increased macrophage presence in +/- animals relative to controls.

In our original proposal we planned to measure the *in vivo* effects of modulating NF-κB activity in macrophages using our HLL reporter transgenics that express luciferase under an NF-κB responsive promoter such that luciferase assay of crude protein extracts can be used to quantify NF-κB activity. While the HLL reporter mice provided valuable information regarding NF-κB activation *in vivo*, three issues led us to construct a second generation of NF-κB reporter transgenic mice. First, although we have attempted to identify NF-κB activation at a cellular level, we were unable to reproducibly identify luciferase protein or mRNA in individual cells despite repeated efforts with immunohistochemistry and *in situ* hybridization. Second, we needed to be able to sort individual cells that have activated NF-κB. Third, the proximal HIV-LTR is an NF-κB dependent promoter that by all indications was a good fidelity as a read-out for NF-κB activation; however, it was a formal possibility that other transcription factors, including Sp1, could influence transcription of this promoter. Therefore, we decided that it would be valuable to have an additional line of reporter mice with another NF-κB

dependent promoter to confirm and validate findings using the HLL mice. We collaborated Dr. Timothy Blackwell to make a new line of transgenic reporter mice that express a green fluorescent protein (GFP)/luciferase fusion protein under the control of a synthetic NF-□B dependent promoter. Since GFP can be detected in individual cells, these reporter mice allow cell specific determination of NF-□B directed transcription, a crucial factor in understanding NF-□B dependent downstream signaling. The luciferase moiety of the fusion protein also enables luciferase assay from protein extracts and *in vivo* imaging as described above for the HLL reporter transgenics.

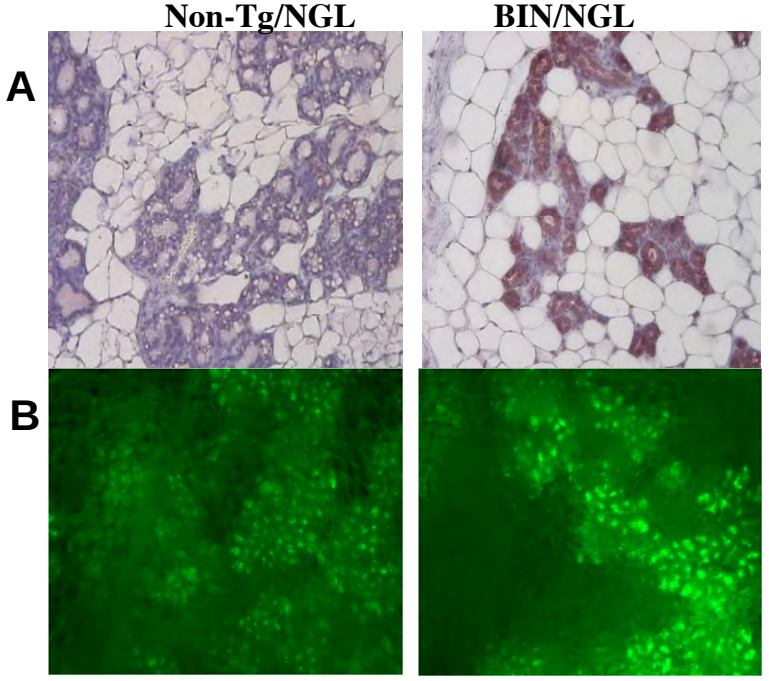

Figure 3 - Immunohistochemistry for GFP expression in single NGL transgenic and double transgenics. Shown are examples of mammary tissue at 16.5dpc. A – immunohistochemistry using a GFP antibody, B – fluorescence in freshly harvested mammary tissue sections.

The new transgenic NF-□B reporter mice contain tandem copies of a 36 base enhancer from the 5' HIV-LTR that includes both NF-□B binding sites. The proximal 169 base pairs of these promoter constructs, including the TATA box, are from the herpes simplex virus thymidine kinase promoter. We constructed plasmids for expression of enhanced GFP (EGFP)/luciferase fusion protein under the control of 8 replicates of the NF-□B enhancer sequence. The CMV promoter present in pEGFP/Luc (Clontech, Palo Alto, CA) was replaced with our synthetic NF-□B dependent promoter. The 8x construct was microinjected by the Vanderbilt Transgenic/ES Cell Shared Resource to generate transgenic lines (C57Bl6/DBA background) named NGL [for NF-□B-GFP/Luciferase]. The NGL reporter transgenics can be used in the same manner as the HLL, giving comparable results. The new NGL transgenics are better than the HLL transgenics as they can also enable visualization of specific cell types in which NF-□B is activated by fluorescence microscopy or immunohistochemistry of tissue sections. Activation of NF-□B results in expression of GFP protein that can be detected by fluorescence microscopy or by immunohistochemical analysis of paraffin embedded sections using an anti-GFP antibody. We tested the efficacy of the new NGL mice by crossing them with transgenics that elevate NF-□B activity in the mammary epithelium. The mice produced from these matings allowed us to visualize where the NF-□B was active (**Figure 3**). The new reporter transgenics make it possible to see both the histological structure of the tissue and to localize and get an indication of NF-□B activity. At 16.5dpc in an NGL transgenic ie. an animal that is effectively wild-type as far as mammary development is concerned but carries the NF-□B reporter, there is diffuse NF-□B activity throughout the epithelial tissue that is proliferating and filling the mammary fat pad. In double transgenics we were able to visualize both the level and localization of NF-□B activity and determine the effect of the transgene that is modulating NF-□B activity. In the double transgenic animals the level of NF-□B activity was higher but confined to a more dense area. **Figure 3A** shows immunohistochemical staining using a GFP antibody to localize NF-□B activity. It is interesting to note that the fluorescent moiety of the reporter also allows us to place freshly harvested tissue on a slide on a fluorescence microscope and begin to get some idea of the expression pattern in three dimensions (**Figure 3B**). The generation of the new reporter transgenics made it feasible to obtain data that was previously not possible to collect.

One of the anticipated benefits of the new reporter transgenics was the ability to assess NF-□B activity in specific cell types. As macrophages are the focus of these studies we were interested to determine whether the NGL reporter transgenics would allow us to quantify changes in NF-□B activity within macrophages. Therefore,

we performed cell culture studies using primary cultures of bone marrow derived macrophages (BMDM) from the NGL reporter transgenics (**Figure 4**). Luciferase assay of cell extracts demonstrate that NF-κB activity is induced at 4 hours post treatment with LPS (a known activator of NF-κB) and that this stimulation can be blocked by pretreatment with an adenovirus expressing a dominant inhibitor of NF-κB (Sadikot et al, 2006). This data provides evidence that the activity of NF-κB within primary NGL macrophages can be easily measured.

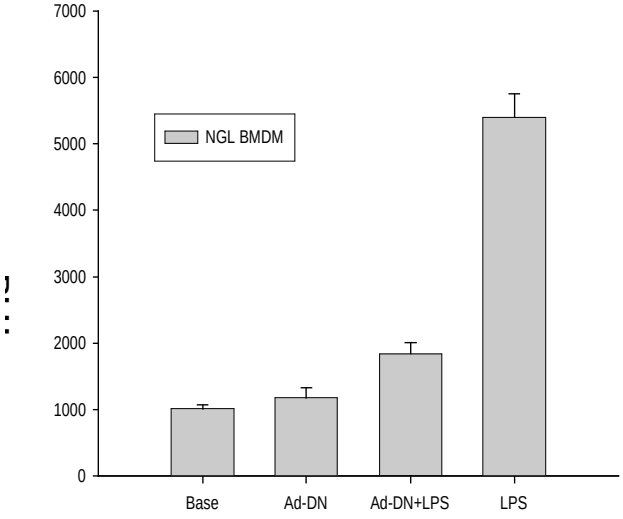

Figure 4– Luciferase assay of NGL BMDM extracts after 4 hrs treatment with LPS in the presence or absence of an NF-κB dominant-inhibitor virus.

In order to carry out more extensive cell culture studies, we have also generated an immortalized NGL bone marrow derived macrophage cell line. The cell surface markers on this line were investigated to confirm that the cells were derived from macrophages and maintained the appropriate characteristics.

Cell surface marker of J2-BM cells (day 14)

Surface marker	% Positive J2-BM cells	Distribution
MAC-1	96.8	Macrophage, granulocytes
Fc receptor	85.7	Macrophage, B Cells
Ly 1.1	2.8	Pan-T cells, some B cells
Lyt 2.1	0.4	T-cell subsets, thymocyte
L3T4	3.2	T-cell subsets, thymocyte
Surface immunoglobulin	0.7	B cells

Having confirmed that the characteristics of the immortalized line were consistent with macrophage cells we tested to determine whether they have the appropriate NF-κB response to LPS stimulation and whether we can measure this using a luciferase assay. The data showed that the response to LPS stimulation of the immortalized cell lines was not significantly different to that of primary BMDC (**Figure 5**). In combination, the studies suggest that we have generated an immortalized macrophage cell line from the NGL mice that can be used in future *in vitro* studies as required.

In addition to investigating our ability to assess NF-κB activity in specific cell types using our NGL reporter we have cultured BMDM from wildtype (IκBα +/+) and IκBα +/- mice. In order to confirm that NF-κB signaling was altered in macrophages derived from heterozygous knockout animals we performed western analyses using cytoplasmic and nuclear extracts from wildtype and heterozygous BMDM and assessed the response to LPS stimulation (**Figure 6**). IκBα+/- BMDM contained decreased IκBα and increased RelA protein at baseline compared to WT BMDM. Four hours after LPS stimulation, increased RelA was detected in both WT and IκBα +/- BMDM; however, IκBα protein was virtually undetectable in IκBα +/- BMDM. While IκBα protein had returned to basal levels by 24 hours after LPS stimulation, nuclear RelA protein was significantly higher in IκBα +/- BMDM compared to WT BMDM. These results demonstrate our ability to

obtain BMDM from both wildtype and heterozygous knockout mice and that NF-κB signaling is altered in heterozygous knockout mice.

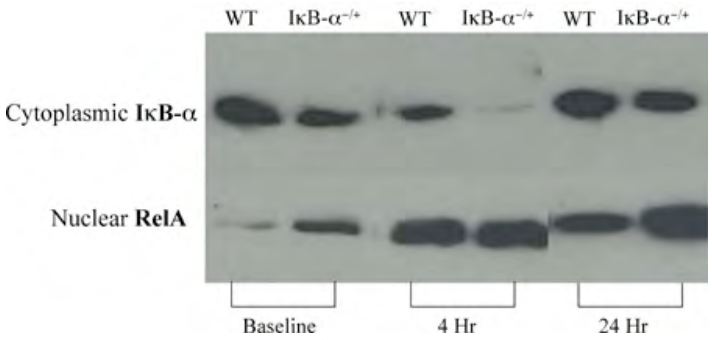

Figure 6– western analysis of cytoplasmic and nuclear extracts from wildtype and IκB +/- BMDM cells showing differential response to treatment with LPS.

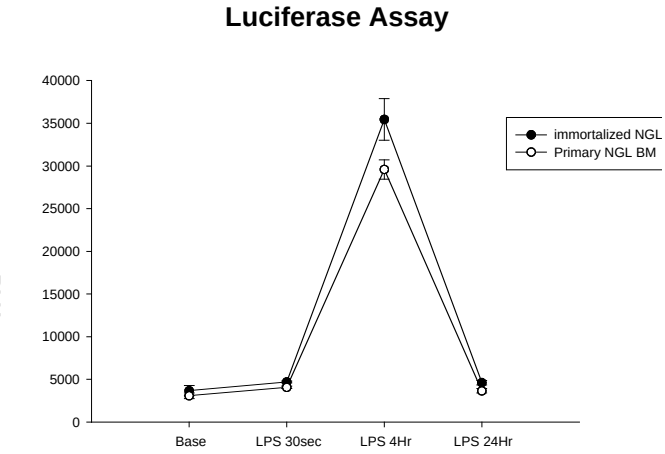

Figure 5– Luciferase assay of extracts from NGL primary and immortalized BMDM cells showing response to treatment with LPS.

In order to carry out more extensive and targeted cell culture studies based on the IκB-α null model, we generated immortalized bone marrow derived macrophage cell lines from both wild type and IκB-alpha null mice. While IκB-α wild type macrophages appear typically small and spherical, the morphological appearance of the IκB-α -/- cells is different. These cells are larger and often multinucleated. Treatment of the cells with M-CSF exacerbates the observed morphological phenotype. MTT assay to determine proliferation rate of wild type and IκB-α -/- macrophages determined that knockout cells proliferate at approximately twice the rate of wild type cells.

We were interested in determining potential downstream NF-κB target genes whose differential expression could be contributing to the observed differences in proliferation rates. RT-PCR analysis suggests that c-myc mRNA expression is increased in IκB-α -/- compared to wild type cells, implicating c-Myc as one of the important target genes whose expression is altered by the constitutive NF-κB activity (**Figure 6A**). Another target gene that can be regulated by NF-κB signaling is matrix metalloproteinase-9 (MMP-9). The regulation of MMP activity is known to be important in epithelial cell branching and normal mammary gland development (Witty et al., 1995; Simian et al., 2001). The expression and activity of MMPs is also associated with mammary tumors and human breast cancer where they contribute to invasion and metastasis (Egeblad and Werb, 2002; Heppner et al.,

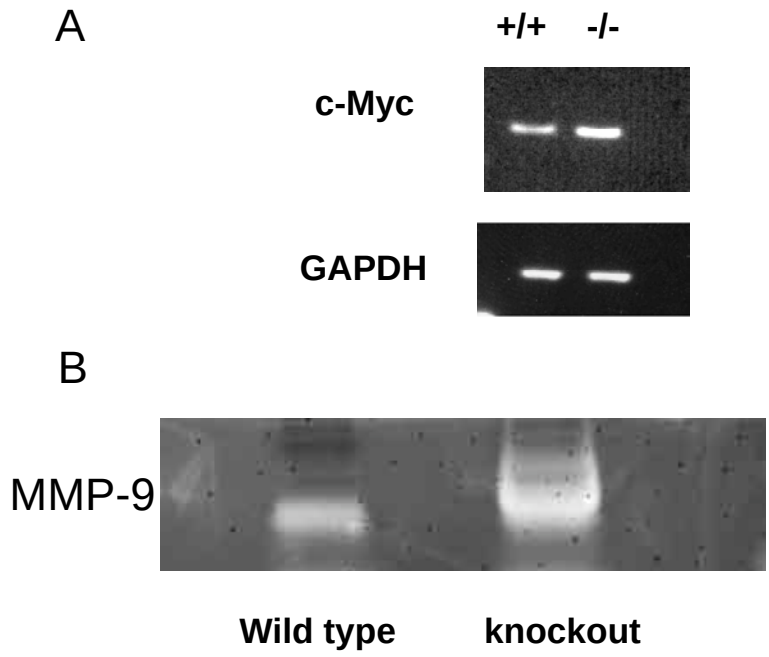

Figure 6A - RT-PCR shows increased levels of c-Myc expression in knockout cell lines. **B**- Gel zymography of conditioned medium (48hrs) from wild type and IκB-α knockout macrophages.

1996). In addition, the expression of MMP-9 has been demonstrated to require activation of NF-κB (Bond et al., 1998) and we have recently shown that MMP-9 activity is affected during postnatal mammary development by NF-κB signaling (Connelly et al., 2007). Given these correlations between NF-κB signaling and mammary development and tumorigenesis we decided to investigate the production of MMP-9 by the macrophage cell lines. Gel zymography and densitometric analysis show a 2-fold increase in MMP-9 in media conditioned by IκB-ζ -/- macrophages compared to wild type cells (**Figure 6B**).

Finally, we were interested in the potential for macrophages in which NF-κB signaling was altered to impact the behavior of adjacent mammary epithelial cells. We cultured normal mammary epithelial cells (NMuMG) in conditioned medium from our macrophage cell lines. Interestingly, our data suggest that the cells cultured in medium from knockout macrophages may survive more effectively than those cultured in wild type medium (**Figure 7**). This provides some evidence that altered macrophages can impact associated epithelium but requires further investigation.

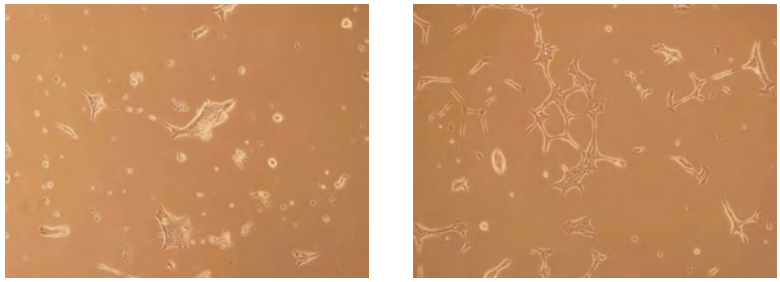

Figure 7. NMuMG mammary epithelial cells cultured for 48 hrs in conditioned medium from wild type or IκBζ knockout macrophages.

Summarizing the data from this section, we have completed fetal liver transplantation studies that suggest that increased NF-κB signaling in cells of the hematopoetic lineage results in decreased virgin mammary ductal development. Heterozygous IκBζ knockout mice have increased ductal development during pregnancy associated with increased numbers of macrophages. We have generated new reporter transgenics that greatly improve our ability to monitor changes NF-κB activity. We have established cell lines from wild type and knockout IκB-ζ mice and using these cell lines we have obtained data concerning the effects of constitutive NF-κB signaling on macrophage cells themselves including increased proliferation rates and increased levels of expression of genes that are known to play roles in both normal development and tumorigenesis. In addition, we have data to suggest that the macrophages with the altered behavior are able to produce mediators that alter the behavior of mammary epithelial cells. Clearly more investigation is required to determine the specific mediators and whether these effects are on survival, proliferation or motility of the epithelial cells.

Task 2. Assess effects on mammary development of induced and inhibited NF-κB activity using novel inducible transgenics (Months 1-36).

a. Investigate postnatal development in doxycycline-induced macrophage-restricted constitutive activator double transgenic mice (IKMRP) and controls (Months 1-36). [300 mice]
b. Investigate postnatal development doxycycline-induced macrophage-restricted dominant inhibitor double transgenic mice in (DNMRP) and controls (Months 1-36). [300 mice]

In collaboration with Dr. Timothy Blackwell and Dr. Michael Ostrowski, we have developed novel conditional transgenic modular mouse models, based on the tetracycline inducible system, to over-express IκB-DN (dominant inhibitor) or cIKK2 (constitutive activator) in response to treatment with doxycycline in drinking water. The components of this system include transgenics expressing the reverse tetracycline transactivator (rtTA) in macrophages, and transgenics in which the tetracycline operator $(tet\text{-}O)_7$ and a minimal CMV promoter drive expression of either the dominant inhibitor (IκB-DN), or a constitutively active IKK2 mutant. Key DNA components for the system were obtained from Dr Jay Tichelaar (Perl et al., 2002). In the presence of

doxycycline, the rtTA binds to tet-O and induces downstream gene expression within 24 hours. In these transgenics, the IκB-DN construct that we have has mutations of the critical phosphorylation targets (serine residues) that are normally phosphorylated in response to signaling resulting in degradation of the inhibitor (Chen et al., 1999). This mutated form of inhibitor is not degraded in response to phosphorylation signals and therefore functions to block NF-κB signaling. To facilitate detection of induced transgene products we attached a FLAG tag to the cIKK2 and a Myc-His tag to the dominant inhibitor. The transgenics expressing the inhibitor are named DN. The transgenics expressing the activator are named IKK. In order to modulate expression in macrophages, we originally collaborated with Dr. John Christman and designed transgenics with macrophage restricted expression of the reverse tetracycline transactivator (rtTA)(Perl et al., 2002). Expression was targeted to macrophages using a promoter based on the mannose receptor promoter (MRP)(Eichbaum et al., 1997) and including 3 repeats of a PU.1 responsive element (DeKoter et al., 2000). The transactivator transgenics are named MRP. With the assistance of the Vanderbilt Transgenic/ES Cell Shared Resource we generated 4 independent lines each of the DN, IKK and MRP transgenics. We confirmed inducible transgene expression in response to doxycycline treatment by crossing the DN lines with an existing, well-characterized lung-specific CC-10rtTA transgenic (Perl et al., 2002). Animals were treated with doxycycline in drinking water (1g/L) for 3 days prior to collection of tissue samples. We demonstrated doxycycline induction of DN expression as measured by western analysis in lung tissue (**Figure 8A**). Results showed no uninduced expression in the absence of doxycycline in the drinking water and no detectable non tissue-specific expression, therefore the system is not leaky.

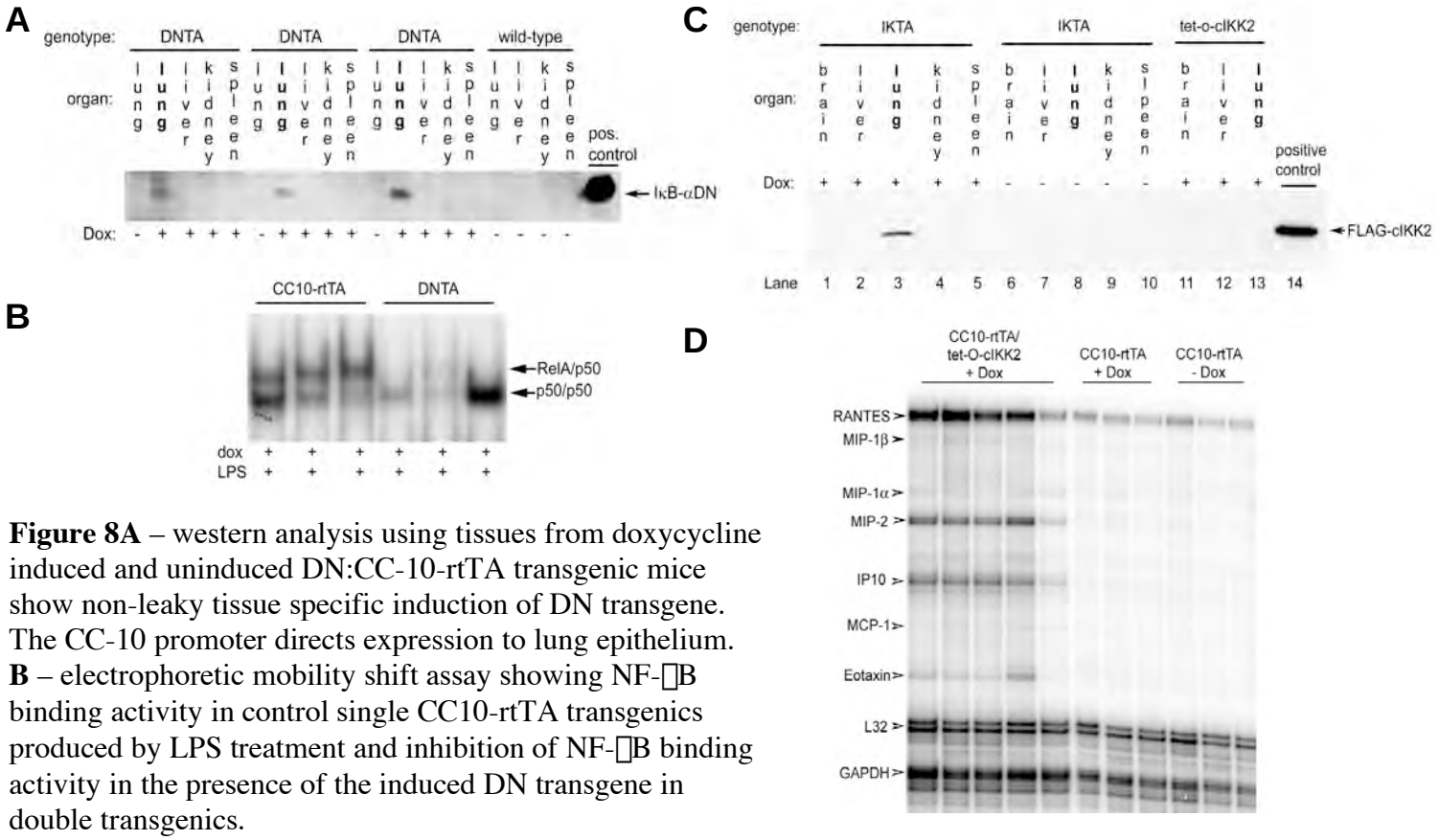

Figure 8A – western analysis using tissues from doxycycline induced and uninduced DN:CC-10-rtTA transgenic mice show non-leaky tissue specific induction of DN transgene. The CC-10 promoter directs expression to lung epithelium.
B – electrophoretic mobility shift assay showing NF-κB binding activity in control single CC10-rtTA transgenics produced by LPS treatment and inhibition of NF-κB binding activity in the presence of the induced DN transgene in double transgenics.
C – western analysis in tissues from doxycycline induced and uninduced IKK:CC-10-rtTA transgenic mice show non-leaky

The induced DN transgene is also able to inhibit NF-κB activation in the lung in response to LPS treatment that would normally be expected to increase NF-κB activity and hence binding in a gel mobility shift assay (**Figure 8B**). We generated 4 lines of IKK transgenics. In equivalent crosses with rtTA transgenics to those decribed above, we confirmed lung specific expression of the constitutive activator upon doxycycline administration and the ability of the transgenic protein to enhance NF-κB activation in the lung (**Figure 8C and D**). We used the lung-targeted form of the modular inducible transgenic system in collaborative studies published in the Journal of Immunology.

We generated 4 independent lines of original MRP transgenics. The mice transmitted the transgene in predicted ratios and we were able to detect the rtTA mRNA using RT-PCR in alveolar macrophages harvested from bronchiolar lavage fluid and in bone marrow derived macrophage cultures. We generated double transgenic animals carrying a combination of the DN and MRP transgenes (DNMP) or the IKK and MRP transgenes (IKMP) and treated double transgenics and controls with doxycycline to induce transgene expression. We were unable to detect expression of the transgenes by western analysis of macrophages harvested from bronchiolar lavage fluid or from bone marrow macrophages cultured from double transgenic animals and appropriate controls despite our ability to easily detect induced expression in the lung targeted system using the same antibodies. We also completed studies in which we treated DNMP and IKMP double transgenics with 2g/l doxycycline in drinking water from 4-8 weeks of age, harvested mammary glands and completed whole mount analyses. Our intention was to determine whether perhaps there were low levels of expression that may be sufficient to produce a phenotype even in the absence of detectable protein expression by western. However, no differences were detected between double transgenics and controls. Taking into consideration all of our data we were forced to conclude that the four lines of MRP transgenics did not result in sufficient expression of the rtTA to be of use for the inducible system.

As we had proposed to target the inducible system to macrophages we sought an alternative strategy. The c-fms gene encodes the receptor for macrophage colony-stimulating factor (CSF-1). The c-fms promoter has been successfully used to generate macrophage specific transgenics (Sasmono et al., 2003; Burnett et al., 2004). In trying to find a source for this promoter we made contact with Professor Michael Ostrowski at Ohio State University, Columbus, Ohio. We discovered that his group were also attempting to make a macrophage-targeted rtTA transgenic. They had founder animals from two different transgene constructs each of which uses a different form of the c-fms promoter. Both types of transgenics express high levels of the transgene as determined by RT-PCR. Dr. Ostrowski kindly agreed to collaborate with us and provided us with founder animals.

We mated these new MRP mice with our IKK and DN transgenics to determine whether they produced sufficient levels of rtTA expression to be effective in our inducible system. Initially, we decided to determine whether we could detect expression of the IKK transgene in *ex vivo* cell culture experiments. We took two double positive IKFM (cfms and IKK) and two control mice and extracted BMDMs, cultured in medium containing M-CSF for 10 days (method according to Connelly et al. 2003). The cells were seeded in 6-well plates and stimulated with doxycycline (1µg/ml) for 24 and 48 hours. Whole cell protein extracts were prepared and western blot analyses performed to detect FLAG-IKK. Despite attempts to load a relatively large amount of protein we were unable to detect a band of the correct size that would indicate successful induction of IKK expression.

In order to extend the period of treatment and optimize the probability of transgene induction, we took one double positive IKFM and one DNFM mouse and controls and administered doxycycline (2g/L) in drinking water for 1 week. Bone marrow cells were harvested and seeded in 6-well plates in the presence of M-CSF and 100ng/ml doxycycline. 100ng/ml doxycycline was added every 2 days to culture medium. Cells were collected at 6, 8 and 10 days from each line and whole cell protein extracts prepared. Western blot analyses were performed using appropriate antibodies to detect FLAG-IKK and myc-DN. Once again, we were unable to detect induced protein expression.

We were concerned about our inability to specifically detect transgene at the level of protein expression and decided to adopt an RT-PCR strategy to attempt to detect transgene expression at the level of RNA.

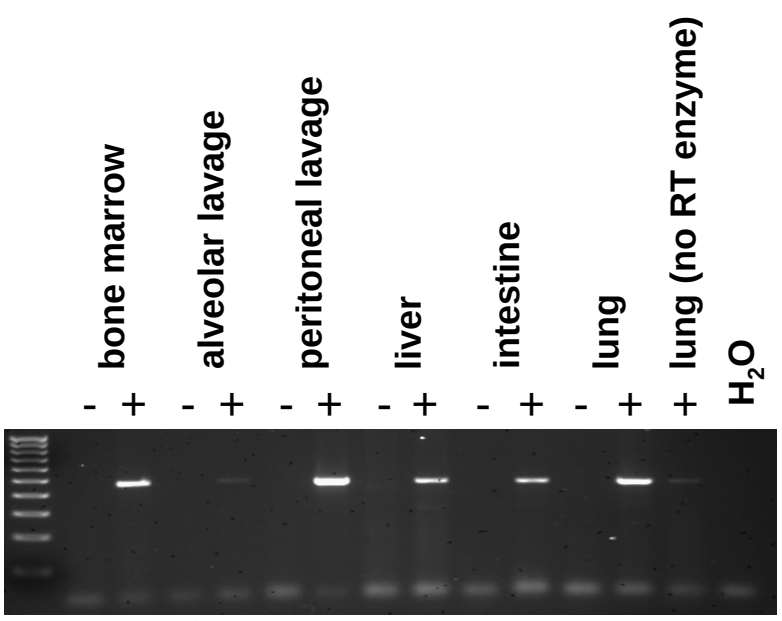

Figure 9 - RT-PCR for DN transgene in DNFM (double positives) and controls (double negative). DNFM mice were treated with 2g/L doxycycline in drinking water for 4 weeks before tissue collecion

We treated two DNFM double positives and two control animals with 2g/L doxycycline in drinking water for 4 weeks. Lung, liver and intestine tissue samples were harvested from each animal and snap frozen in liquid nitrogen. Bronchioalveolar and peritoneal lavages were been completed and bone marrow cells harvested from femurs (pooled cells from double positives and controls to provide one sample from each) and samples used to prepare RNA and perform RT-PCR. We designed new primer pairs to detect FLAG-IKK and DN-Myc by RT-PCR and detected induced expression of the DN and IKK transgenes (**Figure 9**) and data not shown.

We decided that it was possible that the transgene was being induced at low levels that were below the detection limits of our western analysis but which would still result in phenotypic effects. Therefore, we treated IKFM double positive and control mice with 2g/L doxycycline in drinking water from 4 to 8 weeks of age. The mammary glands were harvested and whole mount analysis performed. In these studies we have observed a different phenotype in double positive as compared to controls (**Figure 10**). The example shown in last years report and included here turns out to be one of the more minimally affected cases. Many of the animals placed on doxycycline from 4 to 8 weeks appeared sick by the end of the treatment period. Considerable numbers of the experimental double transgenic mice had severely inhibited ductal development. At this point we are not certain if the phenotype is limited to inhibited invasion of the virgin ductal growth into the mammary fat pad or if there may be other more extensive systemic issues with induction of the IKK transgene and activation of NF-κB in macrophages over this period of several weeks.

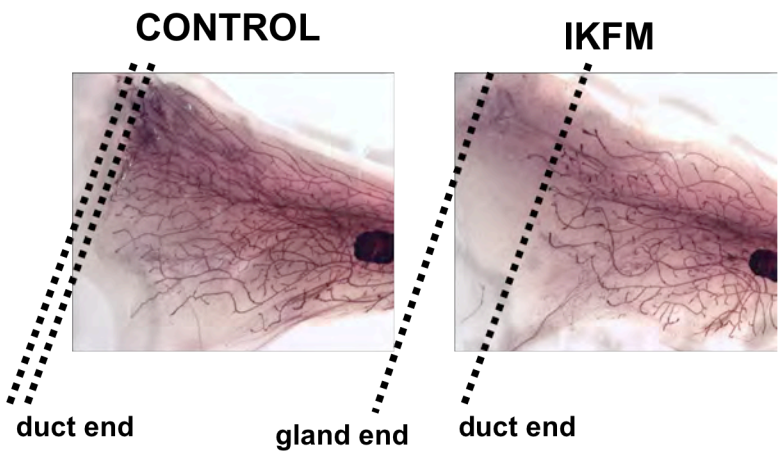

Figure 10 - Whole mount analyses of control and double IKFM transgenics following treatment with doxycycline from week 4-8.

We performed similar strategies to assess whether phenotypic effects were observed by treatment with doxycycline to induce the DN transgene in macrophages. Interestingly, the mice in which the DN transgene is induced show no signs of sickness even after equivalent periods of treatment. In our studies in which the DN transgene was turned on from weeks 4 to 8 our initial preliminary data suggested the persistence of relatively large terminal ductal end structures. However, having added larger numbers of experimental animals to the data set, we would now state that we can not report significant differences during postnatal development. As macrophages clearly play important roles during involution and NF-κB is rapidly increased at the onset of involution we predicted that inhibition of NF-κB in macrophages would have significant effects during

involution. We have also generated a cohort of double transgenic DNFM animals and appropriate controls treated with 2g/l doxycycline from 1 day prior to 5 days post wean. Disappointingly, our preliminary analysis of samples from these mice has not detected any significant differences. There are at least two possible interpretations of this data. The first would be that NF-□B signaling within macrophages has no significant role during these stages of normal mammary development. The second may be that the inhibitor is only expressed in a subset of macrophages and that the uninhibited population is sufficient for overall normal function.

Task 3. To determine whether manipulation of NF-□B activity within macrophage populations effects tumorigenesis (Months 25-36).

a. Investigate effects on tumorigenesis in PyVT/IKFM doxycycline-induced transgenics and controls. ie. does constitutive NF-□B activity within macrophages exacerbate tumorigenesis? (Months 25-36). [100 mice]
b. Investigate effects on tumorigenesis in PyVT/DNFM doxycycline-induced transgenics and controls. ie. does reduced NF-□B activity within macrophages inhibit tumorigenesis? (Months 25-36). [100 mice]

As originally proposed this task was dependent on establishing the model described in task 2 and was not scheduled to commence until month 25. However, due to the difficulties we experienced in establishing the critical macrophage targeted rtTA transgenic component of the inducible modular system we adopted an intermediate strategy to obtain worthwhile data in the event that we were unsuccessful in developing the modular system in time to make significant progress with this aim.

We obtained PyVT transgenic mice. While this model of mammary cancer has been used in a number of studies, little is known concerning the pattern of NF-□B activation during the development of the tumors. Our new NGL reporter transgenics provided us with a unique opportunity to investigate the stages during tumor progression in which NF-□B is active and the specific cell types involved. We crossed the PyVT transgenics with the NGL reporter transgenics to enable us to investigate the pattern of NF-□B activation at the various stages of tumor development (**Figure 11**). The PyVT mice rapidly develop mammary tumors that are readily visible in whole mount analyses by 7 weeks of age (**Figure 11A**). Using immunohistochemistry to detect GFP expression in double PyVT/NGL reporter transgenics we were able to visualize localized NF-□B activation within the developing mammary tumors (**Figure 11B**). Our reporter transgenics do not distinguish between activation of the classical and alternative NF-□B pathways. Therefore, we completed western blot analyses to detect p52/p100 expression (alternative pathway) and translocation of p65 to the nucleus (classical pathway) (**Figure 11C + D**). These data provided an intriguing hint about the roles of the two pathways in mammary tumor development. Activation of the alternative signaling pathway occurs via processing of the p100 protein to the shorter p52 form. This pathway is active in both control and PyVT mammary tissue at 4 weeks. We believe that this represents activation of a pathway that is important for normal ductal development. However, signaling via the alternative pathway appears to shut down in control animals but be maintained in PyVT mice at 7 weeks. This may indicate that part of the mechanism by which the PyVT induces tumor formation is by maintaining a normal developmental signal, extended into an inappropriate period. Elevated activation of the classical pathway has been associated with breast tumors and cell lines. Thus the activation of this pathway in tissue

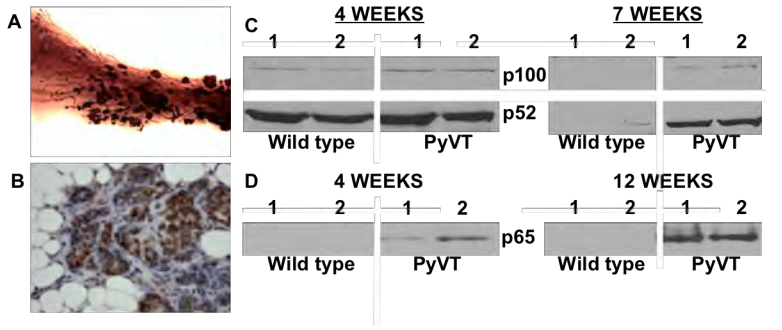

Figure 11 A. Mammary gland whole mount from 7 week old PyVT transgenic. **B**. Immunohistochemistry for GFP in mammary section from 7 week old PyVT/NGL transgenic. **C.** Western blot for p100 and p52 in mammary gland whole cell extract from wild type and PyVT. **D.** Western blot for p65 in mammary gland nuclear extracts from wild type and PyVT.

samples that bear developing mammary tumors was somewhat expected. Interestingly, activation of this pathway was not detected in control tissues.

In order to optimize production of DNFM and IKFM inducible double transgenics, we have generated homozygous forms of the IKK, DN and MRP transgenics. As time and resources were limited during our final no cost extension year we have not been able to generate the originally proposed triple PyVT/IKFM and PyVT/DNFM transgenics to study primary tumor development and metastasis in this model. We decided to adopt a more rapid strategy to at least provide preliminary information on the effects of directly modulating NF-κB signaling within macrophages on metastasis to the lungs. We developed a tail vein metastasis model which we have used in collaborative lung metastasis studies using Lewis Lung Carcinoma (LLC) cells (Stathopoulos et al, 2008; Stathopoulos et al, 2008b). Given our interest in the potential for NF-κB within macrophages to impact metastasis we chose to clodronate treat experimental mice during the process of metastasis to the lung thus depleting macrophages. The data confirmed that resident lung macrophages are crucial contributors to the ability of introduced tumor cells to produce metastatic tumors in the lung (Stathopoulos et al, 2008b).
In order to begin to address the impact of altered NF-κB signaling in macrophages during mammary tumor metastasis to the lungs we have adopted a tail vein metastasis assay using mammary tumor cell lines derived from PyVT mice. We have three different cell lines that we are employing. The first is derived from a single PyVT transgenic and is termed PyVT. This cell line is aggressive and results in visible lung metastases 2 weeks after tail vein injection. We have also derived two lines from double transgenic PyVT plus NGL reporter mice. Our intention was to incorporate the NGL reporter of NF-κB activity in these cell lines. These lines are termed PYG 129 and PYG 134. We have confirmed that they both activate NF-κB signaling in response to TNF-α treatment and that this response can be measured by luciferase assay. The PYG 129 and PYG 134 lines appear to be less aggressive than the PyVT (non-reporter) line and it requires 5 weeks post tail vein injection in order for visible lung metastases to be detectable. Double transgenic IKFM and control mice were placed on 2g/l doxycycline. After 1 week PyVT 1 x 10^6 cells were introduced via tail vein injection and doxycycline treatment continued until lungs were harvested 2 weeks later (**Figure 12**). We were predicting that increased NF-κB activity within the macrophages would be supportive of developing lung metastases. However, the data suggests the opposite. We have also completed an experiment following an identical strategy using the PYG 129 cell line. In this study 9 control mice had no tumors at 5 weeks. 3 out of 7 IKFM double transgenics had tumors (5, 2 and 1; average 1.14). While the numbers of lung metastases are low and we clearly need to optimize the study, it is intriguing to note that this preliminary data is following a trend in agreement with our initial hypothesis. This suggests that the outcome in terms of metastasis is highly dependent on the tumor cell line and we intend to attempt to determine the critical differences between cell lines in future studies. Our preliminary studies have induced NF-κB activity prior to introduction of the metastatic cells. We also intend to address the question of the effects of modulation after the initial implantation stage.

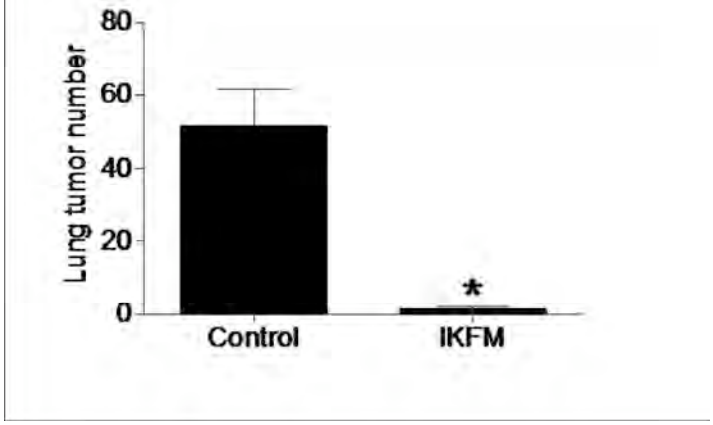

Figure 12. IKFM mice were treated with doxycycline for 1 week then 1 million PyVT cells (mammary tumor cell line isolated from PyVT mice) were injected via the tail vein. Doxycycline treatement was continued for an additional 2 weeks and lungs were harvested and inflated to count tumors (control n=11, IKFM n=8, * $p < 0.0005$).

Clearly there remain many interesting questions that it will be important to address in future studies.

KEY RESEARCH ACCOMPLISHMENTS

1) Results obtained using our fetal liver reconstitution strategy using I□B□ deficient cells and controls suggest that cells of the hematopoetic lineage (including macrophages) play a significant role in development of the mammary ductal epithelium. Our data suggest that contrary to our initial hypothesis, increased NF-□B activity in cells of the hematopoetic lineage may inhibit post-natal mammary ductal development.
2) Our data suggests that in I□B□ +/- mice, constitutive NF-kappaB activity may increase macrophage presence during pregnancy.
3) In collaboration with the group of Dr. Timothy Blackwell, we have generated a novel GFP/luciferase transgenic reporter of *in vivo* NF-kappaB activity that we can use to obtain information concerning NF-kappaB activity at the resolution of single cells on tissue sections. These transgenics have now been fully characterized and have led to a collaborative publication.
4) We have generated immortalized macrophage cell lines from I□B-□ -/- and wild type mice. We have characterized the behavior of the cell lines that have constitutive NF-□B activity and identified effects on cellular proliferation, expression of downstream target genes and the ability of these cells to influence behavior of adjacent epithelial cells.
5) In collaboration with the group of Dr. Timothy Blackwell, we have generated transgenics in which either the dominant inhibitor or a constitutive activator of NF-□B is under the control of an inducible promoter and confirmed that they are functional. These transgenics have now been fully characterized, have been used in published collaborative studies.
6) We have obtained macrophage targeted rtTA transgenic mice from the laboratory of Professor M. Ostrowski, Ohio State University, crossed with our inducible activator and inhibitor transgenics and confirmed inducible expression of both transgenes. Our initial data suggests that activation of NF-□B within macrophages inhibits post-natal mammary ductal development.
7) We have established a colony of PyVT transgenics and established double PyVT/NGL transgenics. Using these mice we have been able to begin to characterize the patterns of NF-□B signaling during mammary tumor development in this model.
8) Our initial studies introducing mammary tumor cell lines via tail vein injection suggest that altered NF-□B signaling within macrophages can significantly affect metastasis to the lung but that the final outcome may be highly cell line dependent.

REPORTABLE OUTCOMES

Publications

In vivo reporter of NF-kappaB activity transgenics. Everhart MB, Han W, Sherrill TP, Arutiunov M, Polosukhin VV, Burke JR, Sadikot RT, Christman JW, Yull FE, Blackwell TS. (2006) Duration and intensity of NF-kappaB activity determine the severity of endotoxin-induced acute lung injury. J Immunol. 176:4995-5005.

Airway epithelium controls development of acute lung injury through the NF-□B pathway (2007). Cheng, D-S.C., Han, W., Chen, S., Sherrill, T.P., Chont, M., Park, G-Y., Sheller, J.R., Polosukhin, V.V., Christman, J.W., Yull, F.E., and Blackwell, T.S. J Immunology 178:6504-13 (the last two authors contributed equally).

Stathopoulos, G.T., Sherrill, T.P., Han, W., Sadikot, R.T., Yull, F.E., Blackwell, T.S., Fingleton, B. (2008) Host nuclear factor kappaB activation potentiates lung cancer metastasis. Molecular Cancer Research 6:364-71.

Meeting abstracts

Sherrill, T., Robinson-Benion, C., Arutiunov, M., Cheng, D-S., Blackwell T. and Yull, F. The role of NF-kappaB signaling in macrophages on mammary development and neoplasia. June 2005. Era of Hope DOD Breast Cancer Research Meeting

Connelly, L., Saint-Jean. L., Cheng, D-S, Han, W., Zabuawala, T., Chodosh, L., Ostrowski, M., Blackwell, T., Yull, F. NF-kappaB signaling in specific cell types plays significant roles in mammary development. Beatson International Cancer Conference, June 2006 Glasgow Scotland

Connelly, L., Saint-Jean, L., Sherrill, T., Newsome, A., Pigg, R., Cheng, D., Han, W., Zabuawala, T., Ostrowski, M., Blackwell, T., Yull, F. Modulation of NF-kappaB in the macrophage lineage: effects on mammary development and tumorigenesis Era of Hope Meeting June 2008 Baltimore

The mouse models that we generated in the process of these studies represent important tools for ongoing research. In particular, we have proposed the use of inducible transgenics targeted to macrophages in several recent grant applications;

"NF-kappaB activity in macrophages is a critical determinant of the metastatic potential of breast tumor cells" DOD Breast Cancer Program – Concept Award (applied 2008 – not funded)

"The NF-kappaB alternative pathway (p100/p52) regulates COX-2 expression and contributes to mammary tumorigenesis" DOD Breast Cancer Program - IDEA award (applied 2007 – not funded; 2008 application pending)

"NF-kappaB activity in macrophages determines impact on mammary tumor development and metastasis" Susan G Komen Foundation – Investigator Initiated Proposal (applied 2007 – not funded; 2008 pre-application pending)

"PTSD and lung cancer: NF-kappaB signaling as a critical link" VA Merit award (applied twice in 2007 – not funded; resubmission pending).

Dr. Jaikun Wang was supported for a brief period on this grant prior to acceptance into Meharry Medical School.

Dr. Linda Connelly has developed a strong interest in breast cancer research whilst working on this project and has started to apply for independent funding.

CONCLUSIONS

In summary, we have utilized our I□B-□ -/- in both *in vivo* studies and, after the generation of novel macrophage cells lines, for *in vitro* studies which suggest that altered NF-□B activity within macrophages can have significant effects on normal mammary development. We have established transgenics that are effective tools for measuring NF-□B responses both *in vitro* and *in vivo*. After initial difficulties we have finally succeeded in generating a new modular transgenic system that enables us to inducibly activate or inhibit NF-□B activity within macrophages. Our initial metastasis studies have produced intriguing data. Given the recent report by Hagemann et al, 2008, of results from studies in ovarian cancer in which they propose that NF-□B is important for maintaining the immunosuppressive phenotype of tumor-associated macrophages we believe that we are "on the right track". We are optimistic that obtaining additional funding will make it possible for us to

extend our investigations into the question of whether manipulation of NF-□B activity in the macrophage lineage could be used as a novel therapeutic approach.

PERSONNEL

Personnel receiving salary support during the funding period:

Fiona Yull – Principal Investigator
Linda Connelly – Postdoctoral fellow/Research Instructor
Jiakun Wang – Postdoctoral fellow
Cheryl Robinson-Benion – Research Assistant
Melissa Arutinov (married and now named Melissa Chont) – Research Assistant

REFERENCES

Beg, A.A., Sha, W.C., Bronson, R.T., Baltimore, D. (1995) Constitutive NF-kappa B activation, enhanced granulopoiesis, and neonatal lethality in I kappa B alpha-deficient mice. *Genes Dev*. 9:2736-46.

Bond, M., Fabunmi, R. P., Baker, A. H., and Newby, A. C. (1998) Synergistic upregulation of metalloproteinase-9 by growth factors and inflammatory cytokines: an absolute requirement for transcription factor NF-kappa B. *FEBS Lett* 435: 29-34.

Burnett, S.H., Kershen, E.J., Zhang, J., Zeng, L., Straley, S.C., Kaplan, A.M., Cohen, D.A. (2004) Conditional macrophage ablation in transgenic mice expressing a Fas-based suicide gene. *J Leukoc Biol.* 75:612-23.

Chen, C-L., Yull, F.E., Kerr, L.D. (1999) Differential serine phosphorylation regulates IkB-a inactivation. *Biochem. Biophys. Res. Comm*. 257, 798-806.

Chen, C-L., Singh, N., Yull, F.E., Strayhorrn, D., Van Kaer, L., Kerr, L.D. (2000). Lymphocytes lacking I□B-□ develop normally, but have selective defects in proliferation and function. *Journal of Immunology* 165: 5418-5427.

Chen, C-L., Yull, F.E., Cardwell, N., Nanney, L., Kerr, L.D. (2000b) RAG2-/-, I□B-□-/- chimeras display a psoriasis-like skin disease. *Journal of Investigative Dermatology*, 115: 1124-1133.

Connelly, L., Robinson-Benion, C., Chont, M., Saint-Jean, L., Li, H., Polosukhin, V.V., Blackwell, T.S., Yull, F.E. (2007) A transgenic model reveals important roles for the NF-kappaB alternative pathway (p100/p52) in mammary development and links to tumorigenesis. *J Biol Chem.* 282: 10028-35.

DeKoter, R.P., Singh, H. (2000). Regulation of B lymphocyte and macrophage development by graded expression of PU.1. *Science.* 288: 1439-41.

Eichbaum, Q., Heney, D., Raveh, D., Chung, M., Davidson, M., Epstin, J., Ezekowitz, A.B. (1997) Murine macrophage mannose receptor promoter is regulated by the transcription factors PU.1 and SP1. Blood 90: 4135-143.

Egeblad, M., and Werb, Z. (2002) New functions for the matrix metalloproteinases in cancer progression. *Nat Rev Cancer* 2, 161-174.

Everhart, M.B., Han, W., Parman, K.S., Polosukhin, VV., Zeng, H., Sadikot, R.T., Li, B., Yull, F.E., Christman, J.W., Blackwell, T.S. (2005) Intratracheal administration of liposomal clodronate accelerates alveolar macrophage reconstitution following fetal liver transplantation. *J Leukoc Biol.* 77:173-80.

Everhart, M.B., Han, W., Sherrill, T.P., Arutiunov, M., Polosukhin, V.V., Burke, J.R., Sadikot, R.T., Christman, J.W., Yull, F.E., Blackwell, T.S. (2006) Duration and Intensity of NF-{kappa}B Activity Determine the Severity of Endotoxin-Induced Acute Lung Injury. J Immunol. 176:4995-5005.

Hagemann, T., Lawrence, T., McNeish, I., Charles, K.A., Kulbe, H., Thompson, R.G., Robinson, S.C., Balkwill, F.R. (2008) “Re-educating" tumor-associated macrophages by targeting NF-kappaB. *J Exp Med* 205:1261-1268.

Heppner, K. J., Matrisian, L. M., Jensen, R. A., and Rodgers, W. H. (1996) Expression of most matrix metalloproteinase family members in breast cancer represents a tumor-induced host response. *Am J Pathol* 149, 273-282.
Klement, J.F., Rice, N.R., Car, B.D., Abbondanzo, S.J., Powers, G.D., Bhatt, P.H., Chen, C.H., Rosen, C.A., Perl, A.K., Tichelaar, J.W., Whitsett, J.A. (2002) Conditional gene expression in the respiratory epithelium of the mouse. *Transgenic Research*. 11:21-9.
Sadikot, R.T., Zeng, H., Joo, M., Everhart, M.B., Sherrill, T.P., Li, B., Cheng, D.S., Yull, F.E., Christman, J.W., Blackwell, T.S. (2006) Targeted Immunomodulation of the NF-{kappa}B Pathway in Airway Epithelium Impacts Host Defense against Pseudomonas aeruginosa. *J Immunol*. 176:4923-30.
Sasmono, R.T., Oceandy, D., Pollard, J.W., Tong, W., Pavli, P., Wainwright, B.J., Ostrowski, M.C., Himes, S.R., Hume, D.A. (2003) A macrophage colony-stimulating factor receptor-green fluorescent protein transgene is expressed throughout the mononuclear phagocyte system of the mouse. *Blood* 101:1155-63.
Simian, M., Hirai, Y., Navre, M., Werb, Z., Lochter, A., and Bissell, M. J. (2001) The interplay of matrix metalloproteinases, morphogens and growth factors is necessary for branching of mammary epithelial cells. *Development* 128, 3117-3131.
Stathopoulos, G.T., Sherrill, T.P., Han, W., Sadikot, R.T., Polosukhin, V.V., Fingleton, B., Yull, F.E., Blackwell, T.S. (2008) Use of bioluminescent imaging to investigate the role of nuclear factor-kappaB in experimental non-small cell lung cancer metastasis. *Clin and Exp Metastasis* 25:43-51.
Stathopoulos, G.T., Sherrill, T.P., Han, W., Sadikot, R.T., Yull, F.E., Blackwell, T.S., Fingleton, B. (2008) Host nuclear factor kappaB activation potentiates lung cancer metastasis. *Molecular Cancer Research* 6:364-71.
Witty, J. P., Wright, J. H., and Matrisian, L. M. (1995) Matrix metalloproteinases are expressed during ductal and alveolar mammary morphogenesis, and misregulation of stromelysin-1 in transgenic mice induces unscheduled alveolar development. *Mol Biol Cell* 6: 1287-1303.

APPENDICES

Everhart MB, Han W, Sherrill TP, Arutiunov M, Polosukhin VV, Burke JR, Sadikot RT, Christman JW, Yull FE, Blackwell TS. (2006) Duration and intensity of NF-kappaB activity determine the severity of endotoxin-induced acute lung injury. *J Immunol.* **176**:4995-5005.

Cheng, D-S.C., Han, W., Chen, S., Sherrill, T.P., Chont, M., Park, G-Y., Sheller, J.R., Polosukhin, V.V., Christman, J.W., Yull, F.E., and Blackwell, T.S. (2007) Airway epithelium controls development of acute lung injury through the NF-□B pathway. *J Immunology* **178**:6504-13 (note that last two authors contributed equally to the publication).

Stathopoulos, G.T., Sherrill, T.P., Han, W., Sadikot, R.T., Yull, F.E., Blackwell, T.S., Fingleton, B. (2008) Host nuclear factor kappaB activation potentiates lung cancer metastasis. *Molecular Cancer Research* **6**:364-71.

Duration and Intensity of NF-κB Activity Determine the Severity of Endotoxin-Induced Acute Lung Injury[1]

M. Brett Everhart,[2]* Wei Han,[2†] Taylor P. Sherrill,[†] Melissa Arutiunov,[‡] Vasiliy V. Polosukhin,[†] James R. Burke,[‖] Ruxana T. Sadikot,[†§] John W. Christman,[¶] Fiona E. Yull,[‡] and Timothy S. Blackwell[3]*[†‡§]

Activation of innate immunity in the lungs can lead to a self-limited inflammatory response or progress to severe lung injury. We investigated whether specific parameters of NF-κB pathway activation determine the outcome of acute lung inflammation using a novel line of transgenic reporter mice. Following a single i.p. injection of *Escherichia coli* LPS, transient NF-κB activation was identified in a variety of lung cell types, and neutrophilic inflammation resolved without substantial tissue injury. However, administration of LPS over 24 h by osmotic pump (LPS pump) implanted into the peritoneum resulted in sustained, widespread NF-κB activation and neutrophilic inflammation that culminated in lung injury at 48 h. To determine whether intervention in the NF-κB pathway could prevent progression to lung injury in the LPS pump model, we administered a specific IκB kinase inhibitor (BMS-345541) to down-regulate NF-κB activation following the onset of inflammation. Treatment with BMS-345541 beginning at 20 h after osmotic pump implantation reduced lung NF-κB activation, concentration of KC and MIP-2 in lung lavage, neutrophil influx, and lung edema measured at 48 h. Therefore, sustained NF-κB activation correlates with severity of lung injury, and interdiction in the NF-κB pathway is beneficial even after the onset of lung inflammation. *The Journal of Immunology,* **2006, 176: 4995–5005.**

Although inflammation generated through activation of innate immune pathways is critical for effective host responses to infection, dysregulated inflammation can contribute to tissue injury, thereby preventing recovery of the organism. The factors that govern whether an inflammatory response is adaptive or maladaptive (leading to injury) are not well understood and may vary depending on the initiating stimulus. The NF-κB pathway, which regulates transcription of a variety of proinflammatory mediators, is involved in generation of neutrophilic lung inflammation; however, it is unknown whether specific parameters of NF-κB activation determine whether lung inflammation resolves or progresses to lung injury. Elucidating the relationships between NF-κB activation, lung inflammation, and lung injury could provide important insights into the pathobiology of a variety of human lung diseases, including the acute respiratory distress syndrome (ARDS).[4]

In the lungs, many noxious/inflammatory stimuli have been shown to activate NF-κB, implicating the NF-κB pathway as a focal point for induction of lung inflammation. In vivo activators of NF-κB in the lungs include intact bacteria, Gram-negative bacterial LPS, ozone, and silica delivered directly to the airways, as well as systemic inflammatory insults such as sepsis, hemorrhage, and direct liver injury (1–10). In rodent models of lung inflammation induced by LPS, pretreatment with relatively nonspecific inhibitors of NF-κB activation has been found to diminish lung inflammation (11–13). Additionally, mice deficient in RelA (the transactivating subunit of NF-κB) and TNFR type 1 have impaired neutrophil recruitment to the lungs in response to LPS compared with wild-type controls and TNFR1-deficient mice (14). Together, these studies indicate that NF-κB plays an important role in initiation of inflammatory signaling in the lungs in response to LPS, a prototypical inflammatory stimulus. After establishment of an inflammatory response, however, it has been suggested that NF-κB has a role in resolution of inflammation through antiapoptotic effects and expression of proteins that function to limit inflammation (15). The importance of NF-κB in regulating ongoing lung inflammation or progression to lung injury is unknown.

We hypothesized that specific parameters of NF-κB activation in the lungs, including cellular distribution, intensity, and/or duration of NF-κB activity, determine whether lung inflammation is self-limited or progresses to injury. Further, we proposed that focused intervention to inhibit NF-κB activity could limit lung injury and convert an injurious stimulus to a phenotype of transient inflammation that resolves without significant tissue injury. To investigate this hypothesis, we generated novel transgenic NF-κB reporter mice to allow cell-specific detection of NF-κB activity.

*Department of Cell and Developmental Biology, †Department of Medicine, Division of Allergy, Pulmonary, and Critical Care Medicine, ‡Department of Cancer Biology, Vanderbilt University School of Medicine, and §Department of Veterans Affairs, Nashville, TN 37232; ¶Section of Pulmonary, Critical Care, and Sleep Medicine, University of Illinois, Chicago, IL 60612; and ‖Department of Immunology, Inflammation, and Pulmonary Drug Discovery, Bristol-Myers Squibb Pharmaceutical Research Institute, Princeton, NJ 08543

Received for publication September 19, 2005. Accepted for publication February 2, 2006.

The costs of publication of this article were defrayed in part by the payment of page charges. This article must therefore be hereby marked *advertisement* in accordance with 18 U.S.C. Section 1734 solely to indicate this fact.

[1] This work is supported by Grants HL61419 and HL66196 from the National Institutes of Health, by the U.S. Department of Veterans Affairs, Vanderbilt Ingram Cancer Center, by Grant BCTR02-1728 from the Susan G. Komen Foundation, and by Grant WX1XWH-04-1-0456 from the U.S. Department of Defense Breast Cancer Program.

[2] M.B.E. and W.H. contributed equally to this work.

[3] Address correspondence and reprint requests to Dr. Timothy S. Blackwell, Division of Allergy, Pulmonary, and Critical Care Medicine, T-1218 Medical Center North, Vanderbilt University Medical Center, Nashville, TN 37232-2650. E-mail address: timothy.blackwell@vanderbilt.edu

[4] Abbreviations used in this paper: ARDS, acute respiratory distress syndrome; IKK, IκB kinase; BAL, bronchoalveolar lavage; RLU, relative light unit.

0022-1767/06/$02.00

We determined parameters of NF-κB activation in a mouse model of transient lung inflammation following i.p. injection of *Escherichia coli* LPS and a model of lung inflammation and injury following prolonged delivery of LPS via an osmotic pump implanted into the peritoneum. We then intervened using a selective inhibitor of IκB kinase (IKK) to down-regulate NF-κB activation during a period in which we identified differential NF-κB activation between the two models. Information from these studies provides evidence that inhibition of the NF-κB pathway in vivo can ablate lung injury and identifies NF-κB as a critical target for limiting ongoing, maladaptive inflammation in the lungs.

Materials and Methods

Animal models

Transgenic NF-κB reporter mice were generated that contain four tandem copies of a 36-base enhancer from the 5′ HIV-long terminal repeat (containing two NF-κB binding sites, GGGACTTTCC) placed upstream of the HSV minimal thymidine kinase promoter. This enhancer-promoter construct was cloned into pEGFPluc (BD Clontech) for expression of an enhanced GFP-luciferase fusion protein. The 8xNF-κB-GFP-luciferase construct was excised and purified using a GELase Agarose Gel-Digesting preparation kit following the manufacturer's instruction (Epicentre Technologies). This construct was then injected at the Vanderbilt Transgenic/ES Cell Shared Resource to generate NGL (NF-κB-GFP-luciferase construct) transgenic mouse lines on C57B6/DBA background. Founder animals were genotyped by Southern blot and then further generations were genotyped by PCR analysis for increased efficiency.

Male and female NGL transgenic mice weighing between 20 and 25 g were used for these studies. *E. coli* LPS (serotype O55:B5) was obtained from Sigma-Aldrich. LPS was delivered by a single i.p. injection of 3 μg/g body weight (1 μg/μl solution in sterile PBS). For prolonged delivery of LPS, an osmotic pump (2001D Alzet pump; ALZA) was filled with LPS solution (1 μg/μl in PBS) and surgically implanted in the peritoneal cavity using sterile technique. The pump delivered 8 μg LPS (8 μl) per hour for 24 h. A priming dose of 3 μg of LPS/g body weight was injected i.p. following pump implantation.

A selective inhibitor of IKK, BMS-345541, was obtained from Bristol-Myers Squibb. The compound was formulated as a 7.5 mg/ml solution in 3% Tween 80 and sterile water. Body weight (75 μg/g) of this solution or an equivalent volume of vehicle (without BMS-345541) was administered by peroral gavage after anesthesia with inhaled isoflurane.

Neutrophil depletion was performed as previously reported (16). Undiluted rabbit antineutrophil Abs (200 μl; Accurate Chemical and Scientific) or control rabbit IgG (1 μg/μl; Sigma-Aldrich) were administered by i.p. injection daily for 2 days. On days 3 and 4, 300 μl of a 1/15 dilution of Ab preparations (in 1× PBS) were injected i.p. On day 5, peripheral white blood cell counts and differentials were measured to verify neutrophil depletion.

The experimental protocol was reviewed and approved by the Institutional Animal Care and Use Committee at Vanderbilt University (Nashville, TN).

Bioluminescence imaging and photon count quantification

Mice were anesthetized and shaved over the chest before imaging. Luciferin (1 mg/mouse in 100 μl isotonic saline) was administered by i.v. injection and mice were imaged with an intensified charge-coupled device (ICCD) camera (IVIS 200; Xenogen). For the duration of photon counting, mice were placed inside a light tight box that housed the camera. Light emission from the mouse was detected as photon counts by the ICCD camera and customized with image processing hardware and software (Living Image software; Xenogen). The imaging duration (30 s) was selected to avoid saturation of the camera during image acquisition. Quantitative analysis was performed by defining a standard area over the mid-lung zone and determining the total integrated photon intensity over the area of interest. For presentation, a digital false-color photon emission image was generated for each captured image.

Bone marrow-derived macrophage experiments

Bone marrow-derived macrophages were generated from NGL mice as previously described (17). Adenoviral vectors expressing a dominant inhibitor of NF-κB (IκBdn), which represents a S36-40A mutant of the avian IκB-α that cannot be phosphorylated or degraded, and β-galactosidase have been previously reported (10, 18). Cells were treated with adenoviral vectors (multiplicity of infection = 300) 48 h before LPS treatment. LPS was added to cultures (200 ng/ml) and cells were harvested 4 h later. In separate experiments, cells were treated with BMS-345541 (20 μM) 30 min before LPS.

Histology and immunohistochemistry

After euthanasia, lungs were inflated with 1 ml of 10% neutral buffered formalin. Lungs were then removed en bloc after tracheal ligation and preserved in 10% neutral buffered formalin for 24 h at 4°C, and subsequently embedded in paraffin. Lung tissue sections (5 μm) were prepared in the Mouse Pathology Core Facility (Vanderbilt University). H&E stains were performed using standard protocol. For GFP immunohistochemistry, 5-μm sections were cut and placed on charged slides. Following paraffin removal, sections were rehydrated and placed in heated Target Retrieval Solution (high pH; (DakoCytomation) for 20 min. Tissues were incubated with rabbit anti-GFP 1/200 (BD Clontech) for 30 min. Sections without primary Ab served as negative controls. The Vectastain ABC Elite System (Vector Laboratories) and diaminobenzidine (DAB^+; DakoCytomation) were used to produce localized, visible staining. Slides then were lightly counterstained with Mayer's hematoxylin, dehydrated, and coverslipped.

Measurement of neutrophil influx

For tissue neutrophil quantification, H&E-stained lung tissue sections were used to count the number of neutrophils per high power field. For each slide, neutrophils were counted in a blinded fashion on 10 sequential, non-overlapping high power fields (magnification, ×400) of lung parenchyma beginning at the periphery of the section. Three separate H&E-stained sections were evaluated per mouse, and the mean number of neutrophils per high power field was reported.

Lung lavage neutrophil counts

For bronchoalveolar lavage (BAL) neutrophil quantification, BAL cells were collected after lavage with 3 aliquots of 1 ml of sterile PBS. BAL was combined and centrifuged at 400 × *g* for 10 min to separate cells from supernatant. Supernatant was saved separately and frozen at −70°C. The cell pellet was suspended in PBS with 1% BSA, and total cell counts were determined on a grid hemocytometer. Differential cell counts were determined by staining cytocentrifuge slides with a modified Wright stain (Diff-Quick; Baxter Scientific Products) and counting 200–300 cells in complete cross-section.

Tissue luciferase assay

Lungs were removed en bloc and homogenized in 1 ml of lysis buffer (Promega) using a dounce homogenizer. After pulse centrifugation, luciferase activity was measured in a Monolight 3010 Luminometer (Analytical Luminescence Laboratory) after adding 100 μl of freshly reconstituted luciferase assay buffer to 20 μl of lung tissue homogenate. Results were expressed as relative light units (RLU) normalized for protein content, which was measured by Bradford assay (Bio-Rad).

Western blots

One hundred micrograms of protein from lung tissue homogenates were separated on a 10% acrylamide gel, transblotted, and immunodetected using phosphospecific Abs to an epitope of IKK1 containing phosphorylated serine 176 and serine 180 (BioSource International). The blots were also probed with Abs to MAPK p44 and p42 (Cell Signaling Technology), then stripped and reprobed for total IKK1 (Santa Cruz Biotechnology).

Lung wet to dry ratio

Lungs were removed and the wet weight recorded. Lungs were then placed in an incubator at 65°C for 48 h and the dry weight was determined.

MIP-2 and KC quantification

MIP-2 and KC levels in BAL fluid were measured using a specific ELISA according to manufacturer's instructions (R&D Systems).

Statistical analysis

To assess differences among groups, analyses were performed with GraphPad Instat software using an unpaired *t* test or one-way ANOVA. Results are presented as the mean ± SEM. Two-tailed values of $p < 0.05$ were considered significant.

Results

Construction of reporter mice to identify cell-specific NF-κB activation

After testing a variety of NF-κB-driven promoter constructs, we determined that basal expression and inducibility characteristics were optimal with a construct that contained four tandem copies of a 36-base enhancer from the 5′ HIV-long terminal repeat (containing two NF-κB binding sites, GGGACTTTCC). This NF-κB-dependent promoter was placed upstream of GFP-luciferase expression cassette, and the construct was tested in vitro using multiple cell lines (A549, RAW 267.4, NIH-3T3, HeLa) to ensure reliable expression in a wide range of cell types (data not shown). Subsequently, the NF-κB reporter construct was excised, purified, and microinjected at the Vanderbilt Transgenic/ES Cell Shared Resource to produce transgenic mice (NGL mice).

To investigate regulation of the reporter expression in primary cells, we obtained bone marrow macrophages and treated them in vitro with *E. coli* LPS (200 ng/ml) for 4 h to stimulate NF-κB activation. Adenoviral vectors expressing a transdominant inhibitor of the NF-κB pathway (Ad-IκBdn) (10, 18) were used to specifically block NF-κB activation in these cells. Cells were infected with adenoviral vectors 48 h before experimentation. Expression of the GFP-luciferase reporter was determined by luciferase assays and fluorescence microscopy (Fig. 1, *A* and *B*). By luciferase assay, no difference in reporter activity was detected between untreated and Ad-IκBdn-treated macrophages (1015.2 ± 67.2 vs 1257.3 ± 174.17 RLU, respectively). Compared with untreated and Ad-IκBdn-treated macrophages, LPS stimulation resulted in a significant increase in luciferase activity (5450.0 ± 265.59 RLU, $p < 0.05$); however, infection of cells with Ad-IκBdn before LPS blocked induction of luciferase expression (1841.3 ± 171.1 RLU). Infection of macrophages with control adenoviral vectors did not affect LPS-induced luciferase activity (data not shown). Using fluorescence microscopy to detect GFP expression before cell harvest, we corroborated the results obtained by luciferase assays (Fig. 1*B*). In addition to Ad-IκBdn, we treated macrophages from NGL mice with a specific inhibitor of the NF-κB pathway, BMS-345541 (19) (Fig. 1*C*). In these studies, cells were treated with BMS-345541 (20 μM) or vehicle 30 min before addition of LPS (200 ng/ml) and cells were harvested 4 h later. Similar to IκBdn, BMS-345541 treatment blocked LPS-induced luciferase activity in macrophages. Together, these findings confirm that LPS-induced expression of GFP-luciferase reflects NF-κB activation in NGL cells.

We performed additional studies to determine the half-life of the GFP-luciferase fusion protein in bone marrow-derived NGL macrophages. At 3 h after LPS treatment, cycloheximide (20 μg/ml) was added to cell cultures to block protein synthesis, and luciferase measurements were obtained every 30 min until return to baseline. In these studies, the half-life of the GFP-luciferase fusion protein was determined to be 2.5 h, making it suitable as a reporter of NF-κB transcriptional activity.

Cellular distribution, intensity, and duration of NF-κB activation in LPS-induced lung inflammation and injury

To model transient neutrophilic lung inflammation, a single dose of *E. coli* LPS (3 μg/g) was administered to NGL mice by i.p. injection (IP LPS treatment). Because established models of LPS-induced lung inflammation in mice do not produce consistent lung injury (20), we developed a model of LPS delivery into the peritoneal cavity over 24 h that produces severe lung inflammation and injury (Fig. 2*A*). In this model, an osmotic pump delivering *E. coli* LPS at 8 μg/h for 24 h was surgically implanted into the peritoneal

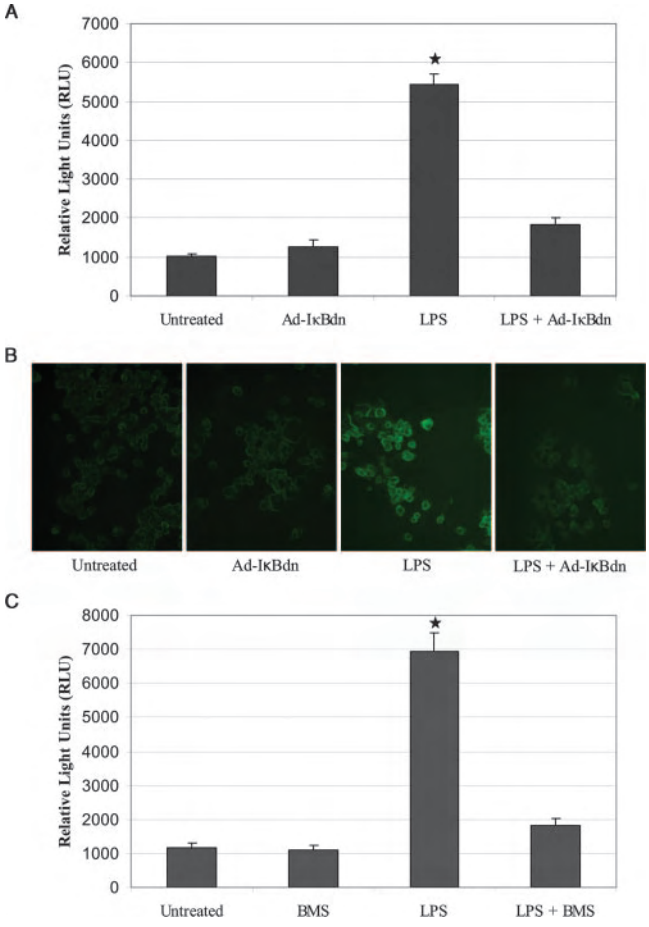

FIGURE 1. NF-κB regulation of the NGL reporter construct in bone marrow-derived macrophages from NGL mice. *A*, Luciferase activity (measured as RLU) from cell homogenates following treatment with LPS (200 ng/ml) for 4 h. Specificity of the reporter for NF-κB was shown by infection with adenoviral vectors expressing a dominant inhibitor of the NF-κB pathway (IκBdn). Cells were infected with adenoviral (multiplicity of infection = 300) 48 h before LPS treatment. Each bar represents the mean RLU ± SEM (for $n = 3$ wells per treatment group) and the experiment was repeated two times (∗, $p < 0.05$ compared with other groups). *B*, Representative fluorescence microscopy images of each treatment group showing GFP fluorescence at the time of harvest. *C*, Luciferase activity from cells treated with NF-κB inhibitor BMS-345541 (20 μM) or vehicle 30 min before LPS and harvested at 4 h. Each bar represents the mean RLU ± SEM (for $n = 3$ wells per treatment group). ∗, $p < 0.05$ vs other groups.

space followed by a priming dose of 3 μg/g LPS by direct i.p. injection (LPS pump treatment). Although single-dose i.p. LPS produced only mild interstitial thickening and cellular infiltrate at 48 h, LPS delivered by osmotic pump caused lung inflammation and injury (edema, interstitial thickening, hemorrhage, and inflammatory cell influx). Persistent lung inflammation in the LPS pump model was confirmed by counting neutrophils on H&E-stained lung tissue sections. Although single-dose IP LPS treatment resulted in a transient influx of neutrophils at 4 h, LPS pump treatment resulted in persistent neutrophil influx through 48 h (Fig. 2*B*). The LPS pump model also resulted in a significant increase in lung edema as assessed by the wet to dry ratio at 48 h (3.81 ± 0.03 in untreated mice vs 4.65 ± 0.04 in the LPS pump group, $p < 0.05$), whereas the lung wet to dry ratio in the IP LPS group was similar to baseline. Delivery of LPS over 24 h into the peritoneum was required to induce this phenotype as treatment with an equal LPS

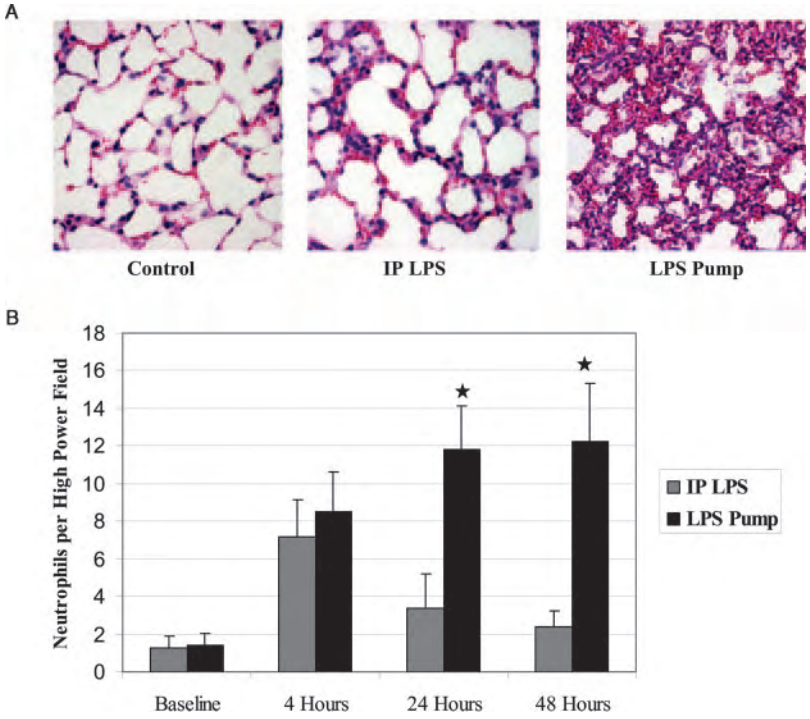

FIGURE 2. A single i.p. injection of LPS (IP LPS treatment) results in transient neutrophilic inflammation, but delivery of LPS by osmotic pump (LPS pump treatment) implanted in the peritoneum leads to persistent neutrophilic lung inflammation and injury. *A*, H&E-stained lung sections from a control NGL mouse and NGL mice harvested 48 h after a single i.p. injection of LPS (IP LPS) or LPS delivered by osmotic pump (LPS Pump). Increased edema, inflammatory cell influx and edema are identified in the LPS pump treatment group. *B*, Quantification of neutrophils per high power field on H&E-stained lung tissue sections. The number of neutrophils per high power field was counted for 10 consecutive, nonoverlapping fields per slide. Each bar represents the mean for each mouse ± SEM (for $n = 6$ mice per group at each time point). ∗, $p < 0.05$ vs IP LPS).

dose by single i.p. injection or implantation of pumps alone did not induce sustained lung inflammation and injury (data not shown).

After establishing these models of transient inflammation without substantial injury and persistent lung inflammation and injury, we investigated whether NF-κB was differentially activated in these models. Expression of the NF-κB-driven reporter in NGL mice was identified by bioluminescence imaging (following i.v. injection of 1 mg of luciferin) to detect luciferase activity in the lungs of intact mice and by immunohistochemistry for detection of GFP in lung sections. Consistent with our previous reports (10, 21), single-dose IP LPS treatment resulted in a transient increase in NF-κB-driven luciferase activity by 4 h. However, by 24 h, photon emission from the lungs returned near baseline, indicating transient NF-κB activation (Fig. 3*A*). In contrast, NGL mice treated with LPS delivered by osmotic pump showed sustained lung luciferase activity at 4, 24, and 48 h. Peak photon emission from the lungs at 4 h did not differ between the two models.

We correlated bioluminescence imaging of luciferase activity in the lungs of NGL mice with cellular localization of NF-κB activity by immunohistochemistry for GFP on lung sections (Fig. 3*B*). At baseline, minimal GFP staining was identified in the lungs. LPS treatment (either IP LPS or LPS pump) resulted in widespread GFP staining in multiple lung cell types at 4 h, including airway epithelium, endothelium, and leukocytes (macrophages and neutrophils). GFP staining was also noted in alveolar epithelium, particularly type II cells. At 24 h after IP LPS treatment, GFP immunoreactivity in the lungs was limited to a few, scattered positive cells, and by 48 h, GFP staining returned to baseline. In the LPS pump model, widespread GFP staining persisted in the lungs through 48 h, consistent with bioluminescence detection of NF-κB driven transgene expression. Together, these studies indicate that endotoxemia induces NF-κB activation in a variety of lung cells. Although the cell-specific pattern of NF-κB activity and peak intensity of lung NF-κB intensity did not differ depending on the method of LPS delivery, prolonged duration of high-level NF-κB activation in the lungs correlated with LPS-induced lung injury.

Early NF-κB inhibition limits neutrophilic lung inflammation whereas late NF-κB inhibition prevents lung injury

To evaluate the role of NF-κB in determining the course of lung inflammation and injury, we used BMS-345541, which is a selective inhibitor of IKK1 and IKK2 (19). In prior studies, BMS-345541 at doses as high as 100 μg/g daily for 6 wk in mice showed no toxicologic changes, either by gross or by histopathologic evaluation, of major organs including the liver (22).

In the IP LPS treatment model, BMS-345541 (75 μg/g) or vehicle was administered to NGL mice by peroral gavage 2 h before injection of LPS and again 4 h after LPS treatment. By bioluminescence imaging, photon emission from the lungs was reduced at 8 h after IP LPS in the group that received BMS-345541 compared with controls treated with vehicle, although no significant difference between the groups was identified at 4 h (Fig. 4, *A* and *B*). At the time of harvest (8 h), luciferase activity in lung homogenates was also significantly reduced in mice treated with BMS-345541 before LPS (1347 ± 51 RLU/μg protein in the BMS-345541 group vs 2089 ± 134 RLU/μg protein in the control vehicle-treated group, $p < 0.05$) (Fig. 4*C*). Neutrophil influx was quantified on lung sections as a measure of lung inflammation. As shown in Fig. 4*D*, a marked reduction in lung neutrophils was identified in lungs treated with BMS-345541 before LPS compared with controls treated with vehicle before LPS. These experiments indicate that treatment with BMS-345541 inhibits lung NF-κB activation and neutrophilic lung inflammation in response to IP LPS treatment.

Based on the differential NF-κB activation that we observed between the IP LPS and LPS pump treatment models, we investigated whether sustained lung NF-κB activation in the LPS pump model mediates lung injury. Therefore, we targeted the late phase of NF-κB activation by beginning BMS-345541 after the establishment of lung inflammation in NGL mice treated with LPS via osmotic pump. Mice were treated with BMS-345541 or vehicle by

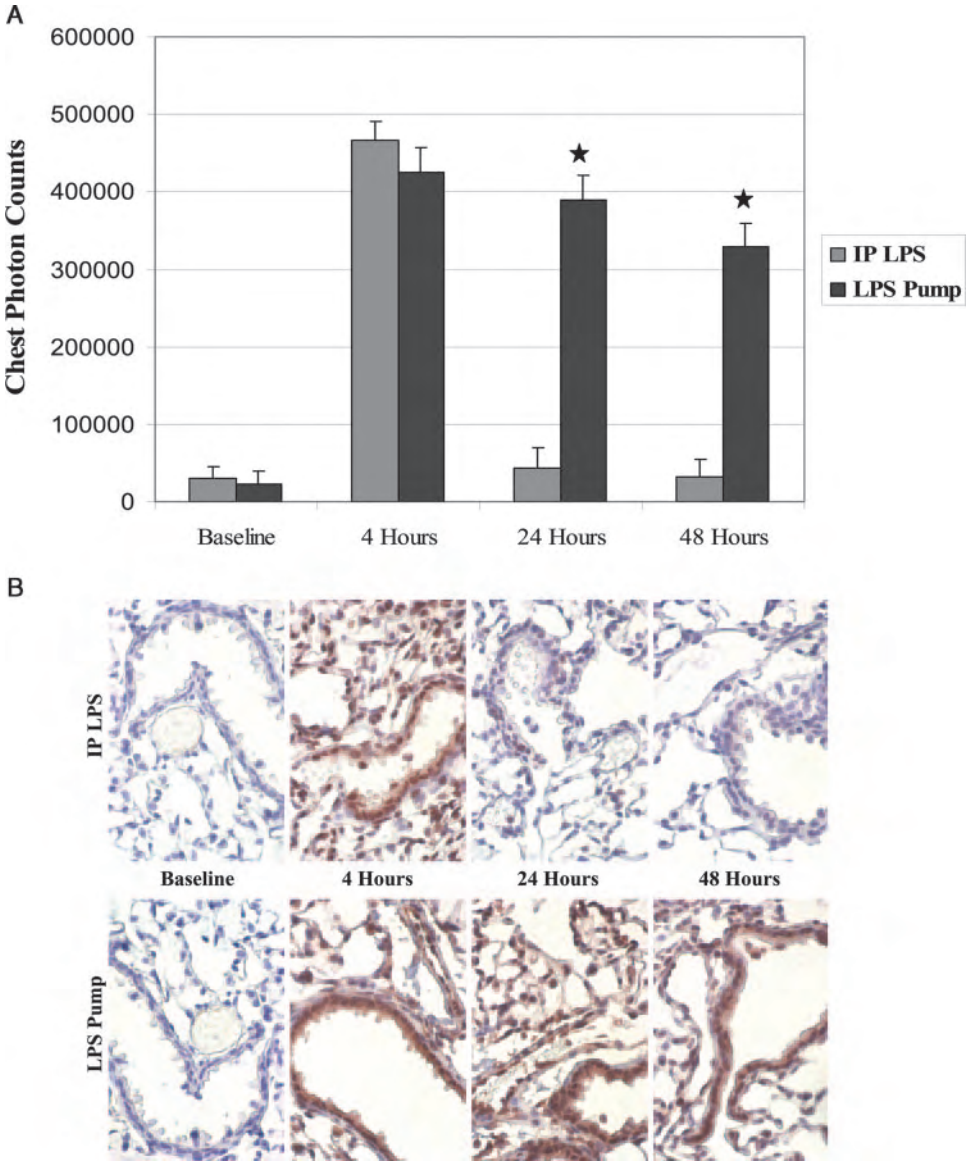

FIGURE 3. Differential NF-κB activation in lungs following a single i.p. dose of LPS (IP LPS) or LPS delivered by osmotic pump (LPS Pump) is identified by reporter gene expression in NGL mice. *A*, Bioluminescence imaging of NGL mice to determine luciferase activity in lungs at baseline, 4, 24, and 48 h after LPS delivered by single i.p. injection or LPS pump. Images were obtained after i.v. injection of 1 mg luciferin and photon detection was quantified over a standard region of the anterior chest corresponding to the mid-lung zones. Each bar represents the mean ± SEM (for $n = 6$ mice per group). ∗, $p < 0.05$ vs IP LPS. *B*, Representative immunohistochemistry for GFP^+ cells in lung sections from NGL mice.

peroral gavage beginning at 20 h after osmotic pump implantation. BMS-345541 dosing was repeated every 4 h for a total of five doses. Multiple doses were used because of the relatively short half-life of the compound in vivo (19). Bioluminescent imaging was performed at baseline, 20, 24, and 48 h after initiation of LPS to evaluate NF-κB-dependent reporter gene expression (Fig. 5, *A* and *B*). In both, vehicle or BMS-345541 treatment groups, similar induction of photon emission from the lungs was observed at 20 h, before intervention. By 24 h, there was a trend toward lower chest bioluminescence in the group treated with BMS-345541, and at 48 h, a marked reduction in photon emission from the lungs was observed in the group treated with BMS-345541 compared with vehicle-treated controls. Treatment with BMS-345541 resulted in ~50% reduction in chest bioluminescence compared with the measurement before treatment (20 h). These findings were confirmed by postmortem measurement of lung tissue luciferase activity. Luciferase activity in BMS-345541 treated mice was 1061 ± 233 RLU/μg protein compared with 2521 ± 462 RLU/μg protein in the vehicle-treated group ($p < 0.05$) (Fig. 5*C*). To show that treatment with BMS-345541 reduces IKK activation in the lungs, we performed Western blot analysis for IKK1 using Abs that specifically identify the phosphorylated (activated) kinase. Fig. 5*D* indicates that IKK1 phosphorylation was reduced in lungs treated with BMS-345541 at 48 h after LPS pump implantation. Therefore, oral delivery of the IKK inhibitor was sufficient to reduce IKK activity and thereby block NF-κB activation in the lungs.

To examine the impact of BMS-345541 therapy on the distribution of cells with active NF-κB, we performed immunostaining for GFP on lung tissue sections from NGL mice (Fig. 6). Interestingly, we found that BMS-345541 treatment broadly diminished GFP staining compared with vehicle-treated controls. Less GFP staining was observed in epithelium, endothelium, and leukocytes at 48 h after LPS pump implantation in BMS-345541-treated mice compared with vehicle-treated mice. By evaluation of H&E-stained lung sections, we observed a dramatic reduction in lung inflammation and injury in mice treated with the IKK inhibitor (Fig. 6). Mice treated with BMS-345541 showed preserved alveolar architecture with minimal edema, septal thickening, and hemorrhage.

To quantify lung inflammation and injury, we measured lung neutrophils, chemokine concentration in BAL fluid, and lung edema at 48 h after implantation of LPS pumps. Lung neutrophil influx was evaluated by counting of neutrophils on H&E lung tissue sections and by quantifying the number of neutrophils in BAL.

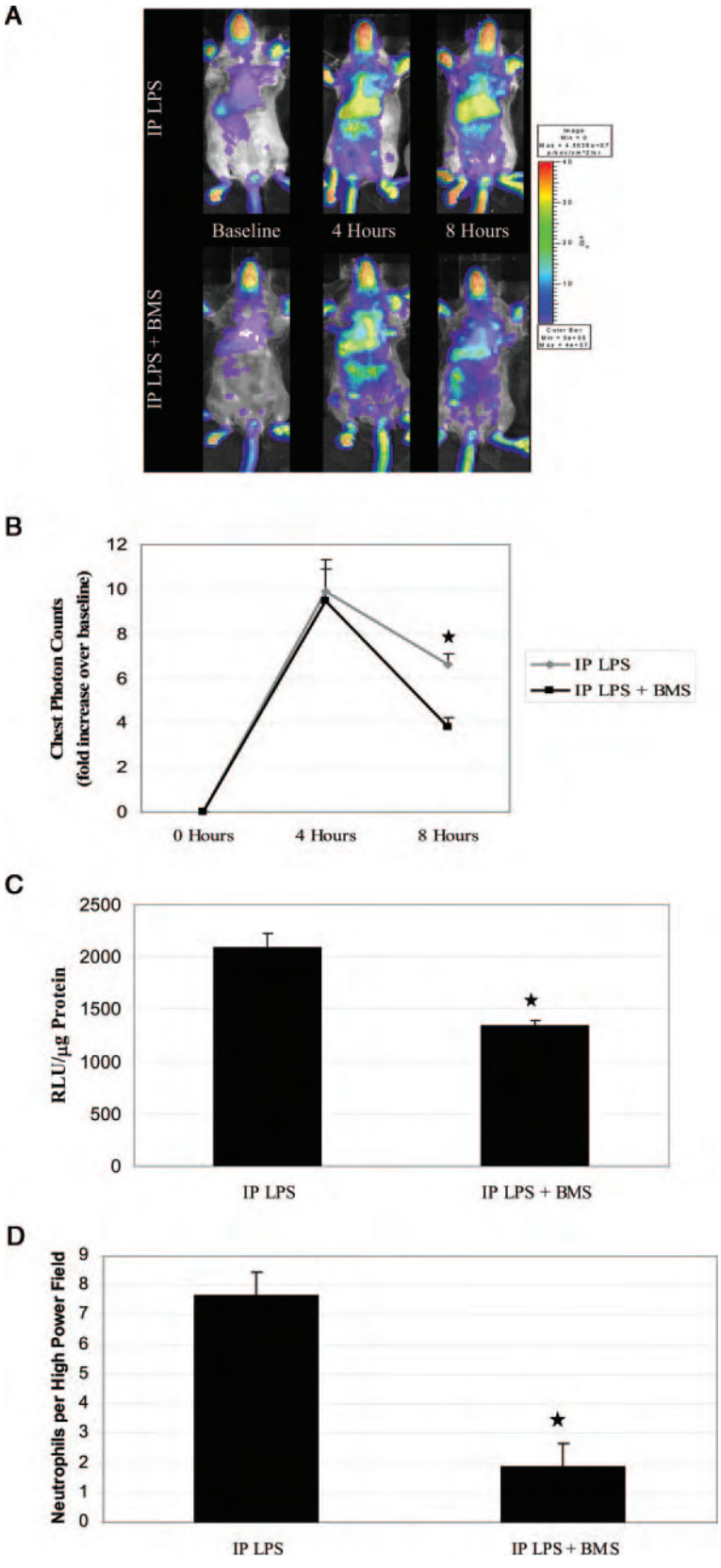

FIGURE 4. Treatment with the specific NF-κB inhibitor BMS-345541 results in decreased NF-κB activity and lung inflammation following a single i.p. dose of LPS. BMS-345541 or vehicle was delivered by gavage (75 μg/g) 2 h before and 4 h after i.p. injection of LPS (3 μg/g). *A*, Representative bioluminescence images of NGL mice obtained before LPS (0 h) and 4 and 8 h after i.p. dose of LPS (IP LPS). *B*, Quantification of chest photon emission from bioluminescence images (fold increase over baseline) (n = 6 mice). ∗, $p < 0.05$ vs IP LPS+BMS group. *C*, Luciferase activity measured in lung tissue homogenates at the time of harvest (RLU/μg protein) for $n = 6$ mice per group. ∗, $p < 0.05$). *D*, Measurement of neutrophils per high power field on H&E lung tissue sections. Each bar represents the mean ± SEM for $n = 6$ mice per group. ∗, $p < 0.05$.

A significant decrease in the number of neutrophils per high power field was detected on lung sections from BMS-345541-treated mice compared with vehicle treated mice (Fig. 7*A*). Similarly, a significant reduction of neutrophils was identified in BAL from mice treated with BMS-345541 (Fig. 7*B*). Because LPS-induced neutrophilic alveolitis in mice is largely determined by expression of the CXC chemokines MIP-2 and KC (23), we measured levels of these mediators in lung lavage fluid from mice treated with BMS-345541 or vehicle in addition to LPS pump treatment. BMS-345541 treatment resulted in deceased production of both MIP-2

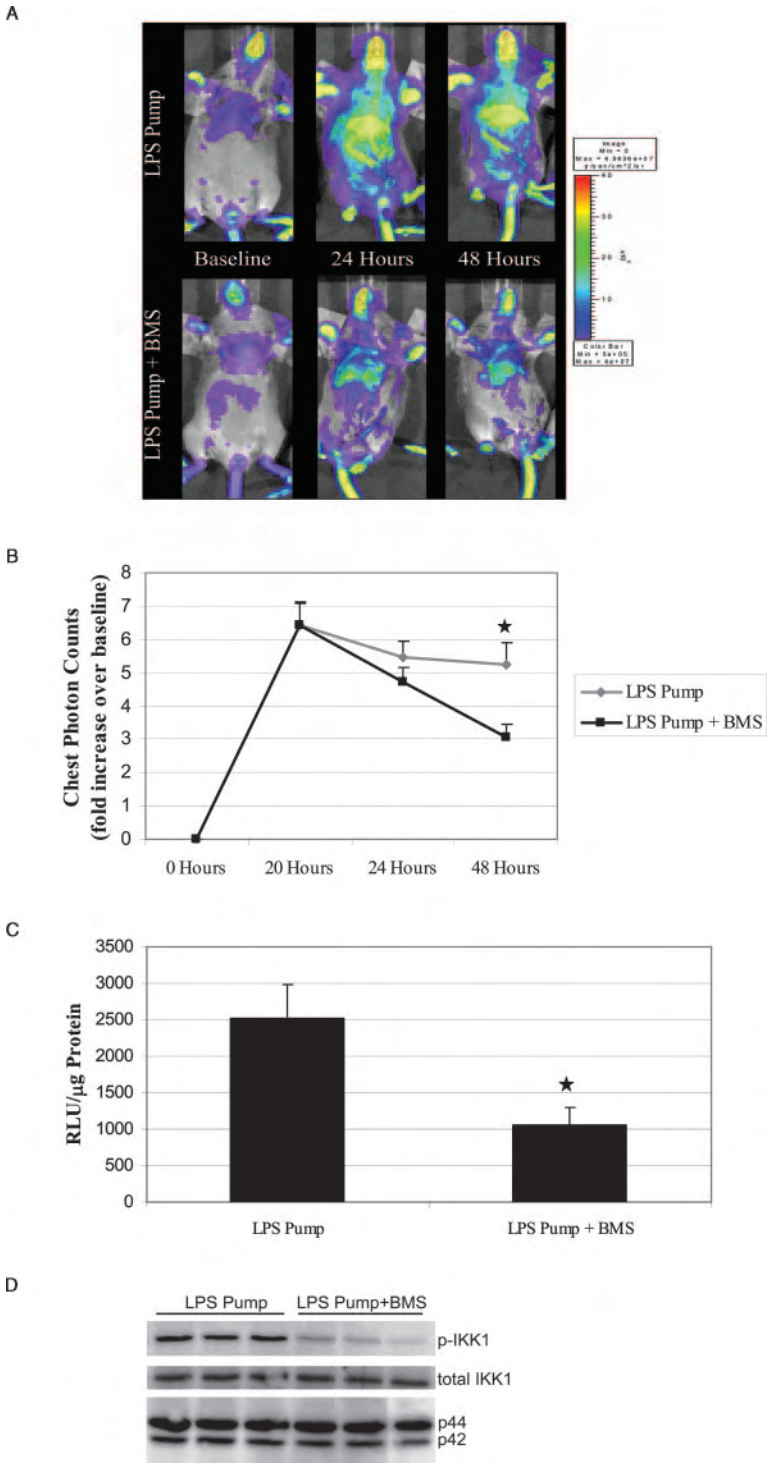

FIGURE 5. Treatment with BMS-345541 after the onset of inflammation in the LPS pump model reduces lung NF-κB activation. BMS-345541 or vehicle was delivered by gavage (75 μg/g) beginning at 20 h after LPS pump implantation and repeated every 4 h for total of five doses. *A*, Representative bioluminescence images of NGL mice obtained before LPS (0 h) and 24 and 48 h after implantation of osmotic pump (LPS Pump). *B*, Quantification of chest photon emission from bioluminescence images (fold increase over baseline) for $n = 12$ mice per group. *, $p < 0.05$ vs group treated with vehicle. *C*, Luciferase activity is measured in lung tissue homogenates at the time of harvest (RLU/μg protein). Each bar represents the mean ± SEM ($n = 12$ per group). *, $p < 0.05$. *D*, Western blot for phosphorylated IKK1 (p-IKK1) in lung tissue homogenates at 48 h after LPS pump implantation, normalized for total IKK1 and p44 and p42 MAPK. Each lane represents protein from a different mouse.

(127.4 ± 48.9 pg/ml in vehicle-treated mice vs 13.9 ± 3.7 pg/ml in BMS-345541-treated mice, $p < 0.05$) and KC (531.2 ± 34.0 pg/ml in vehicle-treated mice vs 21.6 ± 17.9 pg/ml in BMS-345541-treated mice, $p < 0.05$). Lung edema was evaluated by determining lung wet to dry ratio (Fig. 7*C*). The increased wet to dry ratio observed in vehicle-treated mice was completely ablated by BMS-345541 treatment, consistent with the histological improvement observed in the lungs of these mice. Together, these studies show that specific inhibition of NF-κB activation after establishment of lung inflammation reduces lung inflammation and prevents injury.

Neutrophil depletion reduces lung inflammation and injury

To evaluate whether reduction of neutrophil recruitment to the lungs accounts for prevention of lung injury resulting from NF-κB inhibition, we depleted neutrophils and determined the impact on LPS-induced lung inflammation and injury. Neutrophil depletion was achieved by repeated i.p. injection of antineutrophil Abs using a previously published protocol (16). After 4 daily injections of antineutrophil Abs, we detected an 80% reduction in peripheral neutrophil counts compared with mice treated with control IgG (Fig. 8*A*). After documenting PMN depletion, LPS pumps were

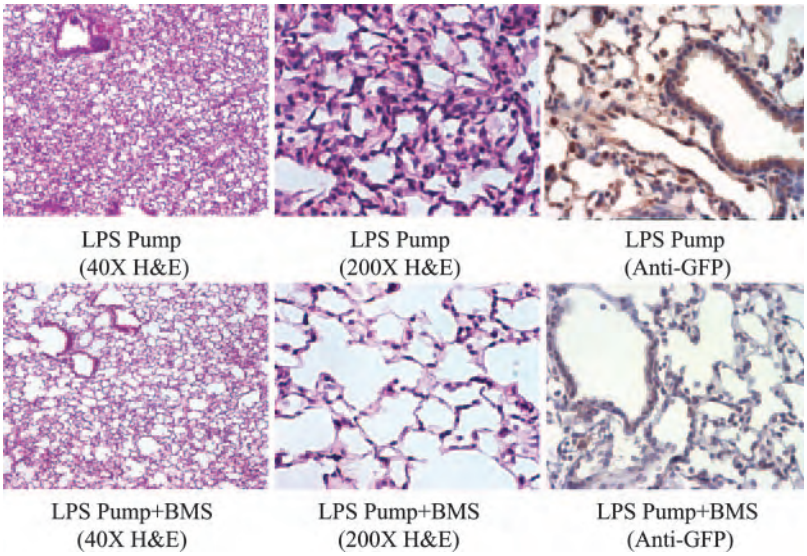

FIGURE 6. Treatment with NF-κB inhibitor after the onset of inflammation in the LPS pump model reduces lung inflammation and injury at 48 h. Representative H&E-stained lung sections were obtained from mice treated with BMS-345541 (LPS Pump+BMS) or vehicle (LPS Pump) in addition to LPS by osmotic pump. Immunohistochemistry for GFP demonstrates widespread reduction in NF-κB-driven reporter expression following treatment with BMS-345541.

implanted and bioluminescent detection of NF-κB-dependent luciferase expression was performed at 24 and 48 h (Fig. 8*B*). As shown, reduction of circulating neutrophils did not affect luciferase expression in NGL mice, implying that neutrophils do not make major contributions to the total lung NF-κB activation in this model. At 48 h, neutrophils were found to be reduced in BAL (Fig. 8*C*) and the lung wet-to-dry ratio was significantly decreased in neutrophil-depleted mice compared with IgG-treated controls (Fig. 8*D*). However, the wet-to-dry ratio in the lungs of neutrophil-depleted mice treated with LPS pump was significantly greater than the ratio in untreated controls, indicating that the achieved degree of neutrophil depletion was only partially effective in preventing lung edema formation. By histological examination of lung sections, mice treated with antineutrophil Abs were found to have a reduction in lung neutrophil influx with a mild diminution in edema and evidence of lung injury compared with IgG-treated controls (data not shown). Accounting for the reduction in neutrophils, immunohistochemistry for GFP did not show any differences in intensity or distribution of GFP staining in the lungs of mice treated with antineutrophil Abs or control IgG before LPS pumps.

Discussion

To comprehensively determine the extent of NF-κB activation in vivo, we developed a reporter system that allows identification of NF-κB-positive cells using GFP detection, as well as quantification of NF-κB activity in cells and tissue using luciferase detection methodologies. The NGL reporter construct was validated as an indicator of NF-κB activation in cell lines, primary cells from transgenic mice, and intact animals. Following a single i.p. injection of LPS, the time course for increased bioluminescence over the chest was similar to our previous report with NF-κB reporter mice that express luciferase under the control of the proximal promoter for the 5′ HIV-long terminal repeat (21).

LPS activates NF-κB in cells directly by interaction with cell surface molecules CD14 and TLR4. Although initial studies identified TLR4 on leukocytes, more recent studies have identified TLR4 expression in other cell types, including endothelium and bronchial epithelial cells, indicating that LPS may directly stimulate inflammatory signaling in a variety of cell types (24, 25). In addition to direct cellular effects, inflammatory signaling by LPS is amplified by rapid production and secretion of "proximal" cytokines, including TNF-α and IL-β, by macrophages. Through specific receptors, these molecules have the ability to activate NF-κB signaling and amplify the host inflammatory response. In NGL mice, we showed that NF-κB was efficiently activated throughout the lungs in response to systemic LPS. Within 4 h, most cells in the lungs were GFP^+; however, in the absence of continued activation, inflammation resolved without substantial tissue injury.

We evaluated NF-κB activation in the lungs in a model of transient lung inflammation (single-dose IP LPS treatment) and a model of LPS-induced lung inflammation that progresses to lung injury (LPS pump treatment). One limitation of previously reported models of LPS-induced lung inflammation in mice is that they produce relatively minor lung injury, even at near lethal doses; therefore, we chose to deliver LPS over 24 h by osmotic pump in a model that resembles subacute LPS release from i.p. infection. Using these two models, we observed clear differences in NF-κB activation. Like other parameters of the inflammatory response, NF-κB activation was transient in the IP LPS model but persisted in the LPS pump model up to 24 h after LPS delivery ceased. In the LPS pump model, obvious lung injury was present by 48 h after implantation of the osmotic pump. In our studies, mice were harvested at 48 h in the LPS pump model because substantial mortality was observed when mice were followed beyond this time point. The cellular distribution of NF-κB activation as measured by GFP^+ cells, and peak intensity of NF-κB activation as determined by bioluminescence imaging of luciferase activity did not differ between the IP LPS and LPS pump treatment models, indicating that these parameters are not the critical determinants of progression to lung injury. However, widespread sustained cellular activation of NF-κB correlated with lung injury.

To evaluate whether a causal relationship exists between sustained lung NF-κB activation and lung injury, we used a specific inhibitor of the NF-κB pathway. BMS-345541 is a selective inhibitor of the catalytic subunit of IKK2 (IC_{50} = 0.3 mM) and IKK1 (IC_{50} = 4 μM) through binding to an allosteric site (19). Peroral administration of BMS-345541 inhibits serum TNF-α production following LPS injection in a dose-dependent manner (19). Additional studies support the use of BMS-345541 as a selective NF-κB inhibitor and anti-inflammatory agent, including findings of reduced joint inflammation and destruction in a collagen-induced arthritis model, reduced severity

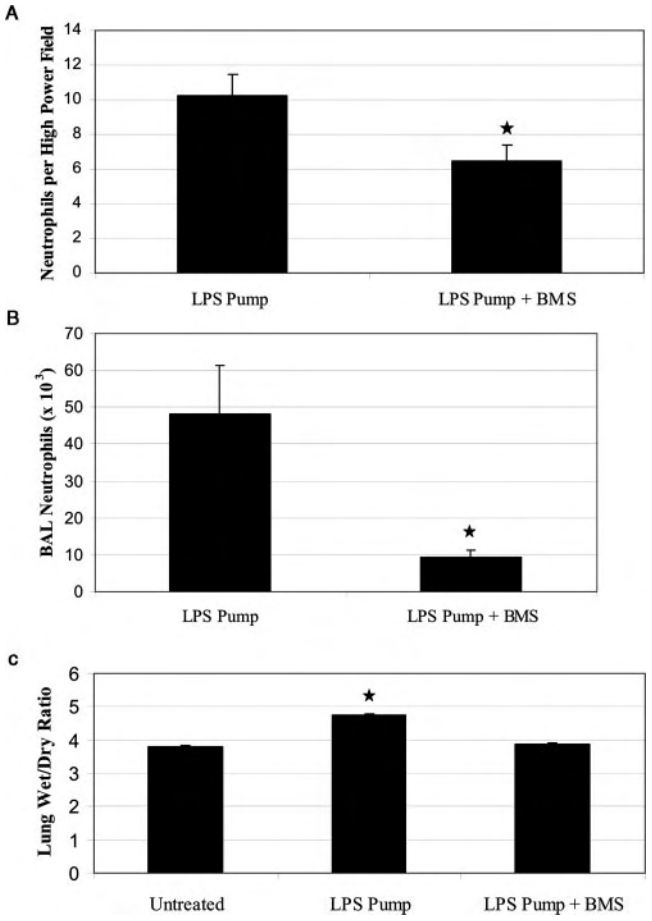

FIGURE 7. Treatment with NF-κB inhibitor decreases neutrophil influx into the lungs and eliminates lung edema in the LPS pump model. Lungs were harvested at 48 h after initiation of LPS treatment in mice treated with BMS-345541 (LPS Pump+BMS) or vehicle (LPS Pump). *A*, Quantification of lung neutrophils on H&E-stained lung sections for $n = 6$ mice per group. *, $p < 0.05$. *B*, Total neutrophils in BAL fluid for $n = 6$ mice per group. *, $p < 0.05$. *C*, Lung wet-to-dry ratio is represented. Each bar represents the mean ± SEM for $n = 6$ mice per group. *, $p < 0.05$ vs the other two groups.

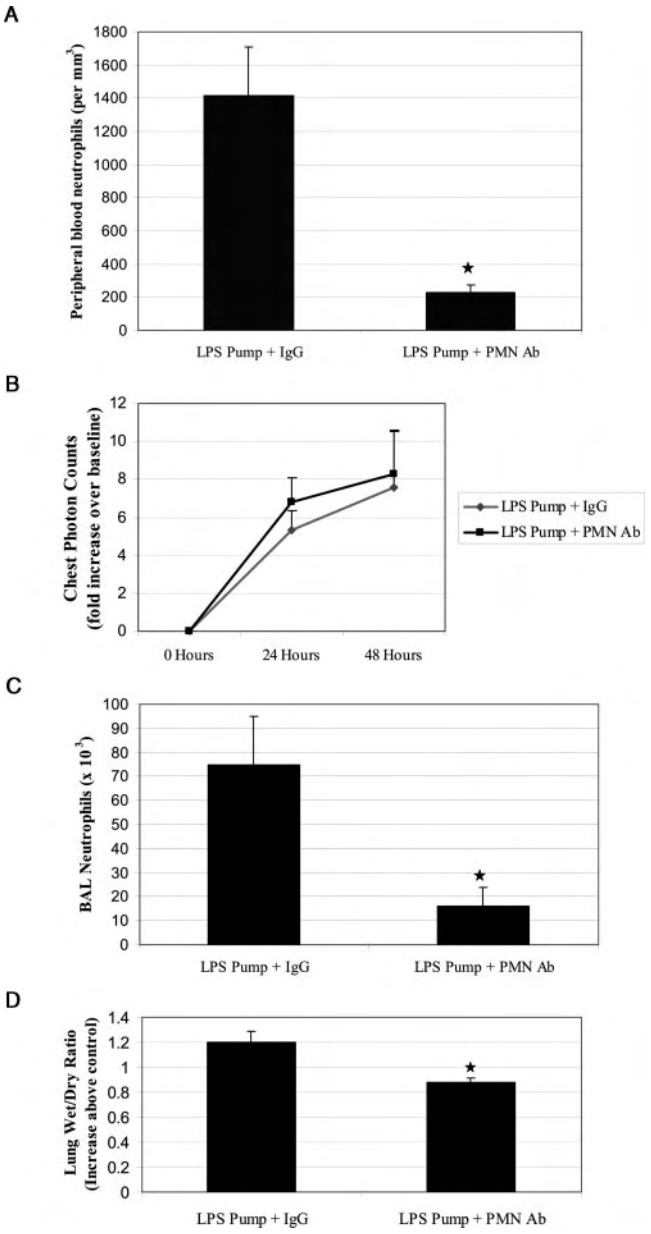

FIGURE 8. Neutrophil depletion reduces lung edema but not NF-κB activation in the LPS pump model. NGL mice were treated with antineutrophil Abs (PMN Ab) or control IgG before implantation of LPS pumps. Mice were harvested at 48 h. *A*, Peripheral blood neutrophils (PMN) were quantified after Ab treatment and before implantation of LPS pumps. *B*, Quantification of chest photon emission from bioluminescence images of mice at baseline, 24, and 48 h after LPS pumps. *C*, Total neutrophils in BAL fluid. *D*, Lung wet-to-dry ratio is reported as the increase above the mean value for an untreated control group. Each bar represents the mean ± SEM for $n = 5$ mice per group for each end point. *, $p < 0.05$ vs IgG control.

of colitis in a dextran sulfate sodium-induced colitis model, and improved graft survival in a murine model of cardiac graft rejection (22, 26, 27). In our experiments, we found that when administered before LPS, BMS-345541 treatment decreased NF-κB activation and neutrophilic lung inflammation measured at 8 h. Subsequently, we treated mice with BMS-345541 during the period when NF-κB activity was differentially up-regulated in the LPS pump model to investigate whether attenuation of NF-κB activation would convert this model of lung injury to one of transient inflammation. We initiated treatment with BMS-345541 at 20 h after LPS pump implantation. At the time of harvest, NF-κB activation, CXC chemokine production, and neutrophilic inflammation were markedly reduced in mice by BMS-345541 treatment. In addition, the histological appearance of lungs from BMS-345541-treated mice was improved and lung edema formation, as measured by wet-to-dry ratio, was eliminated. It appears that part of the benefit of NF-κB depletion results from reducing the neutrophil influx into the lungs consequent to LPS pump implantation. Activated neutrophils produce a variety of oxidants and proteases that have the potential to disrupt the alveolar-capillary barrier and contribute to lung injury (28). By treatment with antineutrophil Abs, we were able to reduce lung neutrophil influx (measured in BAL) to a similar degree as that achieved by treatment with the NF-κB inhibitor; however, the NF-κB inhibitor had a much more profound benefit in protecting from lung injury. These findings imply that NF-κB inhibition reduces lung injury in this model by reduction of neutrophil recruitment to the lungs and through other mechanisms (currently not well defined) that prevent disruption of the alveolar capillary barrier.

In contrast with our findings, a study by Lawrence et al. (15) found that NF-κB played opposing roles in the onset and resolution of inflammation in rat carrageenin pleurisy and mouse carrageenin air pouch models. Using nonspecific inhibitors, decreased NF-κB activation after establishment of inflammation was associated with protracted inflammation and prevention of leukocyte clearance, suggesting NF-κB may not be a suitable target for therapeutic intervention to limit and/or resolve established inflammation. Our findings, however, indicate that NF-κB could be an important target for limiting injury in the setting of ongoing inflammation in the lung parenchyma. The differences in our findings and those previously reported may be related to differences in the models of inflammation and/or the specificity of the agents used to inhibit the NF-κB pathway.

In humans, lung injury resulting from pneumonia, systemic infection, or trauma can cause ARDS (29, 30). The inflammatory phenotype associated with ARDS supports a role for NF-κB in the pathogenesis of this syndrome, including increased concentrations of a variety of NF-κB-linked cytokines and chemokines in BAL fluid from patients with ARDS (31–33). Increased concentration of the NF-κB-dependent CXC chemokine IL-8 correlates with neutrophilia in BAL, and prolonged neutrophilic alveolitis is associated with increased mortality in patients with ARDS (34–37). In addition, NF-κB activation has been identified in alveolar macrophages from humans with ARDS (38). Together, these data from human studies implicate the NF-κB pathway as a potentially important determinant of lung injury in humans with ARDS. Based on our findings in relevant rodent models of lung inflammation and injury, NF-κB may prove to be a beneficial target for therapeutic intervention to treat ongoing lung inflammation and prevent or limit lung injury. Although NF-κB inhibition has the potential to reduce lung injury, innate immune functions that depend on NF-κB may be required for adequate lung host defense against infection (39); therefore, application of these findings to human disease should proceed with caution. Hopefully, a better understanding of the intricacies of proinflammatory pathways that contribute to lung injury and host defense will lead to targeted therapies that limit injury while preserving lung defenses.

Disclosures

J. R. Burke is employed by Bristol-Myers Squibb Pharmaceutical Research Institute, the company that manufactured BMS-345541, which was used in these studies.

References

1. Blackwell, T. S., E. P. Holden, T. R. Blackwell, J. E. DeLarco, and J. W. Christman. 1994. Cytokine-induced neutrophil chemoattractant mediates neutrophilic alveolitis in rats: association with nuclear factor κB activation. *Am. J. Respir. Cell Mol. Biol.* 11: 464–472.
2. Haddad, E. B., M. Salmon, H. Koto, P. J. Barnes, I. Adcock, and K. F. Chung. 1996. Ozone induction of cytokine-induced neutrophil chemoattractant (CINC) and nuclear factor-κb in rat lung: inhibition by corticosteroids. *FEBS Lett.* 379: 265–268.
3. Shenkar, R., M. D. Schwartz, L. S. Terada, J. E. Repine, J. McCord, and E. Abraham. 1996. Hemorrhage activates NF-κB in murine lung mononuclear cells in vivo. *Am. J. Physiol.* 270: L729–L735.
4. Sacks, M., J. Gordon, J. Bylander, D. Porter, X. L. Shi, V. Castranova, W. Kaczmarczyk, K. Van Dyke, and M. J. Reasor. 1998. Silica-induced pulmonary inflammation in rats: activation of NF-κB and its suppression by dexamethasone. *Biochem. Biophys. Res. Commun.* 253: 181–184.
5. Browder, W., T. Ha, L. Chuanfu, J. H. Kalbfleisch, D. A. Ferguson, Jr., and D. L. Williams. 1999. Early activation of pulmonary nuclear factor κB and nuclear factor interleukin-6 in polymicrobial sepsis. *J. Trauma* 46: 590–596.
6. Mizgerd, J. P., J. J. Peschon, and C. M. Doerschuk. 2000. Roles of tumor necrosis factor receptor signaling during murine *Escherichia coli* pneumonia. *Am. J. Respir. Cell Mol. Biol.* 22: 85–91.
7. Mizgerd, J. P., M. R. Spieker, and C. M. Doerschuk. 2001. Early response cytokines and innate immunity: essential roles for TNF receptor 1 and type I IL-1 receptor during *Escherichia coli* pneumonia in mice. *J. Immunol.* 166: 4042–4048.
8. Sadikot, R. T., E. D. Jansen, T. R. Blackwell, O. Zoia, F. Yull, J. W. Christman, and T. S. Blackwell. 2001. High-dose dexamethasone accentuates nuclear factor-κB activation in endotoxin-treated mice. *Am. J. Respir. Crit. Care Med.* 164: 873–878.
9. Blackwell, T. S., J. P. Debelak, A. Venkatakrishnan, D. J. Schot, D. H. Harley, C. W. Pinson, P. Williams, K. Washington, J. W. Christman, and W. C. Chapman. 1999. Acute lung injury after hepatic cryoablation: correlation with NF-κB activation and cytokine production. *Surgery* 126: 518–526.
10. Blackwell, T. S., F. E. Yull, C. L. Chen, A. Venkatakrishnan, T. R. Blackwell, D. J. Hicks, L. H. Lancaster, J. W. Christman, and L. D. Kerr. 2000. Multiorgan nuclear factor κB activation in a transgenic mouse model of systemic inflammation. *Am. J. Respir. Crit. Care Med.* 162: 1095–1101.
11. Lauzurica, P., S. Martínez-Martínez, M. Marazuela, P. Gómez del Arco, C. Martínez-A, F. Sánchez-Madrid, and J. M. Redondo. 1999. Pyrrolidine dithiocarbamate protects mice from lethal shock induced by LPS or TNF-α. *Eur. J. Immunol.* 29: 1890–1900.
12. Liu, S. F., X. Ye, and A. B. Malik. 1999. Pyrrolidine dithiocarbamate prevents I-κB degradation and reduces microvascular injury induced by lipopolysaccharide in multiple organs. *Mol. Pharmacol.* 55: 658–667.
13. Blackwell, T. S., T. R. Blackwell, E. P. Holden, B. W. Christman, and J. W. Christman. 1996. In vivo antioxidant treatment suppresses nuclear factor-κB activation and neutrophilic lung inflammation. *J. Immunol.* 157: 1630–1637.
14. Alcamo, E., J. P. Mizgerd, B. H. Horwitz, R. Bronson, A. A. Beg, M. Scott, C. M. Doerschuk, R. O. Hynes, and D. Baltimore. 2001. Targeted mutation of TNF receptor I rescues the RelA-deficient mouse and reveals a critical role for NF-κB in leukocyte recruitment. *J. Immunol.* 167: 1592–1600.
15. Lawrence, T., D. W. Gilroy, P. R. Colville-Nash, and D. A. Willoughby. 2001. Possible new role for NF-κB in the resolution of inflammation. *Nat. Med.* 7: 1291–1297.
16. Abraham, E., A. Carmody, R. Shenkar, and J. Arcaroli. 2000. Neutrophils as early immunologic effectors in hemorrhage- or endotoxemia-induced acute lung injury. *Am. J. Physiol.* 279: L1137–L1145.
17. Sadikot, R. T., H. Zeng, F. E. Yull, B. Li, D. S. Cheng, D. S. Kernodle, E. D. Jansen, C. H. Contag, B. H. Segal, S. M. Holland, et al. 2004. p47^{phox} deficiency impairs NF-κB activation and host defense in *Pseudomonas* pneumonia. *J. Immunol.* 172: 1801–1808.
18. Sadikot, R. T., W. Han, M. B. Everhart, O. Zoia, R. S. Peebles, E. D. Jansen, F. E. Yull, J. W. Christman, and T. S. Blackwell. 2003. Selective IκB kinase expression in airway epithelium generates neutrophilic lung inflammation. *J. Immunol.* 170: 1091–1098.
19. Burke, J. R., M. A. Pattoli, K. R. Gregor, P. J. Brassil, J. F. MacMaster, K. W. McIntyre, X. Yang, V. S. Iotzova, W. Clarke, J. Strnad, et al. 2003. BMS-345541 is a highly selective inhibitor of IκB kinase that binds at an allosteric site of the enzyme and blocks NF-κB-dependent transcription in mice. *J. Biol. Chem.* 278: 1450–1456.
20. Rojas, M., C. R. Woods, A. L. Mora, J. Xu, and K. L. Brigham. 2005. Endotoxin-induced lung injury in mice: structural, functional, and biochemical responses. *Am. J. Physiol.* 288: L333–L341.
21. Yull, F. E., W. Han, E. D. Jansen, M. B. Everhart, R. T. Sadikot, J. W. Christman, and T. S. Blackwell. 2003. Bioluminescent detection of endotoxin effects on HIV-1 LTR-driven transcription in vivo. *J. Histochem. Cytochem.* 51: 741–749.
22. McIntyre, K. W., D. J. Shuster, K. M. Gillooly, D. M. Dambach, M. A. Pattoli, P. Lu, X.-D. Zhou, Y. Qiu, F. C. Zusi, and J. R. Burke. 2003. A highly selective inhibitor of IκB kinase, BMS-345541, blocks both joint inflammation and destruction in collagen-induced arthritis in mice. *Arthritis Rheum.* 48: 2652–2659.
23. Gonçalves, A. S., and R. Appelberg. 2002. The involvement of the chemokine receptor CXCR2 in neutrophil recruitment in LPS-induced inflammation and in *Mycobacterium avium* infection. *Scand. J. Immunol.* 55: 585–591.
24. Muir, A., G. Soong, S. Sokol, B. Reddy, M. I. Gomez, A. Van Heeckeren, and A. Prince. 2004. Toll-like receptors in normal and cystic fibrosis airway epithelial cells. *Am. J. Respir. Cell Mol. Biol.* 30: 777–783.
25. Fan, J., R. S. Frey, and A. B. Malik. 2003. TLR4 signaling induces TLR2 expression in endothelial cells via neutrophil NADPH oxidase. *J. Clin. Invest.* 112: 1234–1243.
26. MacMaster, J. F., D. M. Dambach, D. B. Lee, K. K. Berry, Y. Qiu, F. C. Zusi, and J. R. Burke. 2003. An inhibitor of IκB kinase, BMS-345541, blocks endothelial cell adhesion molecule expression and reduces the severity of dextran sulfate sodium-induced colitis in mice. *Inflamm. Res.* 52: 508–511.
27. Townsend, R. M., J. Postelnek, V. Susulic, K. W. McIntyre, D. J. Shuster, Y. Qiu, F. C. Zusi, and J. R. Burke. 2004. A highly selective inhibitor of IκB kinase, BMS-345541, augments graft survival mediated by suboptimal immunosuppression in a murine model of cardiac graft rejection. *Transplantation* 77: 1090–1094.
28. Matthay, M. A., and G. A. Zimmerman. 2005. Acute lung injury and the acute respiratory distress syndrome: four decades of inquiry into pathogenesis and rational management. *Am. J. Respir. Cell Mol. Biol.* 33: 319–327.
29. Kollef, M. H., and D. P. Schuster. 1995. The acute respiratory distress syndrome. *N. Engl. J. Med.* 332: 27–37.
30. Ware, L. B., and M. A. Matthay. 2000. The acute respiratory distress syndrome. *N. Engl. J. Med.* 342: 1334–1349.

31. Bhatia, M., and S. Moochhala. 2004. Role of inflammatory mediators in the pathophysiology of acute respiratory distress syndrome. *J. Pathol.* 202: 145–156.
32. Goodman, R. B., R. M. Strieter, D. P. Martin, K. P. Steinberg, J. A. Milberg, R. J. Maunder, S. L. Kunkel, A. Walz, L. D. Hudson, and T. R. Martin. 1996. Inflammatory cytokines in patients with persistence of the acute respiratory distress syndrome. *Am. J. Respir. Crit. Care Med.* 154: 602–611.
33. Schütte, H., J. Lohmeyer, S. Rosseau, S. Ziegler, C. Siebert, H. Kielisch, H. Pralle, F. Grimminger, H. Morr, and W. Seeger. 1996. Bronchoalveolar and systemic cytokine profiles in patients with ARDS, severe pneumonia and cardiogenic pulmonary oedema. *Eur. Respir. J.* 9: 1858–1867.
34. Miller, E. J., A. B. Cohen, S. Nagao, D. Griffith, R. J. Maunder, T. R. Martin, J. P. Weiner-Kronish, M. Sticherling, E. Christophers, and M. A. Matthay. 1992. Elevated levels of NAP-1/interleukin-8 are present in the airspaces of patients with the adult respiratory distress syndrome and are associated with increased mortality. *Am. Rev. Respir. Dis.* 146: 427–432.
35. Donnelly, S. C., R. M. Strieter, S. L. Kunkel, A. Walz, C. R. Robertson, D. C. Carter, I. S. Grant, A. J. Pollok, and C. Haslett. 1993. Interleukin-8 and development of adult respiratory distress syndrome in at-risk patient groups. *Lancet* 341: 643–647.
36. Baughman, R. P., K. L. Gunther, M. C. Rashkin, D. A. Keeton, and E. N. Pattishall. 1996. Changes in the inflammatory response of the lung during acute respiratory distress syndrome: prognostic indicators. *Am. J. Respir. Crit. Care Med.* 154: 76–81.
37. Steinberg, K. P., J. A. Milberg, T. R. Martin, R. J. Maunder, B. A. Cockrill, and L. D. Hudson. 1994. Evolution of bronchoalveolar cell populations in the adult respiratory distress syndrome. *Am. J. Respir. Crit. Care Med.* 150: 113–122.
38. Schwartz, M. D., E. E. Moore, F. A. Moore, R. Shenkar, P. Moine, J. B. Haenel, and E. Abraham. 1996. Nuclear factor-κB is activated in alveolar macrophages from patients with acute respiratory distress syndrome. *Crit. Care Med.* 24: 1285–1292.
39. Sadikot, R. T., H. Zeng, M. Joo, M. B. Everhart, T. P. Sherrill, B. Li, D.-S. Cheng, F. E. Yull, J. W. Christman, and T. S. Blackwell. 2006. Targeted immunomodulation of the NF-κβ pathway in airway epithelium impacts host defense against *Pseudomonas aeruginosa. J. Immunol.* In press.

Airway Epithelium Controls Lung Inflammation and Injury through the NF-κB Pathway[1]

Dong-sheng Cheng,* Wei Han,* Sabrina M. Chen,* Taylor P. Sherrill,* Melissa Chont,† Gye-Young Park,¶ James R. Sheller,* Vasiliy V. Polosukhin,* John W. Christman,§¶ Fiona E. Yull,[2†] and Timothy S. Blackwell[2,3]*†‡§

Although airway epithelial cells provide important barrier and host defense functions, a crucial role for these cells in development of acute lung inflammation and injury has not been elucidated. We investigated whether NF-κB pathway signaling in airway epithelium could decisively impact inflammatory phenotypes in the lungs by using a tetracycline-inducible system to achieve selective NF-κB activation or inhibition in vivo. In transgenic mice that express a constitutively active form of IκB kinase 2 under control of the epithelial-specific CC10 promoter, treatment with doxycycline induced NF-κB activation with consequent production of a variety of proinflammatory cytokines, high-protein pulmonary edema, and neutrophilic lung inflammation. Continued treatment with doxycycline caused progressive lung injury and hypoxemia with a high mortality rate. In contrast, inducible expression of a dominant inhibitor of NF-κB in airway epithelium prevented lung inflammation and injury resulting from expression of constitutively active form of IκB kinase 2 or *Escherichia coli* LPS delivered directly to the airways or systemically via an osmotic pump implanted in the peritoneal cavity. Our findings indicate that the NF-κB pathway in airway epithelial cells is critical for generation of lung inflammation and injury in response to local and systemic stimuli; therefore, targeting inflammatory pathways in airway epithelium could prove to be an effective therapeutic strategy for inflammatory lung diseases. ***The Journal of Immunology,*** **2007, 178: 6504–6513.**

The NF-κB pathway impacts a number of key biological processes, including innate immunity, through transcriptional regulation of target genes. Following cell stimulation, IκBs are phosphorylated on serine residues in the amino terminus by IκB kinase 2 (IKK2),[4] targeting them for destruction by the ubiquitin/proteasome (26S) degradation pathway (1). IκB degradation allows NF-κB nuclear translocation and transcriptional activation of a variety of genes, including cytokines, chemokines, and adhesion molecules (2, 3). In the lungs, many noxious/inflammatory stimuli have been shown to activate NF-κB, including bacterial products, ozone and silica, as well as systemic inflammatory insults such as sepsis, trauma, and hemorrhage.

Innate immunity is critical for host defense against bacterial pathogens, but dysregulated or exaggerated immune responses can result in tissue injury. In the lungs, this form of host-derived tissue injury characterizes the acute respiratory distress syndrome (ARDS). ARDS is a common cause of morbidity and mortality in critically ill patients, resulting from local or systemic infection, trauma, or other inflammatory/injurious stimuli (4, 5). The inflammatory phenotype underlying the pathogenesis of ARDS includes neutrophilic alveolitis and increased levels of a number of cytokines and chemokines in the airways (4, 6). Improved understanding of critical cell types and biological pathways that regulate innate immunity in the lungs could be useful in designing therapies to limit or prevent lung injury in patients at risk for ARDS.

Airway epithelium provides a physical border between host and environment that protects from injurious and infectious stimuli that gain access to the respiratory tract through inspiration or aspiration. Well-recognized functions of airway epithelium include mechanical clearance of offending agents and production of antimicrobial agents; however, critical functions for coordinating the innate immune response or development of lung injury have not been identified. Airway epithelial cells express a number of TLRs, and we have recently shown that local and systemic inflammation results in prominent activation of the NF-κB pathway in these cells (7–9). Therefore, we hypothesized that epithelial cells in the lung are important for transducing NF-κB-dependent inflammatory signals and that prolonged NF-κB activation in airway epithelial cells leads to a dysfunctional (injurious) inflammatory response culminating in lung injury. To evaluate whether airway epithelial cells critically regulate lung inflammation and injury, we generated inducible transgenic mice that express an activator or dominant inhibitor of the NF-κB pathway in CC10-expressing airway epithelial cells. We then determined the effects of cell type-specific NF-κB activation or inhibition on parameters of lung inflammation and injury. Our data indicate that activation of NF-κB in airway

*Division of Allergy, Pulmonary and Critical Care Medicine, Department of Medicine, †Department of Cancer Biology, and ‡Department of Cell and Developmental Biology, Vanderbilt University School of Medicine, Nashville, TN 37232; and §Department of Veterans Affairs and ¶Section of Pulmonary, Critical Care, and Sleep Medicine, University of Illinois, Chicago, IL 60605

Received for publication November 9, 2006. Accepted for publication March 1, 2007.

The costs of publication of this article were defrayed in part by the payment of page charges. This article must therefore be hereby marked *advertisement* in accordance with 18 U.S.C. Section 1734 solely to indicate this fact.

[1] This work was supported by National Institutes of Health Grants HL61419, HL66196, and HL07123; the U.S. Department of Veterans Affairs; Vanderbilt Ingram Cancer Center; Susan G. Komen Foundation Grant BCTR02-1728; and Department of Defense Breast Cancer Program Grant WX1XWH-04-1-0456.

[2] F.E.Y. and T.S.B. contributed equally to this manuscript.

[3] Address correspondence and reprint requests to Dr. Timothy S. Blackwell, Vanderbilt University School of Medicine, T-1218 MCN, Nashville, TN 37232. E-mail address: timothy.blackwell@vanderbilt.edu

[4] Abbreviations used in this paper: IKK2, IκB kinase 2; ARDS, acute respiratory distress syndrome; cIKK2, constitutively active human IKK2; DNTA, IκB-αDN-transactivated mice, transgenic mice expressing IκB-αDN under control of the CC10 promoter; dox, doxycycline; IκB-αDN, IκB-α dominant negative; IKTA, cIKK2-transactivated mice, transgenic mice expressing cIKK2 under control of the CC10 promoter; MTEC, mouse tracheal epithelial cell; RPA, RNase protection assay; rtTA, reverse tetracycline transactivator; tTS, tetracycline-controlled transcriptional silencer; WT, wild type.

epithelial cells is sufficient for generating acute lung injury, and inhibition of NF-κB activation in airway epithelium abrogates lung inflammation and injury induced by Gram-negative bacterial LPS. These findings suggest a paradigm in which airway epithelial cells control parenchymal lung inflammation and injury via production of NF-κB-dependent mediators.

Materials and Methods

Transgenic mouse models

IKTA-transgenic mice. The pBSIIFlag-IKK2 plasmid containing FLAG-cIKK2, a constitutively active form of human IKK2 containing S177E and S181E mutations, was a gift from Dr. F. Mercurio (Signal Pharmaceutical, San Diego, CA). This plasmid was digested with *Bss*HII to obtain a fragment containing the FLAG-IKK2. The ends of this fragment were filled in before ligation into the *Eco*RV site of a modified pBluescript II SK expression vector (pBSII KS/Asc). This vector contains a (tet-O)$_7$-CMV promoter that consists of seven copies of the tet operator DNA-binding sequence linked to a minimal CMV promoter together with bovine growth hormone polyadenylation sequences to ensure transcript termination. The final plasmid ((tet-O)$_7$-FLAG-cIKK2-BGH.poly(A)) was verified by sequencing. To prevent basal leakiness, we used a construct expressing a tetracycline-controlled transcriptional silencer (tTS) under control of the CC10 promoter (CC10-tTS-hGH-poly(A)) (10). The (tet-O)$_7$-FLAG-cIKK2 microinjection fragment was excised from the plasmid as a 3.3-kb *Xmn*I-*Asc*I fragment. We purified both CC10-tTS and (tet-O)$_7$-FLAG-cIKK2 constructs using a GELase Agarose Gel-Digesting preparation kit following the manufacturer's instruction (Epicentre), and these constructs were coinjected at the Vanderbilt transgenic/ES cell shared resource to generate transgenic lines of mice (FVB background) that have cointegrated both the CC10-tTS and (tet-O)$_7$-FLAG-cIKK2 transgenes. Genotyping of founder animals was performed by Southern Blot and later stages of genotyping were performed by PCR analysis. Primers used for PCR of the (tet-O)$_7$-FLAG-cIKK2 transgene are as follows: 5′ primer (located in the CMV minimal promoter) 5′-GAC GCC ATC CAC GCT GTT TTG-3′; and 3′ primer (located in the constitutively active form of IκB kinase 2 (cIKK2) coding region) 5′-CTT CTC ATG ATC TGG ATC TCC-3′. The product size is 452 bp. Primers used for identification of cc10-tTS transgene are as follows: upstream 5′-GAG TTG GCA GCA GTT TCT CC-3′; and downstream 5′-GAG CAC AGC CAC ATC TTC AA-3′. The product size is 472 bp. PCR protocols for both (tet-O)$_7$-FLAG-cIKK2 and CC10-tTS were as follows: 1 cycle 94°C for 2 min; 30 cycles at 94°C for 1 min, 56°C for 30 s, and 72°C for 1 min; and 1 cycle at 72°C for 10 min. Mice transgenic for CC10-tTS/(tet-O)$_7$-FLAG-cIKK2 were mated with cc10-rTTA homozygous mice (gift from Dr. J. A. Whitsett, University of Cincinnati, Cincinnati, OH) to obtain transgenic mice carrying all three transgenes, which were designated IKTA mice. IKTA mice from three separate founder lines were used for these studies.

IκB-αDN-transactivated (DNTA) transgenic mice. To tag the IκB-α dominant inhibitor (IκB-αDN) (8, 11, 12), a 1.35-kb *Bam*HI/*Dra*I fragment was excised from pCMX-pp40 and blunt-end ligated into *Bam*HI/*Eco*RV-digested pEF4/Myc-HisA (Invitrogen Life Technologies). The IκB-αDN-Myc-His-tagged fragment was then excised by *Bam*HI digest, fill-in of the overhanging ends and *Pme*I digestion. The resulting fragment was blunt-end ligated into the pBSII KS/Asc vector described above, which had been *Pst*I digested and filled in. Plasmid constructs were verified by sequencing. A 2.1-kb *Asc*I microinjection fragment was prepared and coinjected with the CC10-tTS microinjection fragment as described above at the Vanderbilt-transgenic/ES cell shared resource to generate transgenic lines of mice (FVB background) that have cointegrated both the CC10-tTS and (tet-O)$_7$-IκB-αDN-Myc-His transgenes. Genotyping of founder animals was performed by Southern blot analysis, and later stages of genotyping were performed by PCR analysis. Primers used for PCR of the (tet-O)$_7$-IκB-αDN-Myc-His transgene are as follows: sense primer, 5′-TGA GGA TGA GGA GAG CAG TGA ATC-3′; and antisense primer, 5′-CAC CCC CCA GAA TAG AAT GAC AC-3′. The product size is 422 bp. Primers used for identification of CC10-tTS transgene (as above). PCR protocols for (tet-O)$_7$-IκB-αDN-Myc-His was as follows: 1 cycle 95°C for 4 min; 30 cycles at 95°C for 30 s, 55°C for 30 s, and 72°C for 1 min; and 1 cycle at 72°C for 10 min. Mice transgenic for CC10-tTS/(tet-O)$_7$-IκB-αDN-Myc-His were mated with CC10-rTTA homozygous mice to obtain transgenic mice carrying all three transgenes, which were designated DNTA mice. DNTA mice from two separate founder lines were used for these studies.

Doxycycline (dox) treatment. All IKTA or DNTA mice (or appropriate controls) were maintained on normal water until transgene activation was desired. At that time, 2 g/L freshly prepared dox (Sigma-Aldrich) was added to the animals' drinking water. Sucrose (2%) was also added to decrease the bitter taste of dox water. The bottle with dox and 2% sucrose water was wrapped with foil to prevent light-induced dox degradation, and dox water was replaced twice per week.

LPS models

Male and female mice weighing between 20 and 25 grams were used for these studies. *Escherichia coli* LPS (serotype 055:B5) was obtained from Sigma-Aldrich. For studies involving aerosolized LPS, 8 ml of a 1 μg/μl LPS solution in PBS was delivered by ultrasonic nebulization in a closed chamber for 30 min using a previously published methodology (13). To deliver systemic LPS, an osmotic pump (2001D Alzet pump; ALZA) filled with LPS solution (1 μg/μl in PBS) was implanted surgically in the peritoneal cavity using sterile technique (9). The pump delivered 8 μg of LPS (8 μl)/h for 24 h. In some experiments, osmotic pumps (1003D) were used. These pumps were filled with LPS solution (8 μg/μl in PBS) to deliver 8 μg/h (1 μl/h) over 72 h. A priming dose of 3 μg of LPS/g body weight was injected i.p. following pump implantation.

Implantation of carotid artery catheter and blood gas analysis

The common carotid artery was separated from the vagus nerve and muscle, and then, two 6-0 silk threads were passed under the artery. The cephalic thread was tied to prevent bleeding, and then, the artery was clamped by small bulldog clamp. A small incision was made just below the ligature, and the catheter was inserted into the lumen. The clamp was taken off, and the catheter was pushed in 10 mm. The catheter was fixed with a second thread and the thread previously used to prevent bleeding. A blunt 16-gauge needle was carefully inserted through the incision and pushed s.c. until the end protruded through the incision in the neck. The incision in the skin was then sutured, and the catheter was connected to a stainless steel tube. The implanted catheter was flushed with saline containing 200 IU heparin/ml and 1 mg ampicillin/ml every day. For blood gas analysis, 100 μl of arterial blood was collected via the catheter and immediately placed in ice. Blood gas analysis was done using an ABL-5 blood gas machine (Radiometer America) at 37°C. Before each measurement, the blood gas machine was calibrated with a standard solution.

Lung histology and immunohistochemistry

Lungs were inflated and fixed with 1 ml of 10% formalin and then were removed en bloc after tracheal ligation. For immunohistochemical analysis, 5-μm paraffin sections were deparaffinized, dehydrated, washed with PBS, treated with 0.05% trypsin, and incubated with 1% BSA in PBS for 20 min before incubation with rabbit polyclonal anti-FLAG Ab (Rockland) or rabbit polyclonal anti-myc Ab (Santa Cruz Biotechnology). After incubation with primary Ab, a standard avidin-biotin complex protocol (Vectastain ABC kit; Vector Laboratories) using anti-rabbit secondary Abs was used. TUNEL assays were performed using a commercially available kit in accordance with the manufacturer's directions (In Situ Cell Death Detection kit; Roche Molecular Biochemicals). Semiquantitative scoring of TUNEL-positive cells was performed on histological specimens by a pathologist blinded to the genotype and treatment group. Ten sequential, nonoverlapping tissue fields of lung parenchyma were evaluated under ×400 magnification. Each tissue field was scored using a 0–4 point system (0, no positive cells; 1, ≤1% positive cells; 2, 1–5% positive cells; 3, 5–10% positive cells; and 4, 10–25% positive cells). A mean score for all fields was calculated for each animal.

EMSA

Tissue nuclear proteins were extracted from whole lung tissue by the method described previously (14). After preparation of nuclear protein extract, EMSA for NF-κB-binding activity was performed using oligonucleotides containing a consensus NF-κB-binding sequence (5′-AGT TGA GGG GAC TTT CCC AGG C-3′).

Western blot analysis

Protein extracts from tissue homogenates (100 μg) were separated on a polyacrylamide gel and transblotted for detection of FLAG-cIKK2 or IκB-αDN-Myc-His. For FLAG-cIKK2, proteins were separated on a 10% acrylamide gel, and anti-FLAG Abs (anti-FLAG conjugated with HRP M_2 mAb; Sigma-Aldrich) were used. HRP was detected by chemoluminescence using Lumi-Light^{PLUS} Western blotting substrate (Roche Diagnostics). For IκB-αDN-Myc-His, proteins were separated on a 12% polyacrylamide gel, and monoclonal anti-myc Abs (Sigma-Aldrich) were used for immunodetection. For detection of RelA in lung tissue nuclear protein fractions, nuclear proteins were prepared as previously described (14), 20 μg of protein was separated on a 10% acrylamide gel, and RelA was

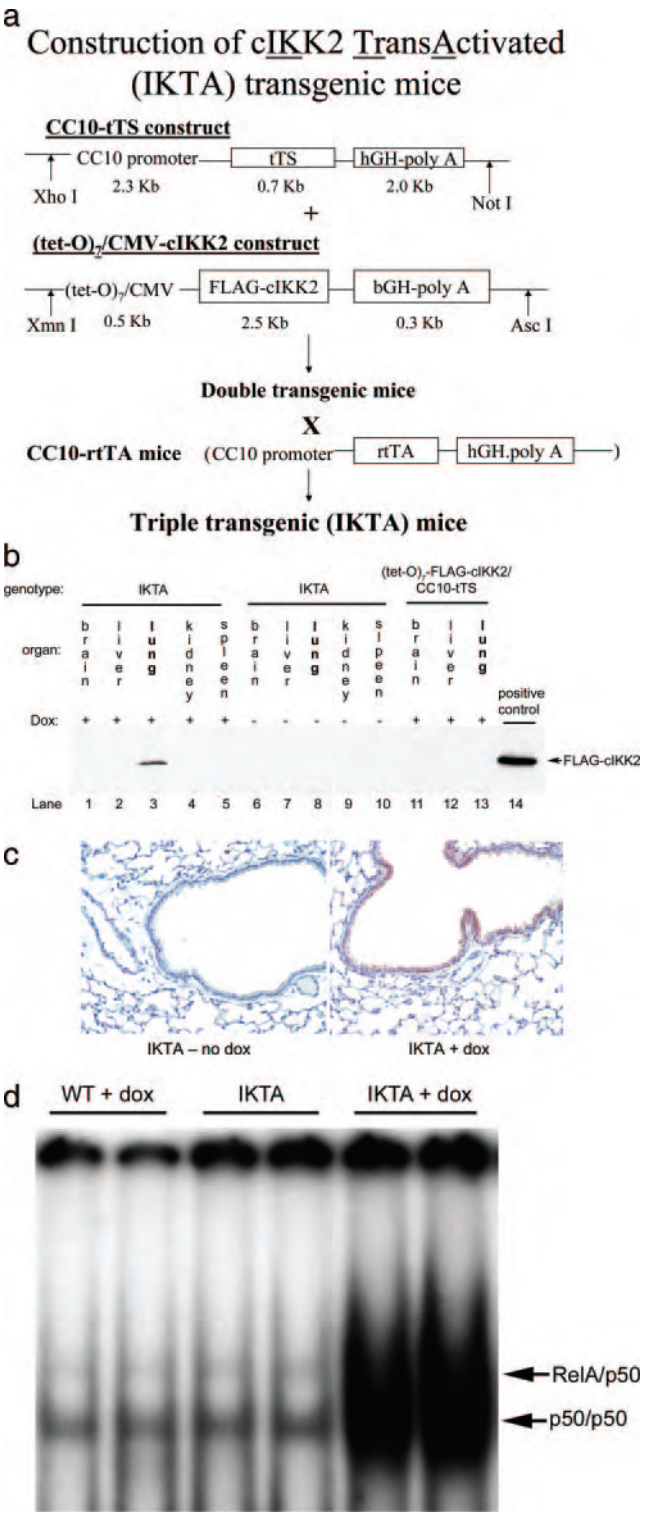

FIGURE 1. Dox-induced expression of FLAG-cIKK2 is localized to lung epithelial cells and sufficient to activate NF-κB. *a*, Schematic for construction of IKTA transgenic mice. *b*, Western blot analysis for FLAG-cIKK2 expression in tissue homogenates obtained from untreated IKTA mice, triple transgenic IKTA mice treated with dox for 3 days, or double transgenic (tet-O)$_7$-FLAG-cIKK2/CC10-tTS mice treated with dox. Transgene expression is detected only in the lungs of IKTA mice following dox treatment. *c*, Immunohistochemistry for FLAG in lung tissue from an untreated IKTA mouse (*left panel*) or an IKTA mouse treated with dox for 3 days (*right panel*). FLAG-cIKK2 staining (brown stain) is localized exclusively in airway epithelial cells in dox-treated IKTA mice. *d*, EMSA for NF-κB binding using lung nuclear protein extracts from WT control mice treated with dox (WT + dox), untreated IKTA mice (IKTA), and IKTA mice treated with dox for 3 days (IKTA + dox). Increased intensity of both NF-κB bands (RelA/p50 and p50/p50) is present in the IKTA + dox group.

immunodetected using rabbit polyclonal anti-RelA Abs (Santa Cruz Biotechnology). TATA-binding protein was detected as a loading control using specific Abs (Santa Cruz Biotechnology).

RNA isolation and RNase protection assay (RPA)

Lung tissue was homogenized in TRIzol reagent (Invitrogen Life Technologies), and RNA was isolated following the manufacturer's instructions. RPA using chemokine template mCK-5 was done with the RiboQuant multiprobe RPA system (BD Pharmingen) according to the manufacturer's direction.

Total and differential cell counts and protein measurement in lung lavage

Lung lavage was performed with 3 aliquots of 800 μl of sterile normal saline. Fluid was combined and centrifuged at 400 × *g* for 10 min to separate cells from supernatant. Supernatant was stored at −70°C for cytokine and chemokine measurements. The total and differential cell counts were done as described previously (12). Protein concentration was quantified using the Bradford assay (Bio-Rad).

Lung wet/dry ratio measurement

Lungs were removed and the wet weight recorded. Lungs were then placed in an incubator at 65°C for 48 h, and the dry weight was determined.

Cytokine and chemokine measurements

Measurement of cytokines and chemokines in lung lavage fluid and cell culture supernatant was done using the Bio-plex mouse cytokine 23-plex kit (Bio-Rad) following the manufacturer's direction and using Luminex technology. MIP-2 and KC levels were measured using a specific ELISA according to the manufacturer's instructions (R&D Systems).

Tracheal epithelial cell culture

Mouse tracheal epithelial cell (MTEC) culture was done by following the previously published protocol with minor modification (15). After removing muscle and vessels, tracheas were incubated in Ham's F-12 pen-strep containing 1.5 mg/ml pronase (Roche Molecular Biochemicals) for 18 h at 4°C to dislodge the epithelial cells. Cells were treated with 0.5 mg/ml crude pancreatic DNase I (Sigma-Aldrich) on ice for 5 min. After incubation in tissue culture plates (BD Biosciences) for 3–4 h in 5% CO_2 at 37°C to adhere fibroblasts, nonadherent cells were collected by centrifugation. Supported polycarbonate and polyester porous (0.4 μM pores) membranes (Transwell; Corning-Costar) were coated with type I rat tail collagen (BD Biosciences) in 0.02 N acetic acid for 18 h at 25°C. Membranes were seeded with cells and incubated with DMEM-Ham's F-12 medium containing 15 mM HEPES, 3.6 mM sodium bicarbonate, 4 mM L-glutamine, 100 U/ml penicillin, 100 μg/ml streptomycin, 0.25 μg/ml Fungizone, 10 μg/ml insulin, 5 μg/ml transferrin, 0.1 μg/ml cholera toxin, and 25 ng/ml epidermal growth factor (BD Biosciences) and 30 μg/ml bovine pituitary extract, 5% FBS, and freshly added 0.01 μM retinoic acid, filling upper and lower chambers in 5% CO_2 at 37°C. Media were changed every 2 days until the transmembrane resistance (R_t) was >1000 Ω · cm^2, as measured by an epithelial Ohm-voltmeter (World Precision Instruments). Media were then removed from the upper chamber to establish an air-liquid interface, and lower chambers only were provided fresh DMEM-Ham's F-12 medium supplemented with 2% NuSerum (BD Biosciences) and 0.01 μM retinoic acid.

Membrane cultures were prepared for scanning electron microscopy, as described previously (16). Briefly, samples were fixed with 2.5% glutaraldehyde, stained with 1.25% osmium tetroxide, critical point dried under liquid carbon dioxide, gold sputter coated, and visualized on a Hitachi S-3000N microscope (Hitachi).

For immunofluorescent detection of FLAG-cIKK2 expression, membranes were fixed with 4% paraformaldehyde (pH 7.4) for 10 min at 25°C and washed in PBS. A piece of membrane was cut and used for staining. Nonspecific Ab binding was blocked using 5% nonspecific serum and 3% BSA in PBS for 30 min at 25°C. Samples were incubated for 18 h at 4°C with anti-FLAG M2-FITC conjugate Ab (Sigma-Aldrich) in blocking solution. Membranes were mounted on slides with VectaShield (Vector Laboratories) containing 4′,6-diamidino-2-phenylindole to stain intracellular

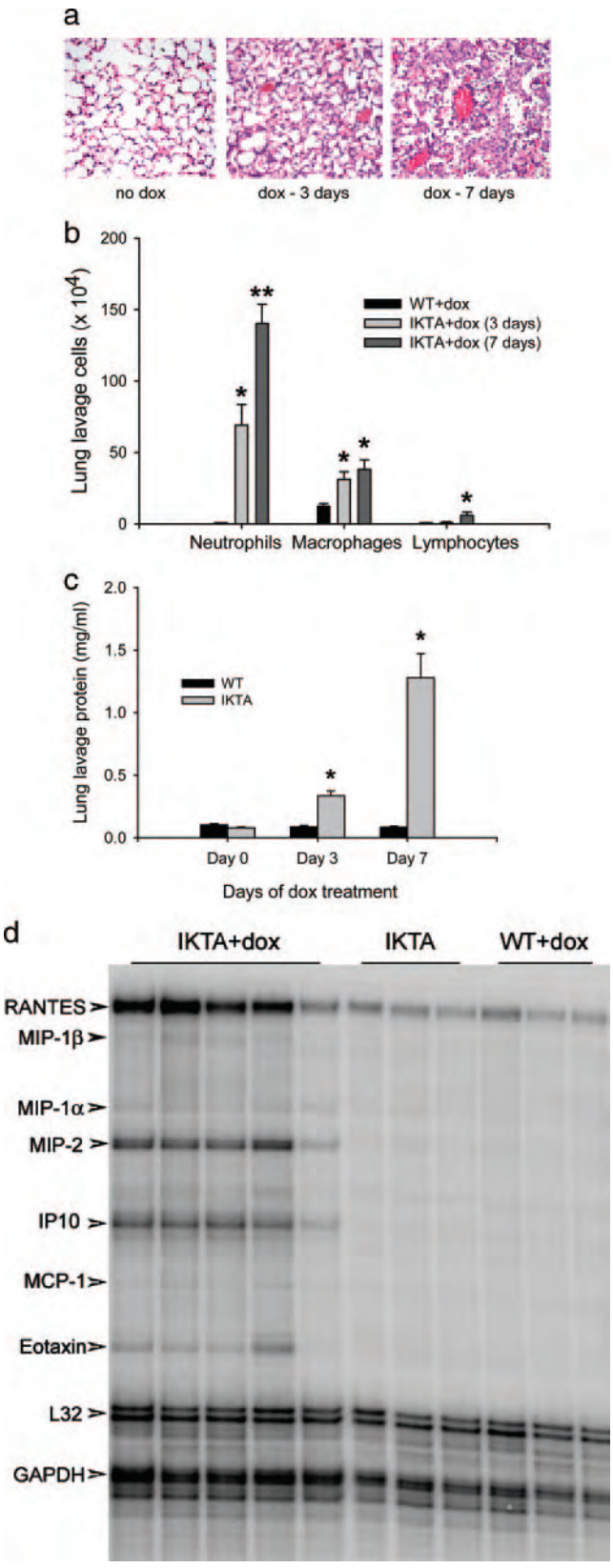

FIGURE 2. NF-κB activation in airway epithelium results in progressive lung inflammation and injury. *a*, H&E-stained lung sections from untreated IKTA mice and IKTA mice (line 3) treated with dox for 3 or 7 days. Although untreated IKTA mice have normal lung histology, a progressive inflammatory cell infiltrate is observed at 3 and 7 days after dox treatment, along with hemorrhage and edema at 7 days. *b*, Total neutrophils, macrophages, and lymphocytes in lung lavage from IKTA mice treated with dox for 3 or 7 days compared with WT mice treated with dox for 7 days ($n = 3$–4/group, $*$, $p < 0.05$ compared with WT, $**$, $p < 0.05$ compared with WT and IKTA mice treated with dox for 3 days). *c*, Lung lavage protein concentration in untreated WT and IKTA mice (day 0) and in both groups after 3 or 7 days of dox treatment ($n = 4$/group, $*$, $p < 0.01$ compared with WT). *d*, Multiprobe RNase protection assays for chemokines from lungs of IKTA or WT mice treated with dox for 7 days and IKTA mice without the addition of dox to drinking water. Each lane represents mRNA from a separate mouse.

Table I. *Lung lavage cytokine levels (picogram per milliliter)*[a]

	WT plus dox	IKTA (no dox)	IKTA plus dox
TNF-α	5.6 ± 3.4	4.6 ± 4.6	32.9 ± 11.0
IL-1α	1.3 ± 0.8	0	11.0 ± 2.3*
IL-1β	0	0	40.0 ± 1.6*
IL-2	12.6 ± 5.8	8.7 ± 1.6	25.8 ± 0.5
IL-5	1.0 ± 0.4	0.6 ± 0.6	12.8 ± 5.7*
IL-6	1.4 ± 0.9	1.2 ± 0.1	197.0 ± 54.0*
IL-9	17.9 ± 0	11.3 ± 10.2	31.6 ± 2.5
IL-10	1.5 ± 0.8	0	7.4 ± 2.6
IL-12p40	80.4 ± 9.5	28.2 ± 5.9	258.9 ± 83.3*
IL-17	1.1 ± 0.6	1.1 ± 0.6	13.7 ± 3.0*
Eotaxin	32.1 ± 26.3	44.8 ± 22.9	130.5 ± 18.6
RANTES	0	0	530.8 ± 106.0*
MIP-2	2.0 ± 0.6	0	35.4 ± 10.7*
MIP-1β	10.4 ± 0.8	11.1 ± 2.4	31.8 ± 9.2
KC	42.9 ± 3.7	65.3 ± 11.0	447.5 ± 125.4*
MCP-1	22.3 ± 10.1	12.1 ± 10.1	567.7 ± 144.2*
G-CSF	2.8 ± 0.4	9.6 ± 7.1	94.5 ± 9.1*
GM-CSF	6.8 ± 3.2	11.4 ± 2.9	37.9 ± 16.6

[a] Values measured by luminex or ELISA are presented as mean (±SEM). n = 3–5/group. $*$, $p < 0.05$ compared with all other groups by ANOVA. Levels of IL-3, IL-4, IL-12p70, IL-13, MIP-1α, and IFNγ were below the limits of detection.

DNA. The microscopic images were obtained by using a Zeiss LSM 510 confocal microscope (Zeiss).

Statistical analysis

To assess differences among groups, analyses were performed with GraphPad Instat (GraphPad) using an unpaired t test or one-way ANOVA. Mortality differences were evaluated using a Fisher's exact test. Results are presented as mean ± SEM. Two-tailed p values <0.05 were considered significant.

Results

Construction of transgenic mice with inducible activation of NF-κB in airway epithelium

To achieve inducible NF-κB activation using the tet-on system, we placed a FLAG-tagged cIKK2 (1) under control of the $(tet\text{-}O)_7$-CMV promoter (Fig. 1*a*). To prevent basal leakiness of transgene expression, a construct expressing tetracycline-controlled tTS under the control of the Clara cell-specific CC10 promoter (obtained from Dr. J. Elias, Yale University (New Haven, CT), with permission of A. Farmer, BD Clontech) was coinjected with $(tet\text{-}O)_7$-FLAG-cIKK2 to generate double transgenic mice. Unbound tTS interacts with tet-O sites and functions as a transcriptional repressor; however, binding of dox to tTS results in dissociation from DNA, allowing rtTA binding and promoter activation (10, 17, 18). Double transgenic mice were bred with transgenic mice expressing rtTA under the control of the rat CC10 promoter (obtained from Dr. J. A. Whitsett) to generate triple transgenic mice, which were designated IKTA (for cIKK2 transactivated).

In initial experiments, IKTA transgenic mice were treated with dox in drinking water (2 g/L) for 3 days. Western blots for the FLAG-tagged transgene product identified cIKK2 expression exclusively in the lungs of dox-treated IKTA mice (Fig. 1*b*). No leakiness of FLAG-cIKK2 expression was detectable in other

Table II. *Mediator concentration MTEC supernatant (picogram per milliliter)*[a]

	IKTA	IKTA plus dox
IL-1α	0	6 (4)
IL-1β	0	6 (1)
IL-6	11 (3)	554 (102)*
IL-12 (p70)	0	0
G-CSF	3247 (199)	9366 (460)*
GM-CSF	236 (61)	3816 (280)*
MIP-1α	0	0
MIP-2	121 (8)	833 (5)*
KC	9859 (507)	15908 (434)*
RANTES	242 (78)	14267 (632)*
TNF-α	0	0
IFN-γ	0	0

[a] Values measured by luminex or ELISA are presented as mean ($\pm$SEM). n = 3/group. *, $p < 0.05$ compared with IKTA cells (without dox treatment).

tissues following dox treatment or in the lungs in the absence of dox. By immunohistochemistry, FLAG-cIKK2 expression was localized to the airway epithelium (Fig. 1*c*). We investigated whether FLAG-cIKK2 expression in airway epithelium was sufficient to activate NF-κB by performing EMSAs using lung tissue nuclear protein extracts. Compared with controls, NF-κB activation was increased in lungs of dox-treated IKTA mice (Fig. 1*d*). Taken together, these data show that treatment of IKTA mice with dox induces expression of FLAG-cIKK2 exclusively in airway epithelial cells at levels sufficient to activate NF-κB.

Sustained NF-κB activation in airway epithelium results in neutrophilic lung inflammation and severe lung injury

Although untreated IKTA mice exhibited normal lung histology, IKTA mice showed progressive lung inflammation and injury after 3 and 7 days of dox treatment (Fig. 2*a*). After 3 days of dox treatment, lungs from IKTA mice showed evidence of edema and a cellular infiltrate consisting of neutrophils and macrophages. By 7 days of dox treatment, however, a massive infiltration of inflammatory cells into the lung parenchyma was present, along with septal thickening, edema, and alveolar hemorrhage. Other organs, including liver, spleen, and kidney, showed no evidence of inflammation or architectural abnormalities (data not shown).

By lung lavage, increased numbers of neutrophils and macrophages were identified in the airways of IKTA mice at 3 days after introduction of dox (Fig. 2*b*). After 7 days of dox treatment, increased numbers of neutrophils, macrophages, and lymphocytes were present in lung lavage from IKTA mice compared with dox-treated wild-type (WT) mice, and neutrophils were further elevated compared with IKTA mice treated with dox for 3 days. We measured protein concentration in lung lavage from IKTA mice and WT controls at baseline and after dox treatment as an indicator of vascular permeability (Fig. 2*c*). Compared with baseline, protein concentration in IKTA mice increased 3-fold by 3 days of dox treatment, and by day 7 of dox treatment, protein concentration had increased >10-fold above baseline. Lung lavage protein concentration was similar in untreated WT and IKTA mice and did not change in WT mice following dox treatment. Consistent with these results, wet/dry ratios were increased in dox-treated IKTA mice treated with dox for 3 days compared with controls (wet/dry ratio for WT mice 4.7 $\pm$ 0.1 for WT mice vs 5.7 $\pm$ 0.2 for IKTA, $p < 0.01$).

Activation of NF-κB in airway epithelium resulted in production of a variety of inflammatory mediators. Table I shows the profile of cytokines and chemokines up-regulated in lung lavage from IKTA mice treated with dox for 7 days compared with dox-treated WT mice and IKTA mice without dox treatment. Significantly increased levels of IL-1α, IL-1β, IL-5, IL-6, IL-12, IL-17, RANTES, MIP-2, KC, MCP-1, and G-CSF were observed in dox-treated IKTA mice. No differences in mediator production were identified between WT mice and IKTA mice in the absence of dox treatment. We used multiprobe RNase protection assays to confirm that mRNA expression of selected chemokines was increased in the lungs of dox-treated IKTA mice (Fig. 2*d*). Protein and mRNA measurements of mediators correlated well with the exception of MCP-1, which was increased in lung lavage fluid by Luminex assay, but increased mRNA expression was not identified in the lungs of dox-treated IKTA mice at this time point. Taken together, these studies show that sustained activation of NF-κB in IKTA mice (in the absence of a specific inflammatory stimulus) results in a pattern of progressive lung inflammation and injury associated with production of a number of NF-κB-regulated cytokines and chemokines.

To determine which inflammatory mediators are produced directly by airway epithelial cells following NF-κB activation, we harvested MTECs and grew them in air-liquid interface conditions to obtain highly differentiated airway epithelium (15). Cultures of MTECs from IKTA mice were treated with dox (0.5 μg/ml) for 48 h, and transgene induction was identified by immunostaining of

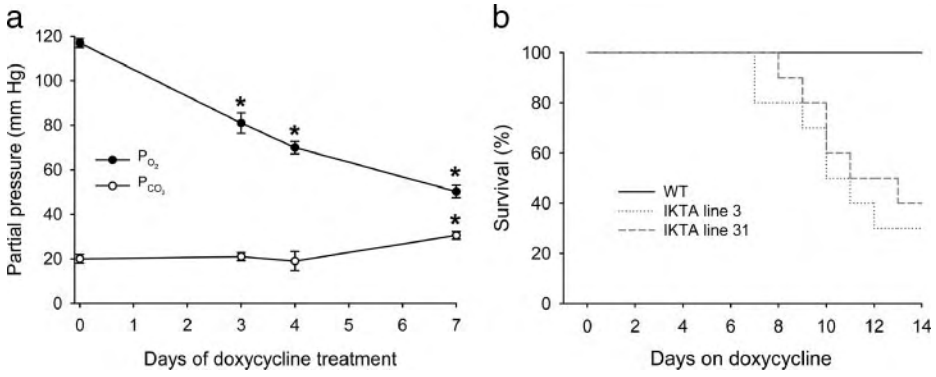

FIGURE 3. Treatment of IKTA mice with dox results in hypoxemia and increased mortality. *a*, Serial arterial blood gas measurements were obtained from indwelling carotid artery catheters. PO_2 and PCO_2 were assessed in IKTA mice at baseline and up to 7 days of dox treatment (n = 3–4/time point, *, $p < 0.01$ compared with baseline). *b*, Mortality rates in mice from IKTA lines 3 and 31 compared with WT controls through 14 days of dox treatment. Although all WT mice survived, 60% of mice in IKTA line 31 and 70% of mice in IKTA line 3 died between day 7 and 14 (n = 10 mice/group).

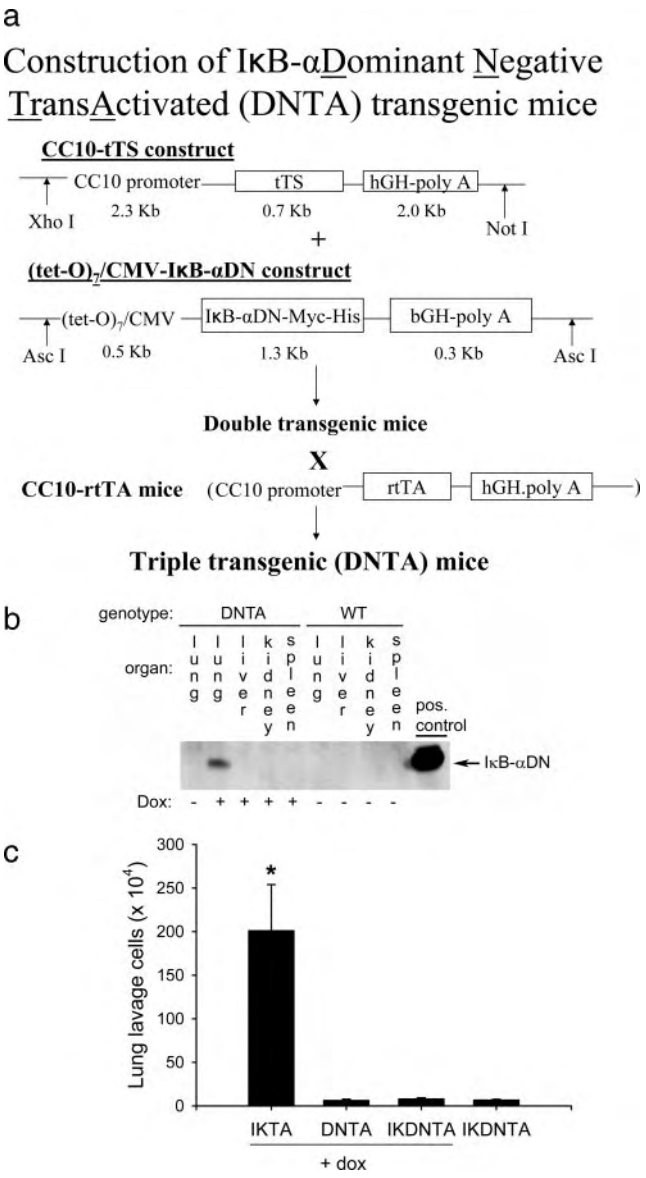

FIGURE 4. DNTA transgenic mice express a dominant inhibitor of the NF-κB pathway in airway epithelium. *a*, Schematic for construction of DNTA transgenic mice. *b*, Western blot analysis for Myc-His-tagged IκB-αDN expression in tissue homogenates obtained from WT and DNTA mice and DNTA mice treated with dox for 7 days. Transgene expression is detected only in the lungs of DNTA mice following dox treatment. *c*, DNTA mice were crossed with IKTA mice (line 26) to create IKDNTA mice that express both transgenes. Total cell counts in lung lavage are shown for IKTA mice (line 26), DNTA mice, and IKDNTA mice following 7 days of dox treatment and IKDNTA mice without dox treatment. The inflammatory cell influx was inhibited in dox-treated IKDNTA mice, indicating that expression of IκB-αDN blocks cIKK2-induced inflammation ($n = 4-8$/group, $*$, $p < 0.05$ compared with other groups).

FLAG-cIKK2 (data not shown). Increased concentrations of IL-6, G-CSF, GM-CSF, MIP-2, KC, and RANTES were identified in cell culture supernatants of dox-treated IKTA cells compared with IKTA cells in the absence of dox (Table II). These findings suggest that direct NF-κB activation in airway epithelial cells is sufficient to produce a number of mediators, including IL-6, G-CSF, MIP-2, KC, and RANTES, that are increased in the lungs of dox-treated IKTA mice. Other mediators that are increased in lung lavage fluid from dox-treated IKTA mice, such as IL-1α, IL-1β, and IL-12p40,

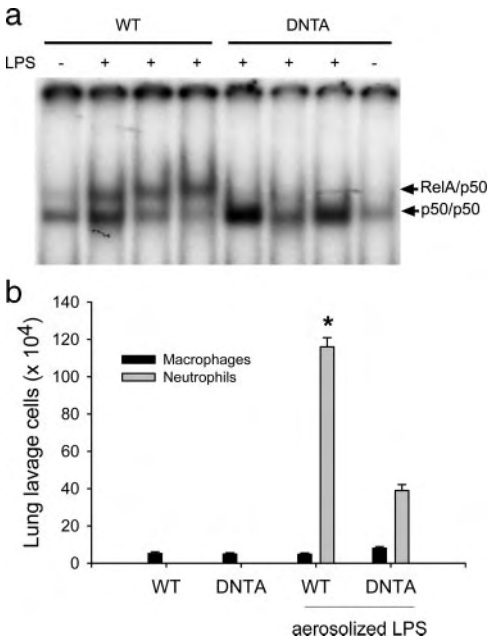

FIGURE 5. DNTA mice have reduced NF-κB activation and neutrophil influx into the airways after aerosolized LPS. WT or DNTA mice were given dox (2 g/L) in drinking water for 1 wk, treated with aerosolized LPS, and lungs were harvested 4 h later. *a*, EMSA for NF-κB binding using lung nuclear protein extracts indicates that induction of the RelA/p50 band is reduced in DNTA mice compared with WT in LPS-treated mice. *b*, Lung lavage cell counts show that LPS-induced neutrophil recruitment is inhibited in DNTA mice ($n = 3$/group, $*$, $p < 0.05$ compared with other groups).

may be up-regulated indirectly through recruitment or activation of inflammatory cells in the lungs.

We sought to determine the physiological effects of lung inflammation/injury resulting from epithelial NF-κB activation in IKTA mice by measuring arterial PO_2. Serial arterial blood gas analysis was done with indwelling carotid artery catheters in unanesthetized IKTA mice treated with dox (Fig. 3*a*). Baseline PO_2 (123.9 ± 4.67 mm Hg) and PCO_2 (20.1 ± 0.93 mm Hg) in IKTA mice were similar to WT controls (data not shown). With continued dox treatment, arterial PO_2 in IKTA mice decreased to 50.3 ± 2.81 mmHg by day 7 and PCO_2 increased to 30.5 ± 4.33 mm Hg. Arterial oxygen saturation decreased from 99 ± 0.1% at baseline to 81 ± 2.7% after 7 days of dox treatment in IKTA mice ($p < 0.001$). WT controls with indwelling carotid artery catheters treated with dox for 1 wk did not show any changes from baseline in arterial PO_2, PCO_2, or arterial oxygen saturation (data not shown).

Continued dox treatment resulted in substantial mortality in IKTA mice between 1 and 2 wk (Fig. 3*b*). In two separate lines of IKTA mice, mortality rates of 60 and 70% were found by 2 wk of dox treatment, whereas no mortality was observed in WT control mice treated with dox for 2 wk. Taken together, these studies demonstrate that persistent induction of NF-κB in airway epithelial cells is sufficient to cause lung inflammation and injury. Lung injury in this model results in progressive hypoxemia with a high mortality rate.

Construction and characterization of transgenic mice that express a dominant inhibitor of NF-κB in airway epithelium

We placed a Myc-His tagged dominant inhibitor of the NF-κB pathway (IκB-αDN) under control of the (tet-O)$_7$-CMV promoter (Fig. 4*a*). IκB-αDN is an avian IκB-α with adenine substitutions at serines 36 and 40 that inhibit phosphorylation and degradation of the protein, therefore blocking NF-κB nuclear translocation (8, 11,

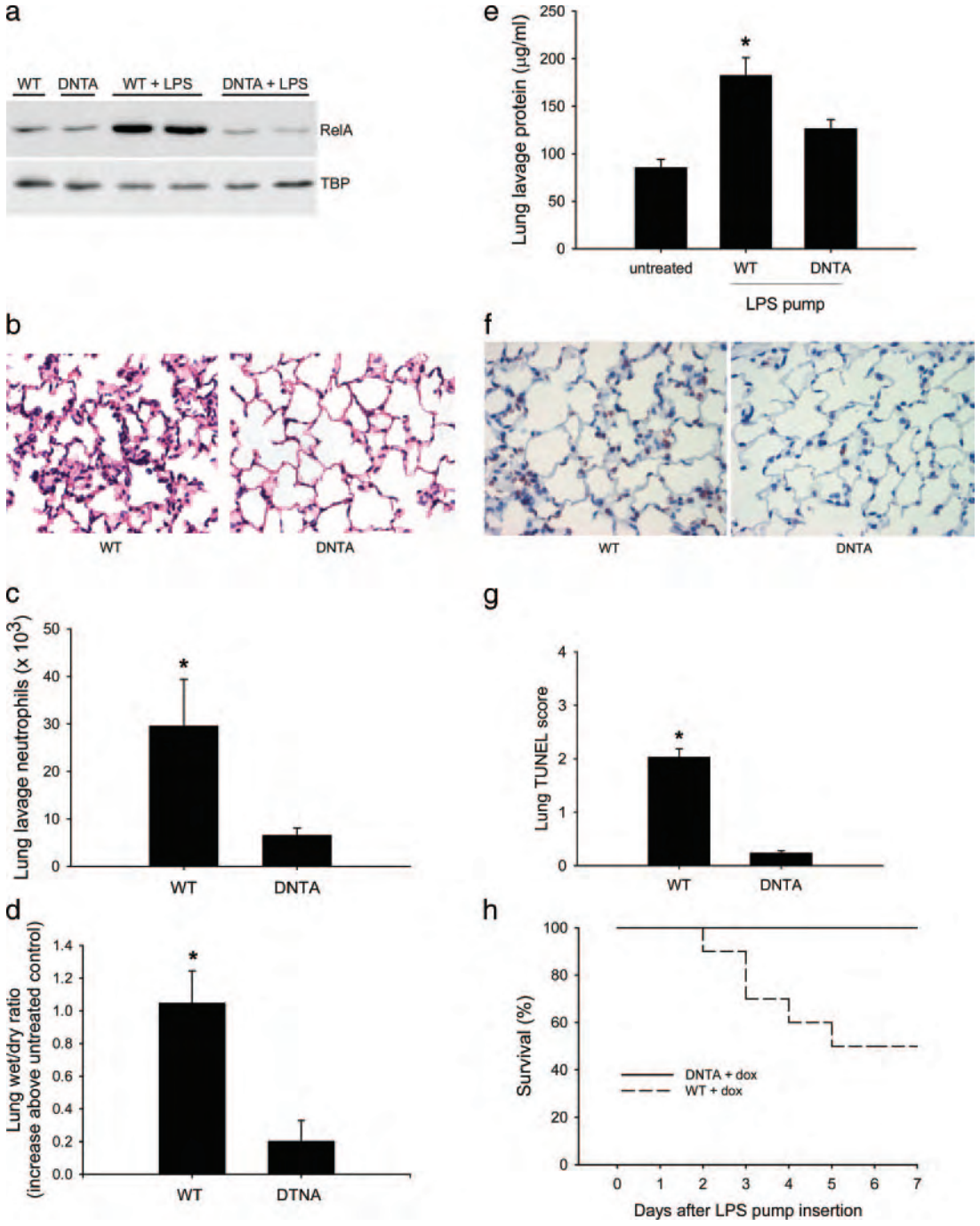

FIGURE 6. DNTA mice are protected from *E. coli* LPS-induced lung inflammation and injury. WT or DNTA mice were treated with dox (2 g/L) in drinking water for 1 wk, followed by i.p. implantation of osmotic pumps delivering LPS. *a*, Western blot analysis from lung nuclear protein extracts showing impaired nuclear translocation of RelA in DNTA mice at 4 h after LPS pump implantation (DNTA + LPS) compared with WT mice (WT + LPS). Samples from DNTA mice and WT mice without LPS pumps are shown as controls. TATA binding protein (TBP) was identified as a loading control. *b*, H&E-stained lung sections from WT and DNTA mice harvested 48 h after i.p. placement of pumps that deliver LPS continuously for 24 h. Lung inflammation and edema were markedly reduced in dox-treated DNTA mice. *c*, Lung lavage neutrophils obtained at 48 h after LPS pump placement ($n = 10$/group; $*$, $p < 0.05$). *d*, Lung wet/dry ratios for WT and DNTA mice treated with LPS pumps presented as increase above untreated controls ($n = 10$/group, $*$, $p < 0.01$). *e*, Lung lavage protein concentration in untreated WT mice and WT and DNTA mice at 48 h after treatment with LPS pump ($n = 6$/group, $*$, $p < 0.05$ compared with untreated mice and LPS pump-treated DNTA mice). *f* and *g*, Representative photomicrographs of TUNEL staining (brown nuclear stain) and scoring of TUNEL$^+$ cells in lung parenchyma from WT and DNTA mice at 48 h after treatment with LPS pumps ($n = 8$/group, $*$, $p < 0.05$). *h*, Mortality rates in dox-treated WT and DNTA mice following i.p. implantation of osmotic pumps that deliver LPS at 8 μg/h over 72 h ($n = 10$/group, $*$, $p < 0.05$).

12). Double transgenic mice containing (tet-O)$_7$-IκB-αDN-Myc-His and CC-10-tTS constructs were produced and cross-mated with CC10-rtTA mice to create triple transgenic mice with inducible expression of IκB-αDN-Myc-His in airway epithelium, which were designated DNTA (for IκB-αDN transactivated). As with IKTA mice, dox treatment resulted in transgene expression exclusively in the lungs (Fig. 4*b*). No leakiness of transgene expression was identified in the absence of dox. Immunohistochemistry for

Table III. *Mediators in lung lavage at baseline and 48 h after implantation of LPS pump (picogram per milliliter)*[a]

	WT	DNTA	WT (plus dox) plus LPS	DNTA (plus dox) plus LPS
TNF-α	0	0	22.7 ± 17.7	1.2 ± 0.5
IL-1α	1.7 ± 0.6	1.8 ± 0.1	81.1 ± 9.3	61.1 ± 6.2
IL-1β	0	0	10.2 ± 6.1	3.7 ± 1.6
IL-2	0	0	24.2 ± 2.4	12.4 ± 4.1**
IL-3	0	0	2.7 ± 0.6	1.0 ± 0.5
IL-5	0	0	3.6 ± 1.1	1.6 ± 0.3
IL-6	0	0	16.2 ± 2.2	9.3 ± 2.2
IL-9	0	0	170.0 ± 31.0	93.0 ± 20.0
IL-10	0	0	7.7 ± 2.8	0
IL-12p40	32.4 ± 5.4	17.8 ± 5.5	65.2 ± 19.1	49.0 ± 10.4
IL-12p70	0	0	8.6 ± 3.8	4.1 ± 2.0
Eotaxin	0	0	76.0 ± 39.3	10.7 ± 10.4
RANTES	2.3 ± 0.8	1.1 ± 0.4	31.8 ± 2.8	19.1 ± 3.0**
MIP-2	0	0	21.9 ± 3.2	4.1 ± 1.5**
MIP-1β	0	0	33.8 ± 8.9	8.9 ± 2.6**
KC	60 ± 3.3	25.0 ± 2.2*	696 ± 77	290 ± 36**
MCP-1	24.3 ± 8.1	16.2 ± 9.3	668 ± 134	288 ± 59**
G-CSF	1.5 ± 0.5	1.9 ± 0	16,597 ± 5,651	2,729 ± 509**
GM-CSF	0	0	23.3 ± 5.3	9.7 ± 2.5**
IFNγ	0	0	8.7 ± 5.4	6.0 ± 3.0

[a] Values measured by luminex or ELISA are presented as mean (±SEM). $n = 4$ mice/group at baseline and 6/group after LPS pump. *, $p < 0.05$ compared with WT group at baseline; **, $p < 0.05$ compared with WT group treated with LPS pumps. Levels of IL-4, IL-13, IL-17, and MIP-1α were below the limits of detection.

the Myc tag on IκB-αDN localized transgene expression to the airway epithelium in dox-treated mice (data not shown). Lungs of dox-treated DNTA mice were histologically normal.

To show that IκB-αDN expression was sufficient to block NF-κB activation in DNTA mice, we crossed IKTA and DNTA mice to obtain mice that inducibly expressed both transgenes (cIKK2 and IκB-αDN-Myc-His). Fig. 4*c* shows that dox treatment of these mice (IKDNTA) results in suppression of lung inflammation induced by cIKK2. These experiments indicate that expression of IκB-αDN in epithelium inhibits NF-κB activation and confirm that cIKK2-induced lung inflammation is transduced through activation of the NF-κB pathway.

Prevention of lung inflammation and injury by blocking NF-κB activation in airway epithelium

After demonstrating that expression of IκB-αDN in epithelial cells blocks NF-κB activation, we undertook studies to identify the effects of inhibiting epithelial NF-κB following treatment with *E. coli* LPS. Initially, WT and DNTA mice were treated with dox for 1 wk to induce transgene expression and then were administered aerosolized *E. coli* LPS (8 ml of a 0.1 μg/ml solution) as reported previously (13). At 4 h after LPS treatment, lungs were lavaged and harvested for determination of neutrophilic alveolitis and NF-κB activation by EMSA. As shown in Fig. 5*a*, dox treatment of DNTA mice reduced nuclear translocation of RelA/p50 heterodimers (the transactivating component of NF-κB) in lung tissue following treatment with aerosolized LPS. Neutrophil influx into the airways was also diminished in DNTA mice (Fig. 5*b*). These findings show that expression of IκB-αDN blocks NF-κB activation and neutrophil recruitment induced by aerosolized LPS.

In addition to direct airway exposure to LPS, we investigated whether blocking NF-κB activation in airway epithelium could reduce lung inflammation and injury resulting from systemic delivery of *E. coli* LPS. We used a model of abdominal sepsis in which LPS is delivered into the peritoneum (8 μg/h) over 24 h via a surgically implanted osmotic pump (9). Using transgenic NF-κB reporter mice, we have recently shown that this model results in persistent lung NF-κB activation that prominently involves airway epithelium (9). For these studies, we treated WT or DNTA mice with dox for 1 wk, followed by implantation of the LPS pump. At 4 h after osmotic pump implantation, NF-κB activation was reduced in DNTA mice as indicated by Western blots for RelA in lung nuclear protein extracts (Fig. 6*a*). At 48 h after implantation, WT mice exhibited histological evidence of lung injury with edema and inflammatory cell influx, which was markedly reduced in DNTA mice (Fig. 6*b*). Consistent with these findings, lung lavage neutrophils were reduced in DNTA mice (Fig. 6*c*). In addition, total lung lavage cells were lower in dox-treated DNTA mice than controls at 48 h after placement of LPS pumps ($16.5 \pm 1.6 \times 10^4$ cells in DNTA mice compared with $35.0 \pm 4.6 \times 10^4$ cells in WT mice, $n = 10$/group, $p < 0.01$). No differences in peripheral white blood cell counts were identified between dox-treated WT and DNTA mice at baseline, 4 h, or 48 h after placement of LPS pumps (data not shown). WT and DNTA mice treated with LPS pumps in the absence of dox treatment had BAL cell counts and peripheral white blood cell counts similar to dox-treated WT mice (data not shown).

We performed multiplex cytokine analysis to evaluate the effects of epithelial NF-κB inhibition on the mediator profile in lung lavage fluid obtained at the time of harvest (Table III). Untreated WT and DNTA mice were included as controls. At 48 h after implantation of LPS pumps, levels of MIP-2 and KC were lower in dox-treated DNTA mice than in dox-treated WT mice, which is consistent with the reduced neutrophilic lung inflammation observed in these mice. Other mediators that were reduced in DNTA mice included RANTES, MIP-1β, MCP-1, G-CSF, and GM-CSF.

At 48 h after implantation of LPS pumps, evidence of disruption of the alveolar capillary barrier was present in dox-treated WT mice with increased lung wet/dry ratios and increased protein concentration in lung lavage compared with control mice in the absence of LPS treatment. Dox-treated DNTA mice, however, were almost completely protected from edema and protein leak after LPS treatment (Fig. 6, *d* and *e*). WT and DNTA mice treated with LPS pumps in the absence of dox treatment had lung wet/dry ratios that were similar to dox-treated WT mice (data not shown). Because disruption of the alveolar-capillary barrier has been linked to

apoptosis of structural cells (both epithelium and endothelium) in lung parenchyma (19–21), we investigated whether LPS-induced alveolar cell death was reduced in DNTA mice compared with WT. As shown in Fig. 6, *f* and *g*, a striking difference in $TUNEL^+$ cells was identified in the lung parenchyma of WT and DNTA mice at 48 h after LPS pump implantation. Frequent $TUNEL^+$ structural and inflammatory cells were identified in lungs of dox-treated WT mice, whereas very few $TUNEL^+$ cells were identified in dox-treated DNTA mice (Fig. 6*f*). Semiquantitative analysis of lung sections from mice treated with dox, followed by LPS pumps, showed a significant reduction in the number of $TUNEL^+$ cells in lungs of DNTA mice compared with WT mice (Fig. 6*g*). TUNEL scores were similar in LPS-treated WT mice with or without dox treatment, and both DNTA and WT mice had very few $TUNEL^+$ cells in lung parenchyma in the absence of LPS treatment (data not shown). Because transgene expression was limited to bronchial epithelium in DNTA mice (as detected by immunohistochemistry), it appears that protection from apoptosis in alveolar cells of DTNA mice is an indirect effect of reduced inflammatory signaling through the NF-κB pathway in airway epithelium.

To determine whether reduced lung injury in DNTA mice could lead to improved survival, we performed peritoneal implantation of osmotic pumps that deliver LPS (8 μg/h) for 72 h into dox-treated WT and DNTA mice. As shown in Fig. 6*h*, delivery of LPS over 72 h resulted in 50% mortality in WT mice at day 7; however, all dox-treated DNTA mice survived.

Discussion

These studies describe the generation, characterization, and use of a novel modular transgenic system that enables regulation of NF-κB activity in specific cell populations. By using this approach to specifically target the NF-κB pathway in airway epithelium, we have defined a pivotal role for epithelial cells in controlling lung inflammation and injury. In DNTA mice, expression of a dominant NF-κB inhibitor in CC10 expressing cells reduces neutrophilic lung inflammation resulting from airway or systemic delivery of LPS and diminishes lung injury and mortality following endotoxemia. In complementary studies using IKTA-transgenic mice, we show that IKK2 expression causes persistent activation of NF-κB in airway epithelial cells, resulting in cytokine production, inflammatory cell recruitment, lung injury, hypoxemia, and high mortality. In IKTA mice, dox treatment induces progressive lung injury with inflammation and edema by 3 days, followed by impaired gas exchange and death after as few as 7 days. Since the onset of detectable transgene expression occurs by 24–48 h after adding dox to drinking water (data not shown), induction of lung injury in dox-treated IKTA mice occurs in a time frame similar to that observed in the systemic LPS model. Taken together, our studies suggest a paradigm in which inflammatory signaling in airway epithelium plays a critical role in orchestrating the lung's response to LPS (and possibly other injurious stimuli) delivered either locally (via the airways) or systemically (via the bloodstream). In this model, the NF-κB pathway in airway epithelium is a focal point for control of lung injury through regulated production of mediators that participate in recruitment/activation of inflammatory cells, induction of alveolar cell death, and disruption of the alveolar capillary barrier.

Although a large number of studies have investigated regulation of inflammatory responses to environmental stress through the NF-κB pathway, the majority of these studies have focused on NF-κB signaling in immune cells. In the lungs, NF-κB is activated in macrophages early after LPS treatment (22), and macrophages are required for maximal activation of NF-κB in the whole lung and the resulting neutrophil influx (23, 24). This information suggests that alveolar macrophages are required for initiation of LPS-induced inflammatory responses in the lungs, likely through activation of NF-κB signaling. However, our data and another recent study (25) indicate that NF-κB signaling in nonimmune cells is critical for determining the lung's response to injurious stimuli. Kisseleva et al. (25) expressed a dominant inhibitor of the NF-κB pathway in endothelial cells using the Tie2 promoter and found that NF-κB blockade resulted in increased vascular permeability in the lungs, increased endothelial apoptosis, and increased mortality in response to systemic LPS. Based on these findings, LPS-induced NF-κB activation in endothelium appears to be primarily protective through maintenance of vascular integrity. In contrast, NF-κB signaling in airway epithelial cells leads to increased vascular permeability in the lungs, and inhibiting LPS-induced NF-κB activation in these cells reduces lung inflammation, edema, and alveolar cell death. Therefore, targeting of NF-κB pathway in specific cell types or compartments (like the airways) may be necessary to effectively reduce lung inflammation and injury.

Previous studies have suggested that lung epithelial cells impact neutrophil recruitment through NF-κB pathway signaling. We found that intratracheal administration of adenoviral vectors expressing NF-κB-activating transgenes in mice results in neutrophilic inflammation (11). Mice deficient in RelA, the primary transactivating component of NF-κB, and TNFR1 exhibit a marked reduction of neutrophilic inflammation in response to airway delivery of LPS (26). In contrast, bone marrow chimeras in which the RelA/TNFR1 deficiency is limited to immune cells (including lung macrophages) have normal LPS-induced neutrophil recruitment, implicating non-bone marrow-derived cells in generation of neutrophilic inflammation in this model. In addition, transgenic mice constitutively expressing a NF-κB inhibitor in lung epithelial cells have reduced neutrophil influx into the airways in response to intranasal instillation of *E. coli* LPS (27, 28). In the gastrointestinal tract, selective deletion of IKK2 in intestinal epithelial cells impairs NF-κB activation and results in decreased lung and systemic inflammation in a gut ischemia-reperfusion model through reduction of TNF-α expression (29). However, local tissue injury in the intestinal mucosa is exacerbated in this model related to increased apoptosis. In combination with the present study, these findings point to the NF-κB pathway in epithelial cells as an important target for therapies designed to modulate inflammation-induced tissue injury.

In humans, evidence supports the role of NF-κB-dependent mediators in inducing lung injury, although the cellular source of these mediators is not well defined. A variety of NF-κB linked cytokines and chemokines has been reported to be increased in lung lavage fluid obtained from patients with ARDS, including TNF-α, IL-1β, IL-6, and IL-8 (6, 30, 31). Increased concentrations of IL-8, a NF-κB-regulated CXC chemokine in humans, are found in lungs of at-risk patients who progress to ARDS, and high levels of IL-8 and neutrophils in lung lavage have been correlated with increased mortality in ARDS patients (32–34). Our mouse model indicates that prolonged activation of NF-κB in epithelial cells is sufficient to produce an inflammatory profile similar to human ARDS, as well as the pathophysiological and histological abnormalities. These findings solidify the NF-κB pathway as an important therapeutic target for interventions targeted to limit lung injury in ARDS. It is intriguing to note that the relatively small percentage of lung cells that constitute the airway epithelium appear to have the potential to play a powerful protective role against lung injury. Airway epithelial cells are relatively accessible to aerosolized agents, and specific inhibition of NF-κB activity by this route could leave intact host defense mechanisms mediated by inflammatory cells in the lung.

In summary, our findings support three major conclusions. First, we have generated a modular transgenic system that can be used to efficiently modulate NF-κB activity in specific cell types. These mice have the potential to be used in a broad range of future research endeavors. Second, our findings implicate the NF-κB pathway in airway epithelial cells is critical for generation of lung inflammation and injury in response to local and systemic stimuli. Indeed, persistent NF-κB activation in epithelium may provide a common pathway for driving the dysregulated inflammatory response that culminates in ARDS. Third, while interventions that reduce inflammation by blocking NF-κB activation in epithelium must be rigorously examined to define their effects on host defense, the airway epithelium may prove to be an important and feasible target for reducing or preventing lung injury in patients at risk for ARDS.

Acknowledgments

We thank Dr. Jeffrey A. Whitsett of the University of Cincinnati College of Medicine for the donation of CC-10 rtTA-expressing transgenic mice used in these studies. We also thank the Vanderbilt University Mouse Metabolic Phenotyping Core, the Vanderbilt Transgenic/ES Shared Resource, and the Mouse Pathology Core for their valuable assistance.

Disclosures

The authors have no financial conflict of interest.

References

1. Mercurio, F., H. Zhu, B. W. Murray, A. Shevchenko, B. L. Bennett, J. Li, D. B. Young, M. Barbosa, M. Mann, A. Manning, and A. Rao. 1997. IKK-1 and IKK-2: cytokine-activated IκB kinases essential for NF-κB activation. *Science* 278: 860–866.
2. Blackwell, T. S., and J. W. Christman. 1997. The role of nuclear factor-κB in cytokine gene regulation. *Am. J. Respir. Cell Mol. Biol.* 17: 3–9.
3. Ghosh, S., M. J. May, and E. B. Kopp. 1998. NF-κB and Rel proteins: evolutionarily conserved mediators of immune responses. *Annu. Rev. Immunol.* 16: 225–260.
4. Ware, L. B., and M. A. Matthay. 2000. The acute respiratory distress syndrome. *N. Engl. J. Med.* 342: 1334–1349.
5. Kollef, M. H., and D. P. Schuster. 1995. The acute respiratory distress syndrome. *N. Engl. J. Med.* 332: 27–37.
6. Bhatia, M., and S. Moochhala. 2004. Role of inflammatory mediators in the pathophysiology of acute respiratory distress syndrome. *J. Pathol.* 202: 145–156.
7. Muir, A., G. Soong, S. Sokol, B. Reddy, M. I. Gomez, A. Van Heeckeren, and A. Prince. 2004. Toll-like receptors in normal and cystic fibrosis airway epithelial cells. *Am. J. Respir. Cell Mol. Biol.* 30: 777–783.
8. Sadikot, R. T., H. Zeng, M. Joo, M. B. Everhart, T. P. Sherrill, B. Li, D. S. Cheng, F. E. Yull, J. W. Christman, and T. S. Blackwell. 2006. Targeted immunomodulation of the NF-κB pathway in airway epithelium impacts host defense against *Pseudomonas aeruginosa*. *J. Immunol.* 176: 4923–4930.
9. Everhart, M. B., W. Han, T. P. Sherrill, M. Arutiunov, V. V. Polosukhin, J. R. Burke, R. T. Sadikot, J. W. Christman, F. E. Yull, and T. S. Blackwell. 2006. Duration and intensity of NF-κB activity determine the severity of endotoxin-induced acute lung injury. *J. Immunol.* 176: 4995–5005.
10. Zhu, Z., B. Ma, R. J. Homer, T. Zheng, and J. A. Elias. 2001. Use of the tetracycline-controlled transcriptional silencer (tTS) to eliminate transgene leak in inducible overexpression transgenic mice. *J. Biol. Chem.* 276: 25222–25229.
11. Sadikot, R. T., W. Han, M. B. Everhart, O. Zoia, R. S. Peebles, E. D. Jansen, F. E. Yull, J. W. Christman, and T. S. Blackwell. 2003. Selective I κB kinase expression in airway epithelium generates neutrophilic lung inflammation. *J. Immunol.* 170: 1091–1098.
12. Blackwell, T. S., F. E. Yull, C. L. Chen, A. Venkatakrishnan, T. R. Blackwell, D. J. Hicks, L. H. Lancaster, J. W. Christman, and L. D. Kerr. 2000. Multiorgan nuclear factor κB activation in a transgenic mouse model of systemic inflammation. *Am. J. Respir. Crit. Care Med.* 162: 1095–1101.
13. Yull, F. E., W. Han, E. D. Jansen, M. B. Everhart, R. T. Sadikot, J. W. Christman, and T. S. Blackwell. 2003. Bioluminescent detection of endotoxin effects on HIV-1 LTR-driven transcription in vivo. *J. Histochem. Cytochem.* 51: 741–749.
14. Blackwell, T. S., T. R. Blackwell, and J. W. Christman. 1997. Impaired activation of nuclear factor-κB in endotoxin-tolerant rats is associated with down-regulation of chemokine gene expression and inhibition of neutrophilic lung inflammation. *J. Immunol.* 158: 5934–5940.
15. You, Y., E. J. Richer, T. Huang, and S. L. Brody. 2002. Growth and differentiation of mouse tracheal epithelial cells: selection of a proliferative population. *Am. J. Physiol.* 283: L1315–L1321.
16. Look, D. C., M. J. Walter, M. R. Williamson, L. Pang, Y. You, J. N. Sreshta, J. E. Johnson, D. S. Zander, and S. L. Brody. 2001. Effects of paramyxoviral infection on airway epithelial cell Foxj1 expression, ciliogenesis, and mucociliary function. *Am. J. Pathol.* 159: 2055–2069.
17. Deuschle, U., W. K. Meyer, and H. J. Thiesen. 1995. Tetracycline-reversible silencing of eukaryotic promoters. *Mol. Cell. Biol.* 15: 1907–1914.
18. Forster, K., V. Helbl, T. Lederer, S. Urlinger, N. Wittenburg, and W. Hillen. 1999. Tetracycline-inducible expression systems with reduced basal activity in mammalian cells. *Nucleic Acids Res.* 27: 708–710.
19. Martin, T. R., N. Hagimoto, M. Nakamura, and G. Matute-Bello. 2005. Apoptosis and epithelial injury in the lungs. *Proc. Am. Thorac. Soc.* 2: 214–220.
20. Kawasaki, M., K. Kuwano, N. Hagimoto, T. Matsuba, R. Kunitake, T. Tanaka, T. Maeyama, and N. Hara. 2000. Protection from lethal apoptosis in lipopolysaccharide-induced acute lung injury in mice by a caspase inhibitor. *Am. J. Pathol.* 157: 597–603.
21. Fujita, M., K. Kuwano, R. Kunitake, N. Hagimoto, H. Miyazaki, Y. Kaneko, M. Kawasaki, T. Maeyama, and N. Hara. 1998. Endothelial cell apoptosis in lipopolysaccharide-induced lung injury in mice. *Int. Arch. Allergy Immunol.* 117: 202–208.
22. Blackwell, T. S., L. H. Lancaster, T. R. Blackwell, A. Venkatakrishnan, and J. W. Christman. 1999. Differential NF-κB activation after intratracheal endotoxin. *Am. J. Physiol.* 277: L823–L830.
23. Koay, M. A., X. Gao, M. K. Washington, K. S. Parman, R. T. Sadikot, T. S. Blackwell, and J. W. Christman. 2002. Macrophages are necessary for maximal nuclear factor-κB activation in response to endotoxin. *Am. J. Respir. Cell Mol Biol.* 26: 572–578.
24. Lentsch, A. B., B. J. Czermak, N. M. Bless, N. Van Rooijen, and P. A. Ward. 1999. Essential role of alveolar macrophages in intrapulmonary activation of NF-κB. *Am. J. Respir. Cell Mol. Biol.* 20: 692–698.
25. Kisseleva, T., L. Song, M. Vorontchikhina, N. Feirt, J. Kitajewski, and C. Schindler. 2006. NF-κB regulation of endothelial cell function during LPS-induced toxemia and cancer. *J. Clin. Invest.* 116: 2955–2963.
26. Alcamo, E., J. P. Mizgerd, B. H. Horwitz, R. Bronson, A. A. Beg, M. Scott, C. M. Doerschuk, R. O. Hynes, and D. Baltimore. 2001. Targeted mutation of TNF receptor I rescues the RelA-deficient mouse and reveals a critical role for NF-κB in leukocyte recruitment. *J. Immunol.* 167: 1592–1600.
27. Poynter, M. E., C. G. Irvin, and Y. M. Janssen-Heininger. 2003. A prominent role for airway epithelial NF-κB activation in lipopolysaccharide-induced airway inflammation. *J. Immunol.* 170: 6257–6265.
28. Skerrett, S. J., H. D. Liggitt, A. M. Hajjar, R. K. Ernst, S. I. Miller, and C. B. Wilson. 2004. Respiratory epithelial cells regulate lung inflammation in response to inhaled endotoxin. *Am. J. Physiol.* 287: L143–L152.
29. Chen, L. W., L. Egan, Z. W. Li, F. R. Greten, M. F. Kagnoff, and M. Karin. 2003. The two faces of IKK and NF-κB inhibition: prevention of systemic inflammation but increased local injury following intestinal ischemia-reperfusion. *Nat. Med.* 9: 575–581.
30. Goodman, R. B., R. M. Strieter, D. P. Martin, K. P. Steinberg, J. A. Milberg, R. J. Maunder, S. L. Kunkel, A. Walz, L. D. Hudson, and T. R. Martin. 1996. Inflammatory cytokines in patients with persistence of the acute respiratory distress syndrome. *Am. J. Respir. Crit. Care Med.* 154: 602–611.
31. Schutte, H., J. Lohmeyer, S. Rosseau, S. Ziegler, C. Siebert, H. Kielisch, H. Pralle, F. Grimminger, H. Morr, and W. Seeger. 1996. Bronchoalveolar and systemic cytokine profiles in patients with ARDS, severe pneumonia and cardiogenic pulmonary oedema. *Eur. Respir. J.* 9: 1858–1867.
32. Miller, E. J., A. B. Cohen, S. Nagao, D. Griffith, R. J. Maunder, T. R. Martin, J. P. Weiner-Kronish, M. Sticherling, E. Christophers, and M. A. Matthay. 1992. Elevated levels of NAP-1/interleukin-8 are present in the airspaces of patients with the adult respiratory distress syndrome and are associated with increased mortality. *Am. Rev. Respir. Dis.* 146: 427–432.
33. Donnelly, S. C., R. M. Strieter, S. L. Kunkel, A. Walz, C. R. Robertson, D. C. Carter, I. S. Grant, A. J. Pollok, and C. Haslett. 1993. Interleukin-8 and development of adult respiratory distress syndrome in at-risk patient groups. *Lancet* 341: 643–647.
34. Baughman, R. P., K. L. Gunther, M. C. Rashkin, D. A. Keeton, and E. N. Pattishall. 1996. Changes in the inflammatory response of the lung during acute respiratory distress syndrome: prognostic indicators. *Am. J. Respir. Crit. Care Med.* 154: 76–81.

Host Nuclear Factor-κB Activation Potentiates Lung Cancer Metastasis

Georgios T. Stathopoulos,[1] Taylor P. Sherrill,[1] Wei Han,[1] Ruxana T. Sadikot,[1] Fiona E. Yull,[2] Timothy S. Blackwell,[1,2,3] and Barbara Fingleton[2]

[1]Division of Allergy, Pulmonary and Critical Care Medicine; [2]Department of Cancer Biology, Vanderbilt University School of Medicine; and [3]Department of Veterans Affairs, VA Tennessee Valley Healthcare System, Nashville, Tennessee

Abstract

Epidemiologic and experimental evidence suggests that a link exists between inflammation and cancer, although this relationship has only recently begun to be elucidated for lung cancer, the most frequently fatal human tumor. Nuclear factor-κB (NF-κB), a transcription factor that controls innate immune responses in the lungs, has been implicated as an important determinant of cancer cell proliferative and metastatic potential; however, its role in lung tumorigenesis is uncertain. Here, we specifically examine the role of NF-κB–induced airway inflammation in lung cancer metastasis using a model of intravenous injection of Lewis lung carcinoma cells into immunocompetent C57Bl/6 mice. Induction of lung inflammation by direct and specific NF-κB activation in airway epithelial cells potentiates lung adenocarcinoma metastasis. Moreover, we identify resident lung macrophages as crucial effectors of lung susceptibility to metastatic cancer growth. We conclude that NF-κB activity in host tissue is a significant factor in the development of lung metastasis. (Mol Cancer Res 2008;6(3):364–71)

Introduction

Although the association between inflammation and cancer was originally postulated long ago, it is only recently that we have begun to understand this relationship (1-3). It is now apparent that carcinogenesis and tumor progression are governed not only by genetic changes in cancer cells, but also by the host environment in which tumors develop and grow (4, 5). Inflammation profoundly affects the host milieu surrounding tumors by recruitment of a variety of inflammatory cells and secretion of a multitude of cytokines, chemokines, angiogenic factors, and matrix-degrading enzymes (4, 6). Although host immune cells are classically believed to mediate antitumor effects (paradigms of immune antitumor surveillance and tumor rejection), immune cells may promote tumor progression and metastasis when aberrantly accumulated at sites of ongoing inflammation (1). In this regard, tumor-associated macrophages have been linked to enhanced tumor progression and metastasis (7, 8).

The nuclear factor-κB (NF-κB) family of transcription factors are ubiquitous heterodimeric or homodimeric proteins that control innate immunity and inflammatory responses (9). Although NF-κB proteins are normally sequestered in the cytoplasm by inhibitory proteins known as IκBs, proteosomal degradation of the IκBs can be triggered by a variety of signals, resulting in translocation of the NF-κB dimer to the nucleus where it can activate transcription of target genes. NF-κB–controlled genes include cytokines, adhesion molecules, angiogenic factors, and enzymes that all have been associated with tumor progression and metastasis (4). Moreover, NF-κB affects neoplastic transformation, cell cycling, apoptosis, invasion, and metastasis in tumor cells (10-15). A recent study revealed that NF-κB activity in metastasizing colon cancer cells is critical in determining the effect of host proinflammatory mediators on the proliferative or apoptotic response of tumor cells (16). Thus, NF-κB is centrally positioned to provide a mechanistic link between inflammation and cancer progression and metastasis.

The lungs harbor the majority of human primary and metastatic neoplasms (17, 18). Although surgery often provides definitive cure and high rates of long-term survival for localized primary disease, the development of metastases precludes surgical treatment and dramatically compromises life expectancy and quality of life (19). In the lungs, conditions that increase the risk of primary lung cancer development, such as cigarette smoking, environmental pollutants, and chronic obstructive pulmonary disease, have been associated with NF-κB activation (20-23). In these studies, we hypothesized that a proinflammatory host lung microenvironment, such as that generated by persistent NF-κB activation, directly increases the host lung permissiveness to cancer cell metastasis. We tested this hypothesis in mice by direct interventions into the canonical NF-κB pathway in the host lungs by infection with NF-κB–modulating recombinant adenoviruses. We studied an adenocarcinoma cell line to emulate the majority of human disease, and we used immunocompetent mice to recapitulate the whole spectrum of host-tumor interactions (24). Here, we show

Received 7/2/07; revised 11/2/07; accepted 11/20/07.
Grant support: The Ingram Charitable Fund (B. Fingleton) and Vanderbilt-Ingram Cancer Center (F.E. Yull), NIH grants HL66196 (T.S. Blackwell) and HL61419 (T.S. Blackwell), the Department of Veterans Affairs (T.S. Blackwell), the Department of Defense Breast Cancer Program grant WX1XWH-04-1-0456 (F.E. Yull), and the Greek State Scholarship Foundation (G.T. Stathopoulos).
The costs of publication of this article were defrayed in part by the payment of page charges. This article must therefore be hereby marked *advertisement* in accordance with 18 U.S.C. Section 1734 solely to indicate this fact.
Note: G.T. Stathopoulos and T.P. Sherrill contributed equally to this work.
Requests for reprints: Barbara Fingleton, Department of Cancer Biology, Vanderbilt University School of Medicine, 734 PRB, 2220 Pierce Avenue, Nashville, TN 37232-6840. Phone: 615-936-5877; Fax: 615-936-2911. E-mail: Barbara.fingleton@vanderbilt.edu

doi:10.1158/1541-7786.MCR-07-0309

that increased NF-κB activity in host lung results in an enhanced metastatic phenotype. Importantly, our results suggest that targeting of host inflammatory cells, particularly macrophages, would confer a protective advantage in premetastatic disease.

Results

Intratracheal Adenoviral Instillation Is a Suitable Method for Increasing NF-κB Activity in the Lung

To generate NF-κB–induced inflammation in the lungs, we instilled adenoviral vectors encoding the active NF-κB molecule, RelA, intratracheally into mice. We have previously shown that intratracheal instillation of adenoviruses expressing NF-κB–activating transgenes results in infection of bronchial epithelial cells, NF-κB activation, and airway inflammation (25). To distinguish specific RelA-induced effects from nonspecific adenoviral-mediated events, we used control viruses (Ad-ctl) encoding either β-galactosidase, green fluorescent protein (GFP), or luciferase. We first used only the luciferase virus in C57Bl/6 mice to establish the time course of expression from intratracheal viral delivery. Efficient transgene delivery was confirmed using 10^9 plaque-forming units (pfu) of Ad-luciferase (Fig. 1A). Following luciferin injection, increased photon emission due to expression of the viral-encoded protein was detectable starting at day 3 (data not shown). Detectable luciferase signal was still present 14 days after virus infection, demonstrating that adenoviral transgene delivery to the lungs produces continued expression over a time period suitable for experimental metastasis assay (Fig. 1B). To show that treatment with Ad-RelA virus results in significant NF-κB activity in the lungs of exposed mice, we took advantage of a transgenic NF-κB reporter mouse model (26). We confirmed that Ad-RelA caused a significant increase in NF-κB–dependent luciferase activity in the lungs at 72 hours postinjection by measurement of chest bioluminescence, whereas control GFP adenovirus had no significant effect [Fig. 1C; luminescence emission (photonsl/s), mean ± SD: baseline = 5,557,183 + 3,965,979; control virus = 8,261,200 ± 3,864,549, $P = 0.36$ compared with baseline; Ad-RelA = 42,761,333 ± 35,490,104, $P = 0.029$ compared with baseline; $n = 3$ mice per group].

Airway Inflammation Resulting from Enhanced Host NF-κB Activity Increases Tumor Take

Experimental metastasis (tail vein) experiments allow testing of the later stages of the metastatic cascade, that is, survival in the circulation, extravasation and survival, and growth at a secondary site. Lewis lung carcinoma cells were originally established from a spontaneous lung tumor occurring in a C57Bl/6 mouse (27). In these experiments, our goal was to assess the effect of airway inflammation, as induced by RelA expression, on the metastatic ability of these cells using the experimental metastasis assay. Because this cell line is syngeneic with C57Bl/6 mice, we were able to examine the inflammatory effects on the background of full immune competence. Based on initial time course studies indicating substantial airway inflammation at 3 days (72 hours) after intratracheal Ad-RelA administration, we instilled 10^9 pfu Ad-RelA or control adenovirus at 72 hours before intravenous injection of LLC cells. Following tumor cell inoculation, the mice were left for 14 days and then euthanized. At this 2-week time point, Ad-RelA–infected mice exhibited >2-fold higher surface tumor numbers than control-infected animals (Fig. 2A). Assessment of tumor burden and size in histologic sections confirmed the increase in tumor number in Ad-RelA–infected mice (Fig. 2B). Furthermore, the size of the tumors was larger in the Ad-RelA mice (median sizes: PBS, 0.05 mm^2; Ad-ctl, 0.04 mm^2; Ad-RelA, 0.10 mm^2; Fig. 2C). Surprisingly, when we analyzed bromodeoxyuridine incorporation as a marker of proliferation or immunostaining for cleaved caspase-3 as a marker of apoptosis in tumor sections from this 2-week time point, no differences were observed between the tumors from the control or Ad-RelA–infected mice (data not shown). These results raised the possibility that the difference in tumor number seen in the Ad-RelA–infected lungs was influenced by increased survival or tumor "take." We therefore assessed whether there was a difference in surviving tumor number in the lungs of virus-infected mice 24 or 48 hours after

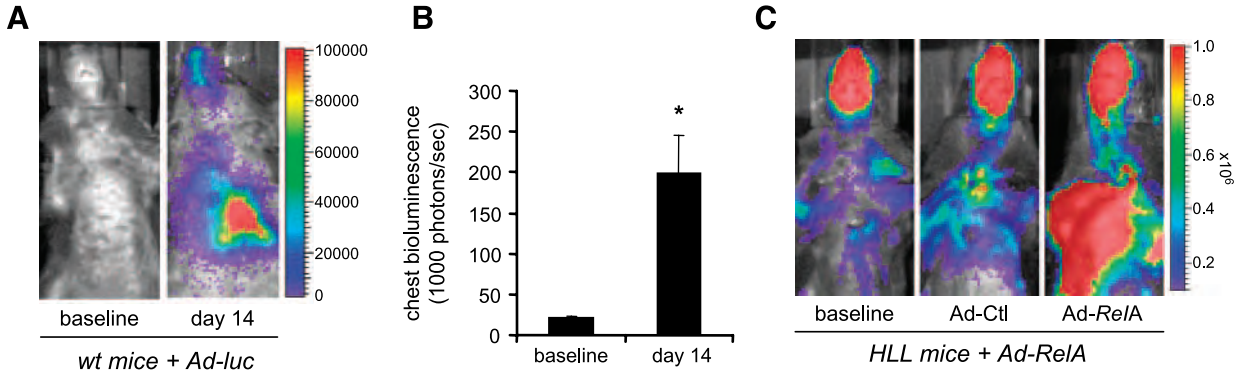

FIGURE 1. Intratracheal adenoviral instillation is a suitable method for increasing NF-κB activity in the lungs. **A.** Prolonged expression of adenoviral-encoded luciferase in the mouse lungs. Wild-type C57Bl/6 mice received 10^9 pfu Ad-luciferase and were serially imaged for bioluminescence after intravenous injection of 1 mg luciferin. Left, image taken before virus instillation; right, image taken after 14 d. **B.** Pooled data from three mice per group treated as in **A** (*, $P = 0.017$ compared with baseline). **C.** Intratracheal Ad-RelA increases NF-κB activity in the lungs. NF-κB reporter mice (*HLL*) on the C57Bl/6 background received 10^9 pfu control adenovirus or Ad-RelA intratracheally. Increased luciferase expression was seen in Ad-RelA–infected (*right*), but not control Ad-GFP–infected (*middle*) *HLL* mice, 72 h after viral delivery.

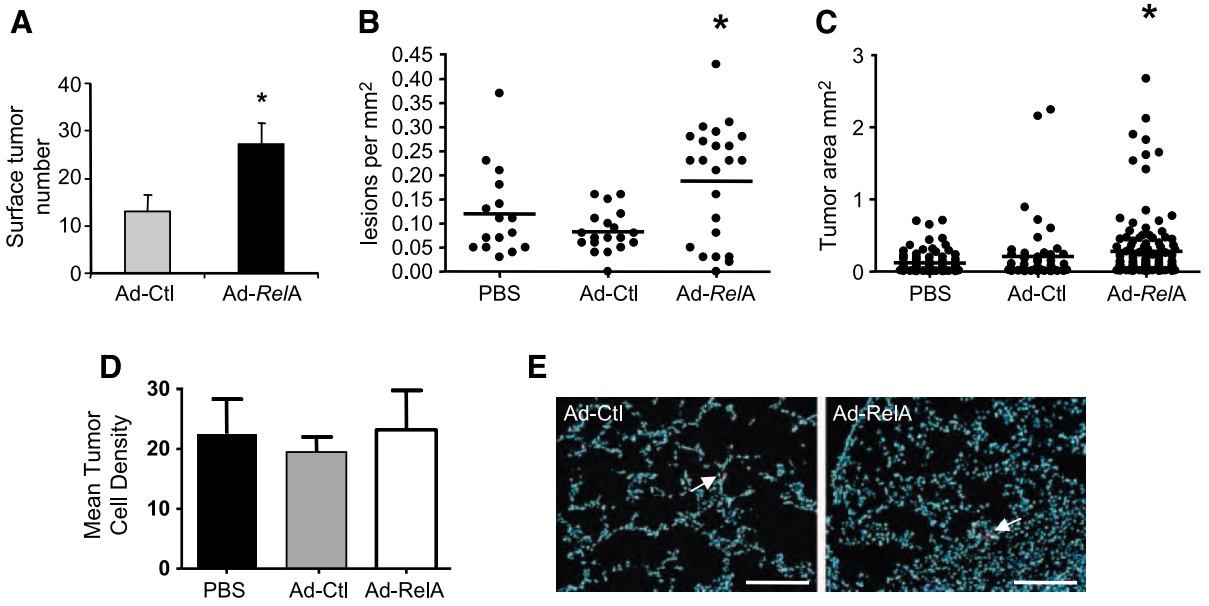

FIGURE 2. Airway inflammation resulting from enhanced host NF-κB activity increases tumorigenicity. **A.** Wild-type C57Bl/6 mice (n = 18/group) received 10^9 pfu Ad-RelA or control adenovirus at 72 h before intravenous injection of 2.5×10^5 LLC cells. Following tumor cell inoculation, the mice were left for 14 d and then euthanized. Intratracheal Ad-RelA resulted in a >2-fold increase in lung tumor numbers (*, P = 0.006 compared with Ad-Ctl). **B.** Four 5-μm histologic sections, each 300 μm apart, were obtained from each lung sample counted in **A**. Using Metamorph software, the area of lung tissue occupied by tumor was calculated for each section and averaged per animal (*, P = 0.033 compared with Ad-Ctl). **C.** Using the same sections as in **B**, the total area of each tumor lesion present in the lungs was calculated using Metamorph software (*, P = 0.034 compared with Ad-Ctl). **D** and **E.** LLC cells were loaded with CellTracker Red CMTPX *in vitro*, and then injected as usual into mice that had been pretreated with Ad-RelA or control virus. Graph in **D** shows the number of red tumor cells per area of lung in four sections each from five mice from each treatment group 24 h after injection of tumor cells. Representative histologic appearance at 24 h is shown in **E**. Tumor cells appear as red (*arrows*); nuclei of lung parenchyma have been counterstained with Hoechst 33258. Bar, 132 μm.

tumor cell injection. The LLC cells were loaded with a red lipophilic dye *in vitro* and then injected as usual into mice that had been pretreated with Ad-RelA or control virus. There was no apparent difference in the number of surviving cells at these time points (Fig. 2D and E and data not shown).

We characterized the inflammatory environment of the lungs both at an early time point (24 hours post-LLC cells) and at the end of study (2 weeks post-LLC cells). This was accomplished by performing bronchoalveolar lavage and assessing cellularity and cytokine levels in the collected fluid. As we have seen previously (25), at early time points following adenoviral delivery of RelA to the lungs, there was a marked increase in neutrophil infiltration (Fig. 3A). Our previous studies have shown that this is a transient early inflammatory response (25). The bronchoalveolar lavage fluid was analyzed by ELISA to measure expression of a number of factors that are indicative of an inflammatory response or that could contribute to tumor growth. Levels of both vascular endothelial growth factor and matrix metalloproteinase 9, two proteins that have been suggested to enhance tumor survival in the lungs, were similar among the different groups of mice at this 24-hour time point (data not shown). In contrast, levels of the NF-κB target gene monocyte chemotactic protein (*MCP-1*) were significantly increased in the Ad-RelA–treated animals compared with the other groups (Fig. 3B). Immunostaining for MCP-1 in tissue sections collected at the 24-hour time point showed that this protein could be detected in airway epithelial cells only in mice exposed to Ad-RelA (Fig. 3C). Similarly, another NF-kB target gene, *interleukin-6* (*IL-6*), could be detected in airway epithelium from Ad-RelA–exposed mice but not those exposed to a control adenovirus or PBS (Fig. 3D).

We then characterized lung inflammation at the 2-week time point following LLC cell injection. At this time point, the inflammatory cell infiltrate in the bronchoalveolar lavage of the Ad-RelA–treated mice was predominantly composed of macrophages (Fig. 3E). Mice infected with a control adenovirus or that received PBS showed no such infiltrate. To confirm that this inflammatory cell influx in Ad-RelA–treated mice was related to host NF-κB activity and not to the presence of tumor cells, additional studies were done with adenoviral vectors (Ad-RelA or control adenovirus) in which no tumor cells were injected and mice were harvested at a similar time point. These studies yielded similar total and differential cell counts in bronchoalveolar lavage to those found in the presence of LLC metastases. We also assayed the bronchoalveolar lavage fluid for the presence of several cytokines that could affect metastasis. We could not detect tumor necrosis factor-α, whereas vascular endothelial growth factor and MCP-5 levels were not different between mice infected with Ad-RelA or control (data not shown). However, at the 2-week time point, levels of the chemokine MCP-1 were increased in bronchoalveolar lavage fluid specifically from Ad-RelA–treated mice (Fig. 3F). As MCP-1 can be expressed by epithelial cells (Fig. 3C; ref. 28), the increased levels are likely a direct result of the Ad-RelA infection of epithelial lining cells and could be responsible for

the observed macrophage influx. The inflammatory response induced by Ad-RelA was confined to the lungs as WBC counts and serum cytokine levels were normal and identical between groups (data not shown).

Taken together, our data show that increasing lung NF-κB activity by adenoviral infection of epithelial lining cells results in a strong up-regulation of chemokine production and concomitant leukocyte influx into the airspaces, composed principally of macrophages at 2 weeks post-LLC cell injection. This inflammatory phenotype correlates with a more permissive environment for outgrowth of metastatic tumors as evidenced by increased lung tumor number and size following intravenous injection of LLC cells.

Alveolar Macrophages Mediate the Effect of Increased Host NF-κB Activity on LLC Metastasis

Because analysis of tumors and bronchoalveolar lavage from multiple experiments revealed a significant correlation between increased tumor number and increased infiltration of macrophages following enhancement of host NF-κB activity, we sought to determine whether this leukocyte population contributed to enhanced tumor cell metastasis. We chose to reduce the numbers of lung macrophages by intratracheal injection of liposomal encapsulated clodronate, which is a bisphosphonate that results in selective apoptosis when phagocytosed by macrophages. When delivered intratracheally, liposomal clodronate targets resident alveolar macrophages and the effect lasts ~5 to 7 days, after which macrophages start to repopulate the lung (29, 30). For these studies, mice received 10^9 pfu Ad-RelA or control adenovirus immediately followed by 75 μL liposomal clodronate or empty liposomes in any combination ($n = 6$ per group). Four animals received PBS followed by PBS (internal control). Three days later, mice received 2.5×10^5 LLC cells via the tail vein and were sacrificed after 14 days for bronchoalveolar lavage and analysis of lung tumors. Despite the relatively short-lived effect of clodronate treatment, we observed partial

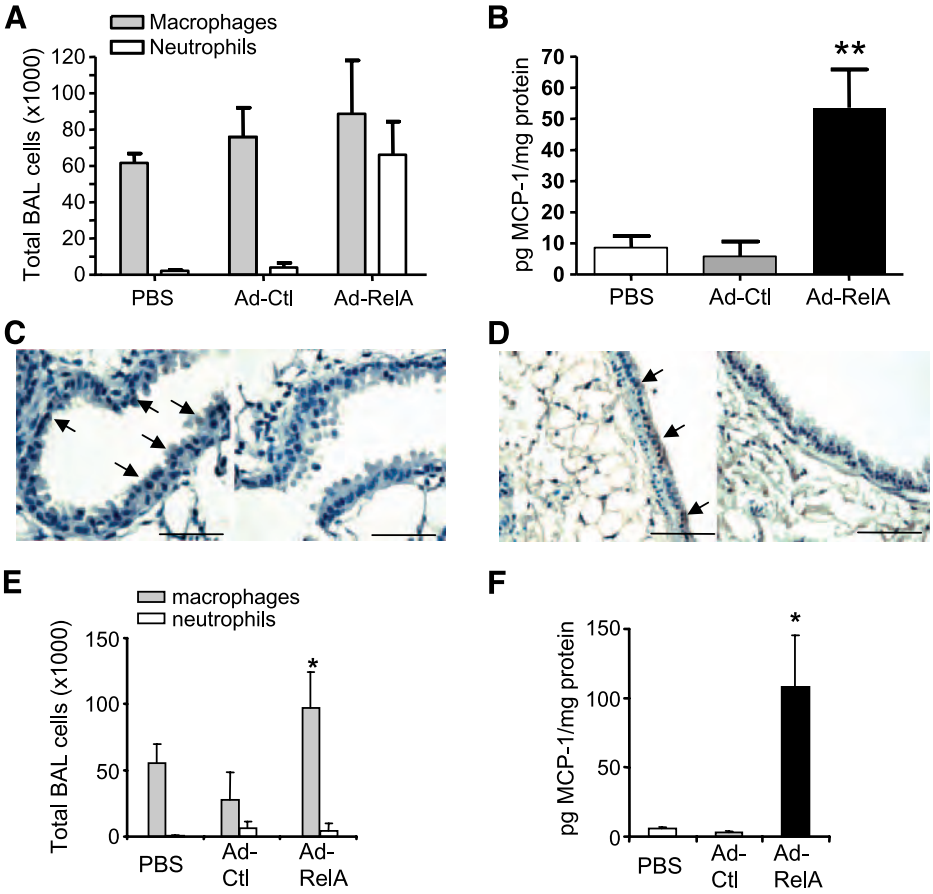

FIGURE 3. Host lungs respond to RelA overexpression with expression of MCP-1. **A.** Bronchoalveolar lavage was done 24 h following LLC cell injection in mice that had been pretreated with intratracheal PBS, control adenovirus, or Ad-RelA ($n = 5$ mice per group). A distinct increase in polymorphonuclear leukocytes was seen in the Ad-RelA–treated group that was not present in the other groups (*, $P < 0.0001$ compared with Ad-Ctl or PBS). **B.** Increased levels of MCP-1 in bronchoalveolar lavage from the mice described in **A** (*, $P < 0.01$ compared with PBS or Ad-Ctl). **C.** Lung tissue harvested from mice 24 h following LLC injection was used for immunohistochemical analysis. MCP-1 was detectable in airway lining epithelial cells (*arrows, left*) in mice exposed to Ad-RelA but not those exposed to a control adenovirus (*right*). Bar, 44 μm. **D.** IL-6, a marker of NF-κB pathway activation, was also present in airway lining cells in Ad-RelA–treated mice (*arrows, left*) but not in control adenovirus–treated mice (*right*). Bar, 68 μm. **E.** Bronchoalveolar lavage was done 2 wk following LLC cell injection in mice pretreated with intratracheal PBS, control adenovirus, or Ad-RelA ($n = 6$ mice per group). Ad-RelA, but not Ad-Ctl or sham PBS injection, caused a mononuclear inflammatory cell influx into the lungs (*, $P < 0.001$ compared with Ad-Ctl or PBS). **F.** Increased levels of MCP-1 in bronchoalveolar lavage from mice treated as described in **E** (*, $P = 0.005$ and $P = 0.007$ compared with PBS and Ad-Ctl, respectively). **E** and **F** were recapitulated without tumor cell injection, with identical results.

abrogation of the inflammatory cell influx induced by Ad-RelA at the 14-day time point (Fig. 4A). Significantly, this reduction in inflammatory cell influx was sufficient to completely negate the Ad-RelA–enhanced metastasis effect (Fig. 4B). There was no effect of clodronate administration on the number of metastatic foci evident in the control virus–treated animals, indicating that the enhanced metastasis seen after Ad-RelA treatment is related to newly recruited or activated macrophages. These data show that short-term ablation of macrophages is sufficient to block enhanced tumor formation resulting from NF-κB–induced airway inflammation.

Discussion

NF-κB is a multifunctional transcription factor that has been shown to affect the pathobiology of a variety of diseases (23, 31, 32). In the present study, we have examined the effects of NF-κB activation in host cells on the development of metastatic tumors in the lung. Increasing the levels of NF-κB activity in the host lung resulted in lung inflammation and a substantial protumorigenic effect. The effector cell population mediating this enhanced tumorigenicity seems to be macrophages, which are recruited to the lungs as a consequence of epithelial cell NF-κB activation. Ablation of lung macrophages using liposomal clodronate is sufficient to block the increase in tumor burden resulting from NF-κB–dependent lung inflammation.

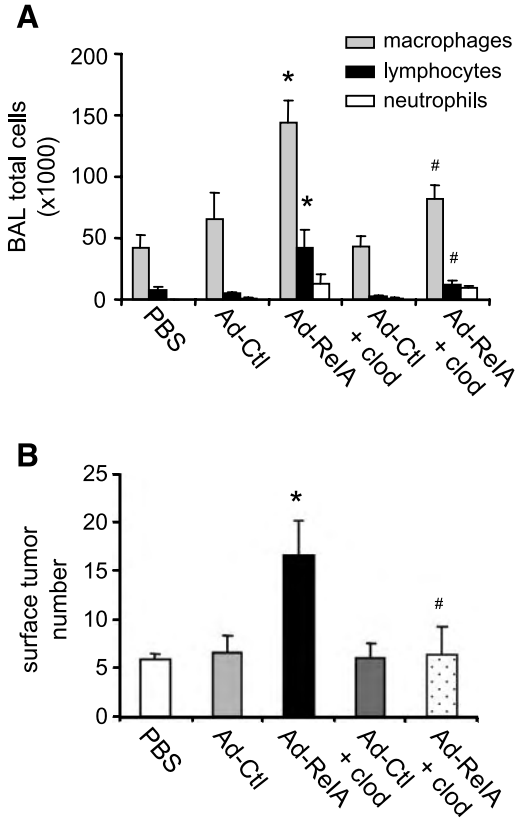

FIGURE 4. Alveolar macrophages mediate the effect of increased host NF-κB activity on LLC metastasis. **A.** Macrophage depletion limits lung inflammation induced by Ad-RelA. C57Bl/6 mice (n = 6 per group) received PBS or 10^9 pfu control adenovirus or Ad-RelA, followed by 75 μL liposomal clodronate (clod groups) or empty liposomes (other groups) intratracheally, 72 h before intravenous injection of 2.5×10^5 LLC cells. After 14 d, clodronate-treated mice had reduced inflammatory cells in bronchoalveolar lavage compared with empty liposome-treated mice (*, $P < 0.05$ compared with PBS and Ad-Ctl; #, $P < 0.05$ compared with Ad-RelA and $P > 0.05$ compared with PBS and Ad-Ctl). **B.** Macrophage depletion limits increased tumor take induced by Ad-RelA. Mice were treated as in **A**, and lung tumors were determined at day 14 (*, $P < 0.05$ compared with PBS and Ad-Ctl, #, $P < 0.05$ compared with Ad-RelA, and $P > 0.05$ compared with PBS and Ad-Ctl).

In contrast to previous studies on the role of NF-κB in tumor progression that have primarily used loss-of-function approaches, we chose to increase host NF-κB levels. Our goal was to recapitulate the increased NF-κB levels reported in the lung tissue of smokers and patients with chronic obstructive pulmonary disease (22, 31) and to generate airway inflammation as occurs in these individuals. In addition to increasing the risk for lung cancer development (33), chronic inflammatory disorders of the respiratory tract may increase the risk for cancer progression and metastasis to the lungs. A striking result of delivery of adenovirus encoding RelA, but not control adenoviruses, was an induction of an inflammatory infiltrate that was composed largely of macrophages at 17 days postinfection. The composition of the RelA-expressing inflammatory infiltrate in the lungs changes from primarily neutrophilic at an early time point following activation of NF-κB in airway epithelium to a primarily macrophage-rich infiltrate later. Interestingly, MCP-1 expression was found to be increased at the early time point, potentially directing the macrophage recruitment. Notably, the presence of the inflammatory infiltrate correlated with an increase in the number of tumor foci. Both the number and the average size of tumor foci were increased in the group overexpressing RelA. There was no difference in the number of tumor cells surviving in the lungs at 24 or 48 hours postimplantation. This would suggest that the inflammatory phenotype associated with RelA overexpression is most critical for outgrowth of implanted tumors. Surprisingly, proliferation and apoptosis variables were not significantly altered between tumors in the Ad-RelA and control adenovirus groups when measured at the 2-week time point. Hence, the critical time when the inflammatory environment contributes to development of metastatic lung tumors seems to be between the early postimplantation stage (48 hours) and the time of harvest (2 weeks).

This idea that NF-κB–induced lung inflammation primarily affects early growth of a metastatic focus is supported by our studies involving macrophage depletion. To determine whether the increase in tumor numbers observed after Ad-RelA infection could be attributed to macrophage infiltration, we depleted macrophages with liposomal clodronate. Previously, we have shown that a single intratracheal dose of liposomal clodronate depletes alveolar macrophages by 77% (30, 34). The depletion lasts ~5 to 7 days (29, 30). In these experiments, partial ablation of macrophages was sufficient to overcome the tumor-promoting effect of lung inflammation resulting from Ad-RelA administration. This finding supports the idea that macrophage recruitment and/or activation occurring proximate to tumor cell implantation determines development of metastatic foci. Although the specific macrophage products or activity that determines metastasis

in this model is not apparent from these studies, our findings support a role for the macrophage in tumor metastasis to the lungs. Literature describing tumor-associated macrophages has suggested various roles for these cells in tumor growth and progression (5, 35, 36). For example, the presence of tumor-associated macrophages has been especially associated with increased angiogenesis, which may be related to vascular endothelial growth factor production by macrophages (3, 5, 7). This does not seem to be a critical factor in our studies as vascular endothelial growth factor levels were similar among the different mouse groups at both early and late time points. A recent article from Condeelis and colleagues has identified a possible paracrine loop that exists between epidermal growth factor receptor–expressing tumor cells and colony-stimulating factor receptor–expressing macrophages that apparently serves as a mechanism to enhance tumor cell migration and hence metastasis (8). As we were using an experimental metastasis assay, migration away from a primary tumor was not required. Further, the number of surviving tumor cells present within the lung parenchyma 24 or 48 hours after tumor cell injection was not different among the various groups, suggesting that emigration from vasculature was not affected. In our experiments, only the enhanced macrophage infiltrate induced by lung inflammation seemed to be related to metastatic focus formation as the clodronate-mediated macrophage depletion did not alter the number of foci in the control animals.

In other studies of NF-κB activation within tumor epithelial cells, the primary result seems to be the generation of a tumor cell intrinsic survival response usually mediated through up-regulation of expression of antiapoptotic Bcl-2 family members (37, 38). In our case, the tumors came from exogenous cells that were inoculated after the infection of the host epithelium with Ad-RelA. By using this system, we have been able to identify another potential function of epithelial NF-κB, that is, the recruitment of tumor-promoting inflammatory cells. Hence, NF-κB in epithelium functions both as an intrinsic tumorigenic promoter by favoring survival and also as an extrinsic promoter by causing the influx of inflammatory cells.

Lung cancer represents an epidemic on the rise (17, 18). At the time of diagnosis, most patients will have local or systemic spread that renders the disease incurable by surgery (39). In addition, metastasis to the lungs from tumors in other organs is a significant clinical problem. Thus, therapies that would halt invasion and metastasis are desperately needed. It is increasingly clear that the biological behavior of lung cancer is influenced not only by progressive changes in cancer cells but also by host factors, including the host immune system. Although an intact immune system may deliver an antitumor effect, an aberrant inflammatory response may actually promote tumor progression/metastasis. Here, we show how increases in host NF-κB activity, a situation known to occur in chronic inflammatory conditions of the respiratory tract as well as in several other organ systems, can enhance the development of tumor lesions in a mouse model of metastatic lung disease. We suggest that the paradigm of treating patients with agents to down-regulate inflammation could be pursued to limit tumor metastasis to the lungs.

Materials and Methods

Cell Line, Plasmid, and Transfection

LLC cells, originally obtained from the National Cancer Institute, were maintained in DMEM (Invitrogen) supplemented with 10% FCS (Invitrogen), glutamine (Invitrogen), and 100 mg/L penicillin and streptomycin (Invitrogen). The LLC clone used for all these experiments was one carrying a NF-κB reporter plasmid, as previously described (40).

Reagents and Drugs

D-Luciferin sodium was obtained from Biosynth AG. Liposomal clodronate or empty liposomes were produced as previously described (30). The lipophilic dye CellTracker Red CMTPX was purchased from Molecular Probes/Invitrogen.

Adenoviral Vectors

Replication-deficient adenoviral vectors that express *Photinus pyralis* luciferase (Ad-luc), β-gal (Ad-βgal), GFP (Ad-GFP) as controls, and the activator of NF-κB (Ad-RelA) were constructed and purified as previously described (25, 41). Briefly, an expression cassette containing a cytomegalovirus promoter driving RelA was inserted into the replication-deficient recombinant adenovirus type 5. Adenoviral vectors were propagated, purified, and stored at −70°C.

Experimental Animals

All animal care and experimental procedures were approved by and conducted according to the Institutional Animal Care and Use Committee guidelines. Mice used for experiments were sex matched, weight matched (20-25 g), and age matched (8-12 wk). C57BL6/J mice were purchased from The Jackson Laboratory, crossed, and inbred. Transgenic mice expressing *Photinus pyralis* luciferase cDNA under control of the proximal 5′ HIV-long terminal repeat, called HIV-LTR/Luciferase (HLL), have been previously reported (26, 42, 43). HLL mice on the C57BL6/J background ($n > 9$) were used for this study. For intratracheal injection, mice were anesthetized with isoflurane, anterior cervical skin and soft tissues were dissected, and 10^9 pfu virus/50 μL PBS or PBS alone followed by 75 μL liposomal clodronate or empty liposomes were injected intratracheally. Three days later, mice received 2.5×10^5 or 5×10^5 LLC cells in PBS or PBS alone via a lateral tail vein. After 24 h or 14 d, mice were euthanized by CO_2 asphyxiation, and lungs were lavaged thrice with 1 mL PBS and fixed in Bouin's solution.

Bioluminescent Imaging

For *in vivo* imaging, mice were anesthetized, received 1 mg of D-luciferin retro-orbitally, and were imaged in an IVIS cooled charged coupled device (Xenogen Corporation) as described previously (25, 43). Data were collected and analyzed using Living Image v.2.50 (Xenogen Corporation) and IgorPro (Wavemetrics) software. Briefly, a photographic image of the animals was first acquired. Then, a bioluminescent image was acquired by integration of photon flux over each group of pixels (bin) in the field of view, and graphically represented using an arbitrary pseudo-color scale. Fifteen seconds of acquisition time were selected in order not to saturate the camera. Standard-sized

circular regions of interest encompassing the murine chest were determined and photon flux was measured over these areas.

Dye Labeling of Tumor Cells

Tumor cells were labeled *in vitro* with the CellTracker Red dye for 30 min at a concentration of 10 μmol/L as per manufacturer's protocol. After washing with PBS, the cells were counted and used for intravenous injection.

Lung Surface Tumor Enumeration

Tumors on the lung surface were enumerated by at least two experienced blinded readers under a dissecting microscope; tumor counts were averaged and statistically analyzed.

Histology

The explanted mouse lungs were fixed in Bouin's fixative solution for 24 h and 70% ethanol for 3 d. Tissues were embedded in paraffin and 5-μm-thick sections were serially cut at a median transverse level of the lungs. The sections were mounted on glass slides and stained with H&E. For assessment of tumor burden, the area of each section that was tumor, as well as the total tissue area, was measured using Metamorph (Universal Imaging Corp.) software. This software was also used to calculate the area of each tumor. Four sections at different depths 300 μm apart were used for these analyses.

Alternatively, lungs were covered in optimum cutting temperature medium and frozen in liquid nitrogen. Sections were rinsed and counterstained with Hoechst 33258 (Sigma), coverslipped using fluorescence-saving mountant (Gel/Mount, Biomeda Corp), and examined using fluorescent microscopy. Four random fields from each section, four sections per animal, were analyzed for the total number of red-labeled tumor cells and the total tissue area using Metamorph software.

Immunohistochemistry

Five-micrometer Bouin's-fixed, paraffin-embedded sections of lungs from either the 24-h or 2-wk time points were assessed for expression of IL-6 and MCP-1 using antibodies purchased from Abcam and following supplier-recommended staining procedures.

Enzyme-Linked Immunosorbent Assays

Tumor necrosis factor-α, MCP-1 and MCP-5, vascular endothelial growth factor, and pro–matrix metalloproteinase 9 were assayed in bronchoalveolar lavage using murine ELISA kits (R&D Systems) according to the manufacturer's instructions (detection limits 3.0, 2.0, 1.58, 5.1, and 8.0 pg/mL, respectively).

Clodronate Treatment

Liposomal encapsulation of clodronate (dichloromethylene diphosphonate) was done as previously reported (30). Liposomes containing PBS were used as a control. Briefly, a mixture of 8 mg cholesterol (Sigma) and 86 mg egg phosphatidylcholine (DOPC, Avanti) was dissolved in chloroform and then evaporated under nitrogen. Chloroform was further removed under low vacuum in a speedvac Savant concentrator. The clodronate solution was prepared by dissolving 1.2 g of dichloromethylene diphosphonic acid (Sigma) in 5 mL of sterile 1× PBS. The entire clodronate solution (5 mL) was added to the liposome preparation and mixed thoroughly. The solution was sonicated and ultracentrifuged at 10,000 × *g* for 1 h at 4°C. The liposome pellet was removed, resuspended in 5 mL PBS, and ultracentrifuged at 10,000 × *g* for 1 h at 4°C. Liposomes were removed, resuspended in 5 mL PBS, and used within 48 h. The final concentration of the liposomal clodronate solution was 5 mg/mL.

Statistical Analysis

All values given represent mean values ± SE. The number of observations (n) is given in parentheses. To compare the two groups, the Student's t and Mann-Whitney U tests were used (for normally or nonnormally distributed data). ANOVA was used to detect significant differences between multiple groups. All P values are two-tailed; P values ≤ 0.05 were considered significant. Statistical analyses were done using the Statistical Package for the Social Sciences Software Version 11.0 (SPSS).

References

1. Dunn GP, Bruce AT, Ikeda H, Old LJ, Schreiber RD. Cancer immunoediting: from immunosurveillance to tumor escape. Nat Immunol 2002;3:991–8.

2. Balkwill F, Coussens LM. An inflammatory link. Nature 2004;431:405–6.

3. Balkwill F, Mantovani A. Inflammation and cancer: back to Virchow? Lancet 2001;357:539–45.

4. Coussens LM, Werb Z. Inflammation and cancer. Nature 2002;420:860–7.

5. Pollard JW. Tumour-educated macrophages promote tumour progression and metastasis. Nat Rev Cancer 2004;4:71–8.

6. Dong G, Chen Z, Kato T, Van Waes C. The host environment promotes the constitutive activation of nuclear factor-κB and proinflammatory cytokine expression during metastatic tumor progression of murine squamous cell carcinoma. Cancer Res 1999;59:3495–504.

7. Lin EY, Pollard JW. Macrophages: modulators of breast cancer progression. Novartis Found Symp 2004;256:158–72.

8. Wyckoff J, Wang W, Lin EY, et al. A paracrine loop between tumor cells and macrophages is required for tumor cell migration in mammary tumors. Cancer Res 2004;64:7022–9.

9. Blackwell TS, Christman JW. The role of nuclear factor-κB in cytokine gene regulation. Am J Respir Cell Mol Biol 1997;17:3–9.

10. Finco TS, Westwick JK, Norris JL, et al. Oncogenic Ha-Ras-induced signaling activates NF-κB transcriptional activity, which is required for cellular transformation. J Biol Chem 1997;272:24113–6.

11. Kim DW, Sovak MA, Zanieski G, et al. Activation of NF-κB/Rel occurs early during neoplastic transformation of mammary cells. Carcinogenesis 2000; 21:871–9.

12. Jiang Y, Cui L, Yie TA, et al. Inhibition of anchorage-independent growth and lung metastasis of A549 lung carcinoma cells by IκBβ. Oncogene 2001;20: 2254–63.

13. Kim DM, Koo SY, Jeon K, et al. Rapid induction of apoptosis by combination of flavopiridol and tumor necrosis factor (TNF)-α or TNF-related apoptosis-inducing ligand in human cancer cell lines. Cancer Res 2003;63: 621–6.

14. Ricca A, Biroccio A, Trisciuoglio D, et al. relA over-expression reduces tumorigenicity and activates apoptosis in human cancer cells. Br J Cancer 2001; 85:1914–21.

15. Andela VB, Schwarz EM, Puzas JE, O'Keefe RJ, Rosier N. Tumor metastasis and the reciprocal regulation of prometastatic and anti-metastatic factors by nuclear factor κB. Cancer Res 2000;60:6557–62.

16. Luo JL, Maeda S, Hsu LC, Yagita H, Karin M. Inhibition of NF-κB in cancer cells converts inflammation-induced tumor growth mediated by TNFα to TRAIL-mediated tumor regression. Cancer Cell 2004;6:297–305.

17. Parkin DM, Bray F, Ferlay J, Pisani P. Estimating the world cancer burden: Globocan 2000. Int J Cancer 2001;94:153–6.

18. Jemal A, Murray T, Ward E, et al. Cancer statistics, 2005. CA Cancer J Clin 2005;55:10–30.

19. Mountain CF, Hermes KE. Surgical treatment of lung cancer. Past and present. Methods Mol Med 2003;75:453–87.

20. Christman JW, Sadikot RT, Blackwell TS. The role of nuclear factor-κB in pulmonary diseases. Chest 2000;117:1482–7.

21. Anto RJ, Mukhopadhyay A, Shishodia S, Gairola CG, Aggarwal BB. Cigarette smoke condensate activates nuclear transcription factor-κB through phosphorylation and degradation of IκB(α): correlation with induction of cyclooxygenase-2. Carcinogenesis 2002;23:1511–8.

22. Fabbri LM, Caramori G, Beghe B, Papi A, Ciaccia A. Physiologic consequences of long-term inflammation. Am J Respir Crit Care Med 1998; 157:S195–8.

23. Caramori G, Adcock IM, Ito K. Anti-inflammatory inhibitors of IκB kinase in asthma and COPD. Curr Opin Investig Drugs 2004;5:1141–7.

24. Krishnan K, Khanna C, Helman LJ. The molecular biology of pulmonary metastasis. Thorac Surg Clin 2006;16:115–24.

25. Sadikot RT, Han W, Everhart MB, et al. Selective IκB kinase expression in airway epithelium generates neutrophilic lung inflammation. J Immunol 2003; 170:1091–8.

26. Yull FE, Han W, Jansen ED, et al. Bioluminescent detection of endotoxin effects on HIV-1 LTR-driven transcription *in vivo*. J Histochem Cytochem 2003; 51:741–9.

27. Mayo JG. Biologic characterization of the subcutaneously implanted Lewis lung tumor. Cancer Chemother Rep 2 1972;3:325–30.

28. de Boer WI, Sont JK, van Schadewijk A, et al. Monocyte chemoattractant protein 1, interleukin 8, and chronic airways inflammation in COPD. J Pathol 2000;190:619–26.

29. Van Rooijen N, Sanders A. Liposome mediated depletion of macrophages: mechanism of action, preparation of liposomes and applications. J Immunol Methods 1994;174:83–93.

30. Everhart MB, Han W, Parman KS, et al. Intratracheal administration of liposomal clodronate accelerates alveolar macrophage reconstitution following fetal liver transplantation. J Leukoc Biol 2005;77:173–80.

31. Barnes PJ, Karin M. Nuclear factor-kB—a pivotal transcription factor in chronic inflammatory diseases. N Engl J Med 1997;336:1066–71.

32. Yamamoto Y, Gaynor RB. IκB kinases: key regulators of the NF-κB pathway. Trends Biochem Sci 2004;29:72–9.

33. Biesalski HK, Bueno de Mesquita B, Chesson A, et al. European consensus statement on lung cancer: risk factors and prevention. CA Cancer J Clin 1998;48: 167–76.

34. Koay MA, Gao X, Washington MK, et al. Macrophages are necessary for maximal nuclear factor-κ B activation in response to endotoxin. Am J Respir Cell Mol Biol 2002;26:572–8.

35. Condeelis J, Pollard JW. Macrophages: obligate partners for tumor cell migration, invasion, and metastasis. Cell 2006;124:263–6.

36. Lewis CE, Pollard JW. Distinct role of macrophages in different tumor microenvironments. Cancer Res 2006;66:605–12.

37. Greten FR, Eckmann L, Greten TF, et al. IKKβ links inflammation and tumorigenesis in a mouse model of colitis-associated cancer. Cell 2004;118: 285–96.

38. Stathopoulos GT, Sherrill TP, Cheng D-S, et al. Epithelial NF-κB activation promotes urethane-induced lung carcinogenesis. Proc Natl Acad Sci U S A. In press 2008.

39. Mountain CF. Staging classification of lung cancer. A critical evaluation. Clin Chest Med 2002;23:103–21.

40. Stathopoulos GT, Zhu Z, Everhart MB, et al. Nuclear factor-κB affects tumor progression in a mouse model of malignant pleural effusion. Am J Respir Cell Mol Biol 2006;34:142–50.

41. Sadikot RT, Zeng H, Yull FE, et al. p47phox deficiency impairs NF-κB activation and host defense in Pseudomonas pneumonia. J Immunol 2004;172: 1801–8.

42. Blackwell TS, Yull FE, Chen CL, et al. Multiorgan nuclear factor κB activation in a transgenic mouse model of systemic inflammation. Am J Respir Crit Care Med 2000;162:1095–101.

43. Sadikot RT, Wudel LJ, Jansen DE, et al. Hepatic cryoablation-induced multisystem injury: bioluminescent detection of NF-κB activation in a transgenic mouse model. J Gastrointest Surg 2002;6:264–70.